GIMA
Geographical Information Management and Applications

Land Use and Land Cover Changes in Monduli District, Tanzania

Analysis of multiple classification methods and satellite sensors in order to perform a multi-temporal post-classification change detection analysis in a difficult to map semi-arid savannah landscape

R.C. van Rosmalen

MSc Thesis

25th of February 2021

Author: Roos C. van Rosmalen

Email: r.c.vanrosmalen@students.uu.nl

Student number: 5716152

Supervisor: Maarten Zeylmans van Emmichoven

Responsible professor: Steven de Jong

Msc Program: Geographical Information Management and Applications

Faculty of Geo Sciences

Utrecht University

Abstract

In this study Land Use and Cover changes in Monduli district, Tanzania, are analysed from 2019 to 1985 with the use of a post classification change detection technique. In Monduli there are several aspects that complicate the classification of the landscape with remote sensing: A semi-arid climate with wet and dry seasons, similarity of spectral signatures of savannah vegetation types, fuzzy transition zones and a small heterogenous agricultural system. As a result of the difficulty of the study area for remote sensing previously conducted studies were unable to map the surface correctly (van den Bergh, 2016; Verhoeve, 2019). In this study measurements have been taken to combat the aforementioned issues and improve the accuracy of the classifications: the number of inputs for the classifier from the ground truth dataset has been increased, the classifiers are trained on each image separately, accuracies have been calculated for each classification, ancillary data and indexes are added and Sentinel 2 imagery (10m spatial resolution) has been incorporated, next to Landsat imagery (30m spatial resolution). Unsupervised ISODATA and supervised maximum likelihood and random forest classification methods have been applied. Sentinel did not result in higher accuracies because of the lower number of spectral bands available. However, of the random forest classifications with Landsat imagery four classifications reached an overall accuracy higher than 0.746 and were used for the change detection analysis. From 1985 to 2019 classes that increased are agriculture (+2.5%), built environment (+0.3%) water (+0.4%) and barren (+1.0%). However, barren shows some fluctuation over the years. As a result of the increase of these classes vegetation (woody savannah, savannah, open shrubland, closed shrubland and grassland) decreased with 2.7%. Additionally, a decrease in forests of 0.4% can be observed which is, next to cloud cover, primarily the result of an increase in woody savannah followed by closed shrub and agriculture.

Key words: *LULC change, semi-arid savannah*, *Landsat, Sentinel, Random Forest, Maximum Likelihood, ISODATA*

Contents

1. Introduction

1.1. Problem

Monduli district is located in the Arusha Region of Tanzania in eastern Africa. In this area Land Use and Cover (LULC) changes are expected as a result of privatization of land, population growth and an increase in the selling of fuelwood (Butz, 2013; Fratkin, 2001; Homewood, Kristjanson & Trench, 2009). Furthermore, there are indications the area is prone to sheet wash, rill, and gully erosion. Soil erosion and consequently land degradation in Africa are often the result of LULC changes. These phenomena have a large impact on the livelihoods of the inhabitants of Monduli, who are mostly pastoralists and farmers (Blake, et al., 2018).

Land cover refers to the physical objects covering the surface such as forests or water. Land use is related to the way the land is used, such as for agriculture or urbanization (Al-doski, Mansor, and Shafri, 2013). By mapping land cover and performing a change detection, specific land use trends can be detected. LULC mapping can be performed with remote sensing. Remote sensing uses electromagnetic radiation in order to obtain information about the surface of the earth (de Jong, van der Meer & Clevers, 2004). With this technique multiple LULC maps can be produced and change detection can be performed.

Previously conducted studies (Kiunsi & Meadows, 2006; van den Bergh, 2016) already demonstrated certain LULC changes in the area. Van den Bergh (2016) used two Landsat images and showed from 1985 to 2016 urban increased (+0.03%), agriculture increased (+2.42%), bare soil increased (+5,73%), water increased (+2.21%) and forests increased (+1.84%). Grassland decreased (-5.77%) and savannah decreased (-3.74%). However, Verhoeve (2019) showed no definitive conclusions could be drawn on the LULC change. In Verhoeve (2019) 32 images are classified and analysed. Even though the accuracy rates are high, the quantities of the LULC classes show big, unrealistic, variations over time that do not match the satellite imagery. The results by Verhoeve (2019) also raise doubts about the accuracy of studies that use less images such as van den Bergh (2016).

The complications encountered in mapping Monduli seem to be a result of the heterogeneity of the landscape which means some LULC classes have relatively similar spectral signatures (Meerman & Sabido 2001; Xie, Sha & Yu 2008), issues in mapping fuzzy transition zones between LULC classes (Feilhauer et al., 2020) and small heterogenic agricultural areas that are difficult to map with higher spatial resolution sensors such as Landsat (Burke & Lobell, 2017; Bégué et al., 2018). Additionally the differences in precipitation patterns, because of the semi-arid climate with dry and wet seasons, result in vegetation to look dry in some satellite images and green in others, which both have very different spectral signatures (Xie et al., 2008). This illustrates Monduli is a difficult area to map and raises questions on how to make an accurate timeseries with remote sensing.

1.2. Objectives

The main priority of this study is analysing the location and quantity of LULC changes in Monduli over a period of 34 years. It is expected some land use types such as agriculture potentially show some level of fluctuation throughout the year because not all pastures are continuously in use and not all crops blossom at the same moment. However, a land cover type such as forests cannot decrease and increase within a small period of time. Components that can have an influence on the accuracy of a classification are the resolution of the satellite sensors (Fisher, Acosta, Dennedy-Frank, Kroeger & Boucher 2018; Karlson et al., 2020), the classification algorithm and also the amount of the collected ground truth used to train the algorithm (Jensen 2004; Millard & Richardson 2015).

The Landsat satellite by NASA is a useful resource for change detection and monitoring because of the long history (Rozenstein & Karnieli, 2011). Landsat has been running since 1972 which means the timeframe Landsat imagery covers is high. However, the Landsat satellite offer a coarser spatial resolution compared to Sentinel-2. Sentinel-2 is a satellite launched by ESA and has a spatial resolution of 10 meters while Landsat-8 has a spatial resolution of 30 meters. With higher spatial resolution imagery it is possible to map classes more precisely which can consequently lead to a more accurate LULC classification (Fisher et al., 2018). Specifically for small heterogenic agricultural systems in Africa Sentinel-2 can be of use (Karlson et al., 2020).

Additionally, each classification method has its own strengths and weaknesses. In this study the unsupervised classification method ISODATA, the supervised more traditional method maximum likelihood method and the supervised machine learning method random forest will be applied. Comparisons between the accuracy of these classifications can provide insights into which method is best suited for this specific study area and will result in the most accurate measurements of the LULC change. Additionally, using multiple approaches to determine LULC changes means the study is not biased to one method.

Verhoeve (2019) specifically demonstrates the transition zones between forests and woody savannah are difficult to map which results in forested areas to fluctuate between years. In Monduli forests transition into (woody) savannah, grassland and shrubland. Forests are characterized by a more closed canopy cover, while woody savannas have more grass cover (Oliveras & Malhi, 2016). Selecting the right training samples is an important element of proper classification of these land cover classes and the ability to analyse changes. Furthermore, an increase in ground truth has a positive influence on the overall accuracy of classifiers (Jensen 2004; Millard & Richardson 2015). The collection of ground truth samples in some areas can be difficult due to accessibility. In this study high-resolution satellite data (0.5-meter spatial resolution) is used to increase the sample size of a previously collected ground truth dataset by Verhoeve (2019). Furthermore, the input for the classifier is increased by collecting random points within the polygons. Increasing the sample size could potentially increase the ability of the classifiers to distinguish between forests and other LULC classes and thus improve issues with mapping transition zones.

1.3. Research questions

As described, there is a need for accurate land use and cover maps in order to measure trends in Monduli. Mapping the landscape provides insight into more complex processes. The main research question of the study is the following:

How has the land use and land cover in the Monduli district in Tanzania changed from 1985 to 2019?

There are a few sub questions formulated based on the components mentioned in the previous section. The first sub questions are related to analysing the results of the different classification techniques. Four Landsat satellite images will be used in order to analyse how much the LULC classes fluctuate in Monduli with the use of each classifier. This results into the following sub research questions:

> *RQ1: How is the land use and cover classified in Monduli with the use of an unsupervised ISODATA classification method?*
>
> *RQ2: How is the land use and cover classified in Monduli with the use of a supervised maximum likelihood classification method?*
>
> *RQ3: How is the land use and cover classified in Monduli with the use of a supervised random forest classification method?*

Furthermore, as mentioned, the difference in Landsat and Sentinel imagery will be explored for recent years as the increased spatial resolution of the Sentinel sensor could potentially improve the classifications. This results into the following sub research question:

> *RQ4: How do the outcomes of the land use and cover classifications of Landsat imagery compare to Sentinel imagery?*

The techniques will be validated with the use of certain validation measurements, further explained in section 3.7. The classifications and resulting accuracies will be compared to answer the firth research question. The best suited method will be applied on all the available images available from 1985 to 2019. Subsequently, the classifications with the highest accuracies will be used to perform a post-classification change detection analysis.

> *RQ5: How does the land use and cover in Monduli change over multiple years from 1985 to 2019 with the best suited method and imagery?*

1.4. Thesis structure

First some theoretical background is provided on the expected LULC changes in Monduli, the use of remote sensing imagery, change detection, LULC classifications techniques, ground truth sampling designs, validation methods and challenges in remote sensing for LULC classifications. Additionally, the results and methods of previously conducted studies in the research area are discussed. Secondly the methods and data used in this study are explained in more detail. What follows is a description of the study area, after which the results of the study are presented. The results are presented in the order of the research questions. First the results of the Landsat

classifications with ISODATA are demonstrated and subsequently with maximum likelihood and random forest. A comparison of Sentinel and Landsat imagery for each method follows to determine if Sentinel could improve the accuracy of the classifications. Lastly the method with the highest accuracy and least unlikely fluctuations is applied on all the available images. Lastly, on the most accurate classifications a change detection analysis is performed. After the results a discussion including recommendations for further research and a conclusion follows.

2. Theory

2.1. Soil erosion and Land Use and Land Cover (LULC) changes

Mapping LULC is important to keep track of the specific changes the environment is undergoing. Certain LULC changes can stimulate the process of soil erosion and land degradation because of the removal of a protective vegetation layer.

Soil erosion occurs when the soil is left unexposed and can be affected by wind and rain. One of the most common types of soil erosion is called sheet erosion. This happens when the rain and wind remove a thin film from the soil (Pimentel, 2006). In figure 1 this process is demonstrated. Soil erosion can consequently cause land degradation because the top layer of the soil has the most nutrients. When this layer is carried away the soil becomes become unfertile which can result into desertification (Bashir, Javed & Bibi, 2018).

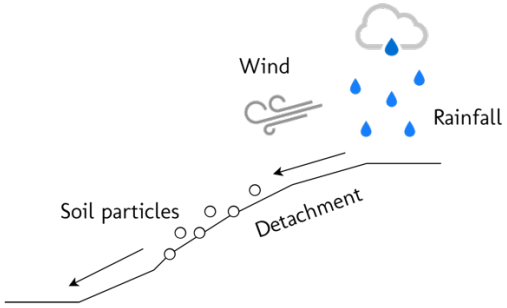

Figure 1
Visualization of the process of soil erosion

The predicted LULC changes in the Moduli district can be connected to changes in the behaviour of the Maasai, a semi-nomadic pastoralist and agro-pastoralist group who inhabit the area (Homewood et al., 2009). Because of the semi-arid savannah climate with dry and wet seasons, there are large differences in precipitation patterns which means the Maasai originally moved around in order for their livestock to have enough vegetation to graze on (Fratkin, 2001; Homewood et al., 2009).

As a result of villagization campaigns by the post-colonial government during the 1960s and 1970s large parts of the Maasai have settled down (Fratkin, 2001). Privatization of land was stimulated, and pastoralists were often left out of the agricultural landscape, as mobility was seen as a subordinate way of conserving resources (Fratkin, 2001; Homewood et al., 2009). Together with the allocation of national parks and commercial farms, this has resulted in restrictions to the movement of the Maasai (Fratkin, 2001). The shift in lifestyle has meant parts of the savannah were cleared to make space for agriculture which results in less vegetation cover to protect the soil (Schmidt, 1997). Furthermore, a component that puts a strain on the environment is the large population growth in the area. From 2002 to 2012 in Monduli district the population increased with 54.4% (National Bureau of Statistics, 2016).

Additionally, there has been an increase in the selling of fuelwood. Currently, wood is extracted at a faster rate compared to the regeneration of the forest which can also result in soil erosion

due to a loss of protective vegetation (Butz, 2013). Other studies in regions in Africa such as Congo demonstrate woody savannah is increasing while there are also indications of deforestation because forests are turned into woody savannahs. These woody savannahs have fewer species and more grasses and pioneer forest species (Oliveras & Malhi, 2016).The transition between forests and savannah is dynamic. However, currently, it seems as if forests are rapidly converted into these land cover types that have less biodiversity (Oliveras & Malhi, 2016).

Population growth, an increase in agriculture, grazing pressure, selling of fuelwood and climate changes can all result in LULC changes and contribute to erosion and consequent land degradation (Blake et al., 2018). Furthermore, something that should be taken into account is the inherently high erodibility of volcanic soils (Mtui, Lepczyk, Chen, Miura & Cox, 2017).

2.2. Remote sensing imagery

2.2.1. Sensors

In remote sensing electromagnetic radiation is used to obtain information about the surface of the earth. It can use a larger part of the electromagnetic field compared to our own eyes, such as near infrared, middle infrared, thermal infrared and microwaves (de Jong et al., 2004). This radiation is detected by satellite sensors. In remote sensing passive and active sensors can be used. Passive instruments detect the reflected and emitted radiation from the earth and active sensors detect information from the earth by providing their own energy (e.g. Radar or Lidar) (Al-doski et al. 2013).

For LULC classification passive satellite sensors are used. There are various types of passive airborne and space-borne sensors that can be used to acquire remote sensing imagery. All these sensors have different spatial, radiometric and temporal resolutions and a different number of spectral bands available. A low or coarse spatial resolution ranges from 30 meters and higher, medium from 2 to 30 meters and high resolution from 0.5 to 2.0 meters (Navulur, 2006). Low resolution imagery can be used to map high levels of LULC classes while lower resolution sensors are able to map more detailed classes. The radiometric resolution refers to the bit size of the imagery and temporal resolution is related to the revisit frequency of the satellite (de Jong et al., 2004). Additionally, the spectral properties of a sensor are of importance. Some sensors have bands ranging from the visible, near infrared to the shortwave infrared while others only capture the visible to near infrared part of the electromagnetic field. Other factors that influence the choice for a certain sensor is that not all imagery is freely available and the timespan a sensor covers, and the swath width can differ. The swath width refers to the area covered by the image.

Landsat sensors by NASA are commonly used for temporal analysis as Landsat TM 4, TM 5 and OLI/TIRS 8 have obtained imagery ranging from 1982 to the present. They have a medium to coarse spatial resolution (30 meters) and higher number of spectral bands available with bands ranging from the visible, to NIR (multispectral) to SWIR. The swath width of Landsat 8, 4 and 5 is 185 which means each scene covers an area of 185 x 185 km (Xie, Sha & Yu, 2008) and they have a temporal resolution of 16 days. Additionally, Landsat 8 has a radiometric resolution of 16-bit and Landsat 4 and 5 of 8-bit.

Sentinel-2 by ESA has a higher spatial resolution of 10 meters. However, even though the satellite is multispectral (MS) and has bands in the shortwave infrared part of the electromagnetic spectrum, not all bands are available in this spatial resolution. In a 10 meter resolution, only the multispectral bands, so the visible and near infrared part of the electromagnetic spectrum can be used (Xie et al., 2008). Another downside of Sentinel-2 for temporal analysis is that the satellite has only been launched in 2015 which means it does not cover as large of a timespan compared to Landsat. Lastly, the radiometric resolution of the sentinel imagery is 12-bit, the temporal resolution 5 days and the swath width is 290 km. Both Landsat and Sentinel are freely accessible.

There are also other sensors available such as Worldview, RapidEye, SPOT, IKANOS or QuickBird. In table 1 the elements relevant for this study of the aforementioned sensors are summarised. MS is short for multispectral (visible to near infrared) and SWIR refers to the short-wave infrared part of the electromagnetic spectrum.

Table 1
Summary of characteristics of some high-resolution satellite sensors

Sensor	Spatial resolution	Sensor bands	Revisit frequency	Radiometric resolution	Data availability	Swath width	Free availability
WorldView-3	1.24m for MS 3.7m for SWIR	8 MS 8 SWIR	4.5 days	11-bits MS 14-bits SWIR	2014-present	13.1 km	Only after project proposal acceptance
RapidEye	5m	5 MS	1 day	12-bits	2008-2020	77 km	Only after project proposal acceptance
SPOT-6&7	6m for MS	4 MS	1 day	12-bits	2012-present	60 km	Only after project proposal acceptance
IKONOS	4m for MS	4 MS	3 days	11-bits	1999-2006	12.2 km	Only after project proposal acceptance
QuickBird	2.6m for MS	4 MS	1-3.5 days	11-bits	2001-2015	16.5 km	Only after project proposal acceptance

One can see some of these sensors have a higher spatial resolution and higher number of spectral bands available compared to Landsat and Sentinel imagery. However, not all of them are as easily accessible and/or have a high data availability. Furthermore, when a swath width is much smaller compared to a study area this means there can be issues encountered in picturing the whole study area at one point in time.

2.2.2. Image pre-processing

Before the satellite imagery can be used to make a LULC classification pre-processing has to take place. In pre-processing noise in the imagery is removed. This step is especially important when multiple images are used for a time-series as it means the images have to be made

compatible with each other. Pre-processing steps include radiometric correction, atmospheric correction, geometric correction, image enhancement and masking of clouds (Xie et al., 2008).

In radiometric calibration errors and distortions of the digital image are corrected and pixels are calibrated. In a value of a pixel not only the reflected and emitted radiation is captured, but also other spectral responses such as scattered radiation by particles in the atmosphere. For the classification only the actual reflection of the surface is needed which is why radiometric correction has to take place (Xie et al., 2008). Furthermore, atmospheric correction should take place as the composition of the atmosphere has an impact on the measured radiance which should be reduced. Geometric correction is performed to remove geometric distortions in images. It is performed by establishing a relationship between the image coordinate system and the geographic coordinate system with the calibration data of the sensor, ground control points, measured data position and altitude. Image enhancement is related to the sharpening of features to make them more interpretable. Lastly, masking of clouds is an important step. Specifically when a larger area is mapped clouds result in noise in the data and have to be removed (Xie et al., 2008).

2.3. Change detection methods

For change detection multiple satellite images at different points in time are used to analyse how the surface has changed between years. The change can be measured in various ways and each method has its own strengths and weaknesses. Some of the most well-known techniques can be divided into pre-classifications and post-classification (Al-doski et al., 2013). In pre- classification techniques the satellite imagery is used directly. The analysis results in a map identifying areas of 'change' and 'no change'. Commonly used are principal component analysis (PCA), Change Vector Analysis (CVA) and image differencing (Lu, Mausel, Brondízio & Moran, 2004). In PCA it is assumed multi-temporal data are highly corelated (Lu et al., 2004). A linear transformation of *n*-bands produces *n* new uncorrelated PC bands which are consequently ordered in terms of the amount of the variance in the image that is explained by the bands. In change analysis it is assumed the band with the highest order represent information that is unchanged between the two dates (Almutairi & Warner, 2010). In image differencing the values of one raster are subtracted from the DN of another raster resulting in a new image indicating the change. CVA is an extension of the image differencing method. It detects all the changes larger than a certain defined threshold. As the direct imagery is used these techniques are accurate and easy to implement. However, when directly using the satellite imagery for change detection there is also more possibility of atmospheric components and sensor differences to have an influence on the outcome compared to post-classification change detection (Al-doski et al., 2013). Additionally, no indication of the specific type of LULC change is provided. A solution for this last issue is to add a LULC classifications to label the pixels the pre-classification technique determined as changed. This method is developed by Pilon, Howarth, Bullock and Adeniyi (1988) (Macleod & Congalton, 1998). Essentially a post-classification technique is applied after the pre-classification in which only the pixels determined as changed are classified.

In post-classification change detection LULC classification maps are generated and compared to each other. This seems to be the most popular technique for change detection (Al-doski et al., 2013). The result of post-classification change detection is a change detection matrix which

demonstrates how much pixels or km2 of each LULC class stayed in the same class or changed to another (Al-doski et al., 2013). In figure 2 an example of a change detection matrix is shown.

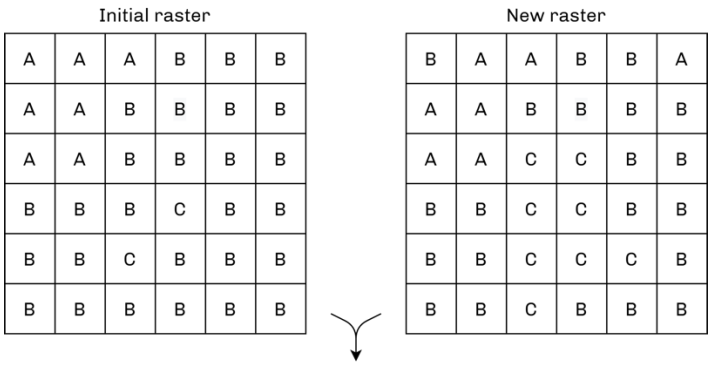

Change detection matrix

New raster \ Initial raster	A	B	C	Total
A	6	1	0	7
B	1	20	0	21
C	0	6	2	8
Total	7	27	2	36
Change	1	7	0	

Figure 2
Example change detection matrix

In this technique there are less issues with atmospheric components and sensor differences (Al-doski, Mansor and Shafri, 2013). However, an important factor in post-classification is that the accuracy of the LULC classifications has a large impact on the results (Civco et al., 2002). Errors in both classifications have an influence on the change detection which is not the case in a pre-classification method (Macleod & Congalton, 1998).

2.4. LULC classification techniques

Since the launch of the first satellite in 1972 various techniques for the interpretation of the obtained imagery have been developed (de Jong et al., 2004). These algorithm-based approaches use the spectral reflectance of the surface within the various parts of the electromagnetic field recorded by the satellite sensor to classify an image. With these techniques it is possible to assign class labels to pixels or objects in an image in order to create a classification, estimate the amount of a certain class such as forests or monitor the classes over time. All these methods use characteristics of the data to detect which LULC class the surface consists off. The elements incorporated by the classifier can be spectral characterises, spatial characterises, temporal characterises or polarization characterises (de Jong et al., 2004).

Not all methods take into account all elements. There are pixel-based image classification techniques and object-based image classification techniques. In a pixel-based technique each pixel is labelled as a certain LULC class. In object-based classification the imagery is segmented into objects before the classification. This means spatial characteristics such as the shape can be taken into account by the classifier. A negative component is that sophisticated parameter tuning is needed during this process. An issue with the use of an object-based approach for a LULC classification is that the size of the segmentation is the same for the whole study area. This means smaller classes can be absorbed because of the segmentation process and the selected scale factor which is not an issue in pixel based methods (Robertson & King, 2011). In this study only pixel-based classification techniques are incorporated.

Remote sensing pixel classification methods can be divided into supervised and unsupervised techniques. In an unsupervised classification it is not necessary to have prior knowledge of the study area while in a supervised classification training samples need to be gathered. This means in an unsupervised classification the data is clustered based on the characteristics of all the data itself (Duda & Canty, 2002), while in a supervised algorithm the spectral characteristics of samples are used. The samples have to be gathered by the researcher. An advantage is that there is control over the collected classes. However, in a supervised classification the quality of the training data has an impact on the accuracy of the classification (Chuvieco & Congalton, 1988). There is always the risk of collecting impure training data which is why an unsupervised classification could possibly be useful as the quality of the training data would have less of an impact. Furthermore, in a supervised classification there may be overlaps between the spectral characteristics of the classes while this would not be the case in an unsupervised classification (Campbell, 2002). However, a downside of an unsupervised classification is that the groups generated by the algorithm and the desired LULC classes might not always overlap.

When applying supervised and unsupervised methods there are various algorithms that can be used. For unsupervised classifications k-means and a variant of k-means called Iterative Self-Organizing Data Analysis (ISODATA) are the most commonly used methods in studies (Li, Zang, Zhang, Li, & Wu, 2014). Regarding supervised methods, a well-tested and more traditional method is maximum likelihood (Brodley & Friedl, 1997). Furthermore various machine learning algorithms have been developed, such as Support Vector Machine, Random Forest, AdaBoost, Naïve Bayes classifier, C4.5, K-nearest Neighbour classifier and logistic (Zhang, Liu, Zhang, & Almpanidis, 2017). In recent years deep learning classification methods have also gained attention (Stoian, Poulain, Inglada, Poughon & Derksen 2019). Specifically Random Forest (Breiman, 2001) and Support Vector Machine (Cortes & Vapnik, 1995) are popular machine learning classification algorithms for LULC classification (Zhang et al., 2017; Li et al., 2014). Support Vector Machine has existed for a longer period of time compared to random forest and is therefore used in more papers, however random forest seems to have a higher average accuracy and demonstrates less variability in LULC classification studies (Sheykhmousa et al., 2020).

2.5. Ground truth sampling techniques

As mentioned, in order to make a supervised classification sample data, also called 'ground truth', is needed to train the classifier. This data is used for both the classification and the validation of the classified map. It is important the samples used are representative of the entire study area

(McRoberts, Tomppo, & Czaplewski, 2014) and should therefore be evenly distributed (Olofsson, Woodcock, Holden, Friedl & Sulla-Menashe 2014). In order to collect the sample data in a proper manner, different sample methods can be used.

The sampling design used determines the way the samples are collected and distributed throughout the study area. Two types of sampling designs can be distinguished called 'probability sampling' or 'subjective sampling'. Subjective sampling means the samples are chosen based on professional judgement to represent all the land use and cover classes (McRoberts et al., 2014). Positive components of this method are that these samples are often accessible and relatively easy to measure. A negative component however is that the samples might not be representative of the total study area. Furthermore the chances of choosing a representative sample are unknown statistically (McRoberts et al., 2014). In probability sampling the samples are chosen objectively. This can be done with simple random sampling, systematic sampling, cluster sampling or stratified sampling (McRoberts et al., 2014). In simple random sampling samples are spread over the research area randomly. This means each location within the study area has an even chance of getting selected. In systematic sampling the study area is divided into a grid and within each grid the chosen samples are located in the middle of the grid. This results into a design where the samples are more evenly distributed as the distance between the samples is maximized. In cluster sampling the samples are clustered together which minimizes costs as it means multiple ground truth samples can be collected in the same location (McRoberts et al., 2014). A fourth method is stratified sampling. In stratified sampling the research area is first divided into groups called strata. Within these strata samples are selected. If these samples are chosen randomly the method is called stratified random sampling (McRoberts et al. 2014). In equalized stratified random sampling the classes also have an equal amount of sampled points. Olofsson et al. (2014) advice to implement a probability sampling design with either a simple random or systematic selection and only choose a method such as clustered sampling when it provides a large costs reduction or if the objectives of the study require clustering.

Next to the sample design the sample size is also an important element. Jensen (2004) states the number of samples has to be equated by 10 times the number of bands that are used. There are also others who argue a similar accuracy can be achieved with a lower amount of samples (Van Niel, McVicar & Datt, 2005). However for some algorithms an increase in samples has a positive influence on the accuracy (Thanh Noi & Kappas 2017). Millard & Richardson (2015) show increasing the sample size for a random forest classification significantly leads to a greater classification accuracy. Furthermore, Olofsson et al. (2014) advices to increase the sample size for rare LULC classes to achieve a similar sample size for each LULC class. Thus, it is important the sample dataset for a classification is large and balanced.

2.6. Validation techniques

An important step after image classification is the validation. Validation can be performed with a visual examination of the map by comparing the classification to the original remote sensing image. This can provide some insights into how well the classified map represents the real world. However, additionally it is important to include a quantitative measurement of the accuracy. In this accuracy assessment the classifications are compared with reference data in order to access the validity (Congalton, 2001).

A validation can be performed with a non-site-specific analysis or a site-specific analysis. In a non-site specific analysis the reference data are statistics that are assumed to be correct (Congalton & Green, 2019). The overall quantities of the different LULC types are compared to the quantities of the reference data. With a non-site-specific analysis one can draw conclusions on which classification is more accurate based on the overall amounts but it not possible to measure which map has a better spatial correspondence. This means a map could be assessed with a high accuracy while the spatial correspondence is actually quite low (Congalton, 2001).

In a site-specific accuracy assessment, the LULC classes in the reference data have a location. The reference data can be a previously classified map, collected from a photo interpretation or ground truth measurements that are assumed to be accurate. With this reference data an error matrix is made. The error matrix demonstrates how effectively pixels were put in the correct LULC class (Congalton, 2001). In figure 3 an example of an error matrix is demonstrated, together with an explanation of the calculation of the descriptive statistics.

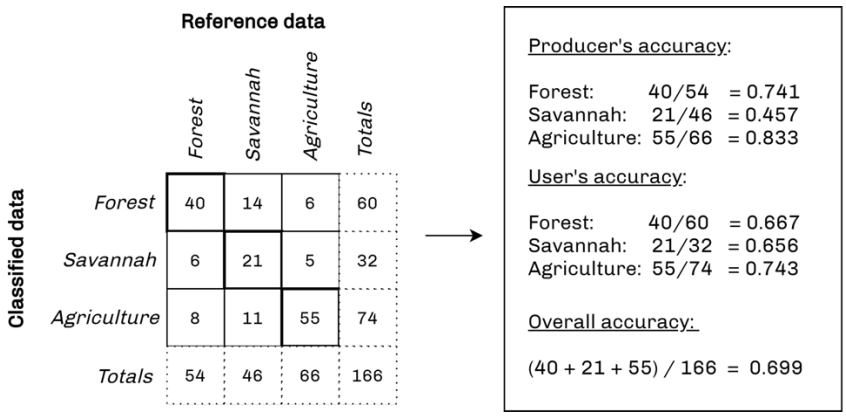

Figure 3
Example of an error matrix
Source: Author, based on Congalton, 2001

The diagonal line in the error matrix shows the correctly classified pixels. From the error matrix the overall accuracy, producer's accuracy and user's accuracy can be calculated. The overall accuracy is calculated by dividing the total correctly classified pixels through the total amount of pixels. The other two statistics are related to the accuracy of the specific LULC classes. For the producer's accuracy the correct pixels are divided by the total number of pixels in the reference data. This is also called the omission error and demonstrates the probability of a real feature to be represented by the correct LULC class on the map. For the user's accuracy the correctly classified pixels are divided by the total number of pixels in the classified data. This is also called the commissions error and shows the probability of a classified pixel in the map to actually demonstrate the correct LULC class (Congalton, 2001).

Another possible assessment of the accuracy of a classification is called the Kappa Coefficient (Cohen, 1960). Kappa can determine if the classified map is significantly better compared to a randomly generated classified map (Congalton, 2001). Including a second accuracy assessment next to the overall accuracy means a more complete conclusion can be provided on which classification is inferior (Congalton, 2001). However, Olofsson et al. (2014) do state the overall accuracy is a better measurement of agreement to report on in regard to the accuracy of a land surface change map. The values of the Kappa statistic range from 1 to -1. However the value

should always be higher than 0 as there is always a positive relationship between the classification and reference data (Congalton, 2001). A value higher than 0.80 can be regarded as a strong agreement between the classification and the reference data, a value between 0.40 and 0.80 as moderate and a value below 0.40 as poor according to Landis & Koch (1977).

An important element here is that the validation samples used in the error matrix are independent from the training samples and the data is randomly sampled across the training and validation as otherwise there is an optimistic bias in the results (Millard & Richardson 2015). It is also important enough samples are used for the reference data. Story & Congalton (1986) advice to use at least 30 inputs per class to make the error matrix. In the study by van den Bergh (2016) and Verhoeve (2019) 20% of the ground truth is used for the accuracy assessment and 80% for training.

2.7. Challenges in LULC classifications with remote sensing

Remote sensing makes the classification of land use and land cover over large areas much more efficient. However, Verhoeve (2019) demonstrated there can be complications encountered. The issues in remote sensing classifications of semi-arid regions stem from various components. To begin with often low to medium spatial resolution sensors such as Landsat are used. In western countries agricultural areas are often made up of large heterogeneous areas which makes it possible to detect the fields with a lower resolution sensor. However, in Africa agriculture frequently consists of small heterogenous systems where the crops are cultivated and the fields are spread out across space, irregular in their shape and can be very small (Burke & Lobell, 2017). Furthermore, large areas are intercropped (Bayala et al., 2015) and often shrubs or trees are integrated within the fields which proposes further complications for traditional remote sensing (Bégué et al., 2018). The launch of Sentinel-2 in 2015 opens up possibilities to accurately map agricultural fields in these areas as a result of the higher spatial resolution of the sensor (Karlson et al., 2020). A downside is however that some information is lost compared to the use of Landsat imagery because of the lower number of spectral bands available. As demonstrated in table 1 there are sensors with a high spatial resolution and high number of spectral bands. However, these sensors often have a low swath width.

Another issue is that in traditional remote sensing classifications pixels can only be assigned to one class which means the result is a categorical map with crisp boundaries. This means the map is easy to read. However, this is not always an identical representation of the real landscape (Feilhauer et al., 2020). In savannah landscapes there are natural transition zones between ecological systems such as woody savannah and forest. These transition zones propose difficulties for mapping the surface as the boundaries are not always clear cut but can appear as fuzzy. A solution could be to add a continuous classification approach (Stuart, Barratt & Place, 2006) or a fuzzy classification (Feilhauer et al., 2020; Xu, Watanachaturaporn, Varshney & Arora, 2005). A positive component of fuzzy classifications is that it contains more information (Feilhauer et al., 2020). However, a negative aspect of these methods is that the results are more difficult to present (Xie et al., 2008) and more difficult to apply a change detection analysis on.

Next to difficulties with mapping transition zones it is quite common vegetation types which seem the same in the field have different spectral features in the image. Additionally, sometimes

different vegetation types have the same spectral signatures which makes them difficult to distinguish regardless of the method used (Xie et al., 2008). Meerman & Sabido (2001) found multiple savannah cover types, that can be distinguished by the amount of grasses or trees, that have similar spectral properties and are difficult to separate consistently (Stuart et al., 2006). To improve the accuracy of classifications of areas that are more homogeneous it is advised to use synthetic methods, which refers to the use of other data in combination with the satellite imagery (Lillesand & Kiefer, 2015). All types of ancillary data, or indexes derived from the satellite imagery can be used to increase the classification. Eiumnoh & Shrestha (2000) demonstrate incorporating a Digital Elevation Model (DEM) and Normalized Difference Vegetation Index (NDVI), made by combing the red and NIR band, improved the classification accuracy with 10% to 20% in a tropical wet-dry landscape in Thailand.

Furthermore, there are large differences in the spectral reflectance of green, photosynthetically active and dry, non-photosynthetically active vegetation which proposes complications in semi-arid climates. In figure 4 the spectral signatures of green vegetation, dry vegetation and soil are shown.

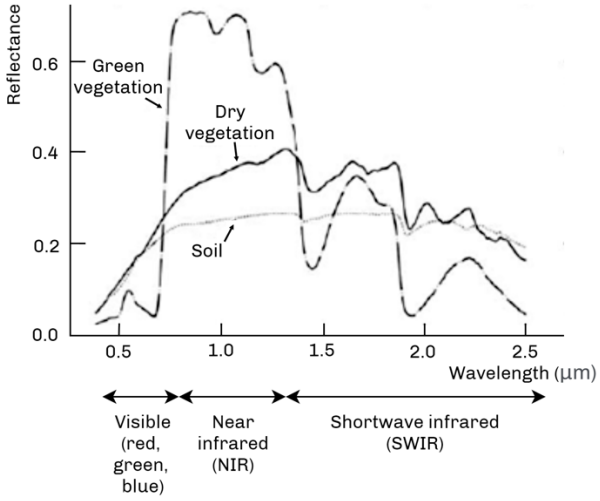

Figure 4:
Illustration of spectral signatures of soil and dry and green vegetation
Source: Adjusted figure of Maisongrande et al., 2007

Green vegetation has a relatively low reflectance in the visible part of the electromagnetic field because the light is absorbed by the pigment in the leaves. Furthermore in the blue and red part of the spectrum chlorophyll absorbs even more light, which is why healthy vegetation looks green to the human eye (Huerte, 2004). This process is not happening in dry vegetation because the vegetation is not photosynthetically active (Xie et al., 2008), which results in dry vegetation to look more similar to soil in the visible part of the spectrum. In the near infrared part reflection of healthy vegetation is much higher compared to the visible part because of the cell structure. The reflection of non-photosynthetically active vegetation is lower here compared to green vegetation. The shortwave infrared wavelength is related to water content. Shortwave infrared light is absorbed by water around 1.4 nm, 1.9 nm and 2.4 nm which is why the spectral signature of the green vegetation shows dips around these wavelengths. The more water present in an object the lower the reflection, and the darker an object will look in the SWIR bands (Observing in infrared, 2014). This means that when there has been a lot of precipitation vegetation can be classified in a very different way compared to a dryer period. To avoid differences in phenology to have a

large impact on classification results in a timeseries images from the same season should be chosen according to Clark & Pellikka (2009). When there is a summer and winter period this is relatively easy. However, in arid climates there is more fluctuation in seasons and rain patterns which makes choosing images with a similar phenology more complicated.

2.8. Previously conducted remote sensing studies

In order to measure the exact amounts of LULC changes in Monduli there have been several remote sensing studies performed on Landsat imagery, such as the study by Kiunsi & Meadows (2006), van den Bergh (2016), Mtui et al. (2017) and Verhoeve (2019).

The study by Kiunsi & Meadows (2006) used 1960, 1991 and 1999 Landsat imagery and demonstrated semi-natural vegetation decreased from 90% in 1960 to 76% in 1991 to 75% in 1999 while agriculture increased from 1% in 1960 to 20% in 1991 and decreased in 1999 to 17%. Bare land increased from 0% in 1960, to 1% in 1991 to 3% in 1999, and water bodies increased from 3% in 1960 and 1991 to 5% in 1999. The ground truth used to train the classifier has been collected by drawing polygons on the satellite imagery and validating the classes in the field. The study is not clear on which supervised classification method is used and does not specify the accuracy of the classifications or demonstrate the classifications (Kiunsi & Meadows, 2006).

The study by van den Bergh (2016) analysed changes from 1985 to 2016 with a maximum likelihood classification on two Landsat images with 7 classes, namely grassland, savannah, forest, agriculture, bare soil, urban and water. Van den Bergh (2016) demonstrated urban areas increased from 0.01% to 0.07%, agricultural areas increased from 2.73% to 5.15%, base soil increased from 12.17% to 17.90%, water increased from 3.88% to 6.09%, forests increased from 2.99% to 4.83%. The amount of grassland decreased from 13.21% to 7.44% and savannah decreased a little bit as well from 59.69% to 55.95%. Furthermore, van den Bergh (2016) showed forests increased from 3.36% to 4.62% from 1985 to 2016. The accuracy reached for the 2016 classification by van den Bergh (2016) is 93.5% based on 20% of the ground truth data used for validation. The urban class has been manually added. There is no description of the sampling method used. Furthermore, there is no accuracy report on the 1985 classification which suggests the classifier of 2016 is used on the 1985 imagery. Additionally, it is stated the images are not atmospherically corrected before classification which is necessary when classifying a timeseries. When analysing the classification manually there are already some indications the classification of 1985 could be less accurate. In figure 5 a part of the classification is visualised next to the satellite image.

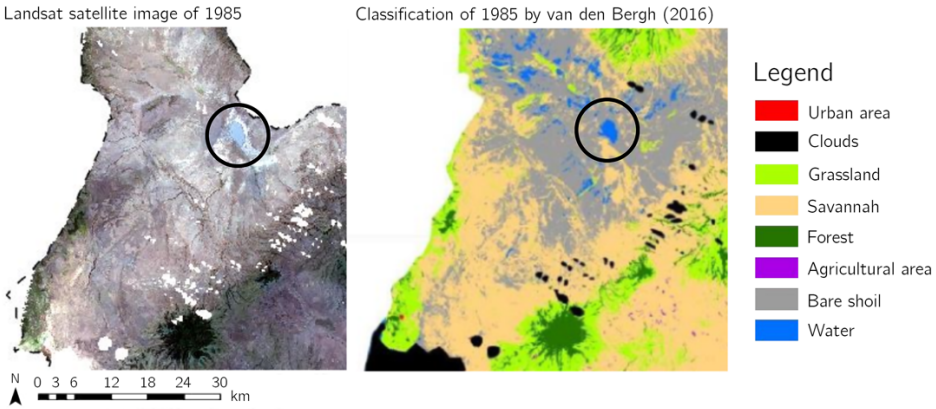

Figure 5

Comparison of part of classification of 1985 by van den Bergh (2016) and Landsat 4 satellite imagery

In the circle a lake can be observed. In the classification by van den Bergh (2016) a large part around the lake is classified as water while one can conclude this is not actually the case through a comparison with the satellite imagery. The predicted lower accuracy of the 1985 classification is possibly a result of the application of the classifier trained on a satellite image of 2016 on an image of 1985, without atmospherically correcting the images.

Mtui et al. (2017) did not directly study Monduli, but landscape changes from 1988 to 2009 and 2011 in a wildlife protected area which neighbours Monduli called Tangarine National park. Tangarine national park is situated on the south-east side of lake Manyana, just outside of the study area. This study also used a maximum likelihood classification on Landsat imagery and derived eight classes, namely woody savannah, savannah, grassland, open and closed shrubland, swamp, water and bare land. They demonstrated an increase in barren land and swamps in and outside the park and a decline in woody savannah as woody savannah had been turned into grassland and barren land. To train the classifier a ground truth dataset consisting of 59 polygons for Tangarine national park, collected in the field in 2012 was used, together with high resolution satellite imagery (SPOT and Geoeye). The ground truth was adjusted based on the high-resolution sensors of 2009 and 2011. The overall accuracy of the classifications of 2009 is 86.8% and 2011 is 84.6%. The accuracy of 2009 has been calculated with the use of a random sample of 1500 points generated and overlaid with the SPOT and/or GeoEye imagery. Only 22 points were located on the imagery of 2009 which meant 98.5% of the validation points were left out. For 2011 a similar method was used.

Verhoeve (2019) classified 32 images from 1985 to 2019 to analyse the LULC change in Monduli. The final maps contained the following classes: Forest, savannah, grass, agriculture, bare, water and urban. Verhoeve (2019) detected big unrealistic fluctuations in land cover such as forested areas between years which cannot be possible and do not correspond to the satellite imagery. This also resulted into doubts about other studies that used less images. Verhoeve (2019) does reach an overall accuracy of 96% for the classification of 2019, with 20% of the ground truth used for validation. However, 20% of the total amount of pixels is sampled, instead of 20% of the ground truth polygons collected which means the training data and samples are not completely independent of each other. This can result in a large positive bias and could be an explanation for the high overall accuracy, but low accuracy from the visual validation. Similar to van den Bergh (2016) Verhoeve (2019) also seems to use the trained classifier of 2019 on the other images, without training the classifier separately for each year. The same issues with the

classification of water encountered by van den Bergh (2016) are present in the classification of 1985 by Verhoeve (2019).

These studies did not add a change detection analysis but do compare the LULC quantities and distributions of multiple classifications. They show urban, agriculture and bare soil and water increased. However, they do not all paint a similar picture of the specific LULC change and there are questions about the accuracy of the results.

3. Methods and data

3.2. Satellite data collection and pre-processing

3.1.1 Sensors

Both Landsat TM and ALI/TIRS, and Sentinel 2 satellite imagery are incorporated in this study. Landsat has covered a large timespan which makes the imagery useful for a timeseries, the spatial resolution of Landsat is relatively low, however the number of spectral bands available is high. Sentinel offers a higher spatial resolution but with a lower number of spectral bands available and lower timespan. Satellite sensors such as worldview-3 have a higher spatial and higher number of spectral bands compared to Sentinel. However, the swath of the scene's is 'only' 13.1 km and the imagery are not as easily accessible. Landsat and Sentinel have a large enough swath width to cover the research area by combining two images and can be easily accessed.

The ground truth used has been collected in February. To avoid making conclusion based on phenology as much as possible images within the same season as the collected ground truth should be chosen. February is at the end of the short dry period and beginning of the rainy season. In order to choose images with a phenology as close to each other as possible images from January, to March are chosen.

To do a temporal analysis at least two images at different points in time have to be used. Using two to three images like other studies did in the same area (Msoffe et al., 2011; van den Bergh, 2016) could mean there is a possibility of drawing false conclusions (Verhoeve, 2019), which is why in this study multiple images are chosen for the analysis. Furthermore, only images with less than 10% cloud cover will be used. If there are multiple images within the same month the one with the lowest cloud cover score is chosen. Sometimes the 10% estimate of cloud score can be too low, which means when examining the image there is a very large part of the study area covered, in these cases the images also will not be used.

For the Landsat imagery the largest part of the study area is located within 2 Landsat tiles, namely path 168, row 62 and row 63. Imagery will be used from the Landsat Thematic Mapper (TM) 5 and 4, and the Landsat Operational Land Imager (OLI) 8. In table 2 the imagery suited for the study is summarized. For the Landsat classification the blue, green, red, NIR, SWIR 1 and SWIR 2 bands will be used.

Table 2
Landsat imagery

#	*Date*	*Satellite*	*Cloud cover %*
1	18 January 1985	Landsat 5 TM	1.31
2	25 February 1987	Landsat 5 TM	3.26
3	17 February 1993	Landsat 4 TM	4.43
6	3 February 2014	Landsat 8 OLI/TIRS	0.89
8	10 March 2015	Landsat 8 OLI/TIRS	1.21
11	28 March 2016	Landsat 8 OLI/TIRS	1.7
15	29 January 2018	Landsat 8 OLI/TIRS	1.76
18	21 March 2019	Landsat 8 OLI/TIRS	1.48

For Sentinel the study area is located within tile numbers T36MZB and T36MZA. The data is available from 2016 to 2019. For each year one image is selected. For Sentinel band 2 (blue), band 3 (green), 4 (red) and 8 (NIR) are available in a 10-meter spatial resolution. In table 3 the suitable imagery is demonstrated.

Table 3
Sentinel imagery

#	*Date*	*Satellite*	*Cloud cover %*
1	3 February 2016	Sentine-2A	0.16
2	8 February 2017	Sentine-2A	2.90
4	24 January 2018	Sentine-2A	0.42
9	20 March 2019	Sentine-2A	0.18

The underlined imagery in figure 6 will be used to apply each classification method on in order to answer the first research questions, the other imagery will only be used to answer the firth research question.

Figure 6
Timeframe of the study area with the used imagery

Sentinel is available in a higher spatial resolution compared to Landsat. However, Landsat has a higher number of spectral bands. Additionally, what can be observed in figure 6 is that Landsat covers a much larger timespan. Something worth noting is the large gap between 2014 and 1993 and 1987 as a result of data (un)availability. This can be explained by the temporal resolution of 16 days of Landsat. This means there is a lower chance of capturing a cloud free image, compared to Sentinel which has a temporal resolution of 5 days. Furthermore, only images around February are picked in this study. During this timeframe there is a relatively high chance of cloud cover as a result of precipitation patterns.

3.1.2. Pre-processing

The Landsat imagery is available as a level 2 product which means they are already geometrically, radiometrically and atmospherically corrected ("Landsat Collection 2: Level 2 Science Products",

n.d.). Sentinel data can be atmospherically corrected with the Sen2Cor processor ("Sen2Cor", n.d.). However, recently Sentinel-2 is also available as a level 2 product ("Level-2", n.d.). This means during the pre-processing steps only the clouds have to be filtered out and the tiles have to be mosaiced.

3.3. Ancillary and derivative data

As explained previously incorporating ancillary data can improve the quality of an image classification. Commonly used are a digital elevation model (DEM) and the normalized difference vegetation index (NDVI). In this study the DEM originating from the Shuttle Radar Topography Mission (SRTM) is used. From the digital elevation the elevation and slope can be derived.

NDVI is an indicator of the density of vegetation. The denser the vegetation in an area the higher the value (Lillesand & Kiefer, 2015). The NDVI uses the near infrared (NIR) and the red band of the sensors. The formula of the NDVI is demonstrated below:

$$NDVI = \frac{(\mathrm{NIR} - \mathrm{Red})}{(\mathrm{NIR} + \mathrm{Red})}$$

In figure 5 it has been demonstrated in the paper by van den Bergh (2016) a large part in the north side of the study area around a small lake is classified as water, while through a visual interpretation it becomes apparent this is not the case in reality. Although in a lesser capacity, in this study this issue has also been encountered. An explanation could be that the lakes in the study area are relatively shallow which means the reflection of the vegetation underneath the water is also detected. This is why for the Landsat imagery the Moisture Stress index (MSI) (Rock, Vogelmann, Williams, Vogelmann and Hoshizaki, 1986) is added. This is an index designed to measure levels of moisture stress in vegetation but can also increase the ability of the classifier to identify water in the study area. A higher value of the index means a higher plant water stress and thus less soil moisture content. This index can potentially also be of use to distinguish other LULC classes in Monduli. Forests have a very different moisture index compared to savannah so adding this index could have a positive impact on ability of the classifier to classify forest transition zones correctly. The MSI uses the near infrared (NIR) and the mid-infrared band (MidIR). This means this index can only be used for the Landsat classifications as a mid-infrared band is not available in a 10-meter resolution for Sentinel. For landsat the MidIR band used is SWIR 1. The formula of the MSI is demonstrated below:

$$MSI = \frac{\mathrm{MidIR}}{\mathrm{NIR}}$$

3.4. Change detection method

In this study the post-classification change detection technique is used. Post-classification minimises issues with atmospheric and sensor differences, and seems to be the most popular

change detection technique (Al-doski et al. 2013). With this method multiple classified images are compared to each other. As the accuracy of the classifications has a large influence on the change detection only the imagery with the highest accuracy is used for this step.

In figure 7 the process from an imagery layer stack to the end result of the change detection is demonstrated.

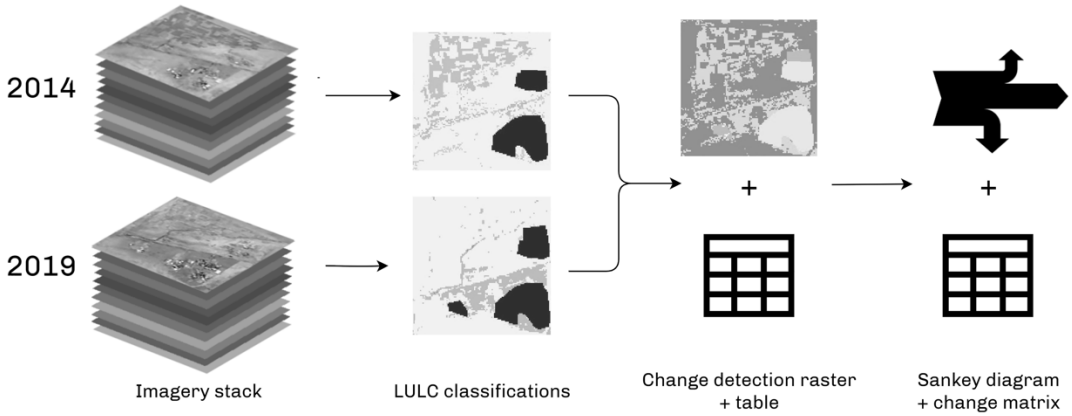

Figure 7
Post classification change detection process

First LULC classifications are created from the imagery stacks. Subsequently, the classified rasters are compared to each other which results in a change detection raster and corresponding table. This raster can be difficult to visualize as there are around 160 classes indicating how a pixel has changed from one LULC class to another. However, the corresponding table can be used to create a Sankey diagram, and change detection matrix. The sankey diagram is a stream diagram and visualizes how LULC classes change between years in a clear way.

3.5. Classification methods

In this study only pixel based classification techniques are incorporated as with this method there are no issues with the absorption of smaller classes because of the segmentation process and the selected scale factor (Robertson & King, 2011). Two more traditional classification methods are used, the unsupervised guided clustering ISODATA and supervised maximum likelihood algorithm, and the newer machine learning classification method random forest. Random forest is one of the most popular machine learning techniques and has demonstrated high accuracies can be achieved (Sheykhmousa et al. 2020).

3.5.1. ISODATA

As mentioned, in this study for the unsupervised classifications a guided clustering method with ISODATA (Iterative Self-Organizing Data Analysis Technique Algorithm) is used. A guided method can potentially achieve a more accurate classification compared to what could be achieved by a pure unsupervised method (Reese et al., 2002). ISODATA calculates class means and clusters pixels by using the least distance. After each iteration means are recalculated and pixels are reclassified which means the amount of pixels is adjusted automatically (Abbas, Minallh, Ahmad, Abid & Khan 2016).

In this method the numbers of clusters created has to be determined by the user. First ISODATA is ran over the satellite imagery with a number of classes around three times the size of the number of classes in the ground truth dataset. Subsequently, the resulting clusters are grouped into the LULC classes of the ground truth dataset. The classes are visually identified with the use of high-quality satellite data (0.5 meter) together with the Landsat and Sentinel data.

3.5.2. Maximum likelihood

In a maximum likelihood technique, the spectral reflectance of the pixels in the different bands is used to classify the pixels in the imagery. Maximum likelihood is a parametric classification method. It assumes the statistics of each class in each band are normally distributed. The probability of pixels belonging to a certain class is calculated and each pixels will be assigned to the class with the highest probability (Lein, 2011). The probability density functions are made on the basis of the spectral signatures of the LULC classes of the training samples (Lillesand & Kiefer, 2015). This process is demonstrated in figure 8. The striped circles refer to the probability contours.

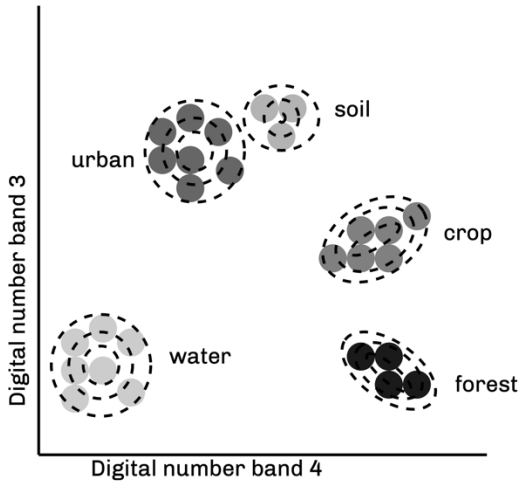

Figure 8
Demonstration of maximum likelihood classification
Source: Author, based on Lillesand & Kiefer, 2015

3.5.3. Random forest

Random forest is a machine learning algorithm invented by Breiman (2001). It processes many decision trees by continuously taking subsets of the input data and of the input bands to determine where to split and start a new tree. This results in a large group of decision trees to determine the final output (Breiman, 2001). Decision trees have some advantages over more traditional techniques such as maximum likelihood as they do not require assumptions in regard to the distribution of the sample data and they are strictly nonparametric (Brodley & Friedl, 1997). In random forest randomness is added which means the tree is split with the use of a subset of predictors that is chosen randomly, and the tree is made using a random feature selection. Random forest is computationally relatively fast, has less issues with overfitting compared to other models, and is not as sensitive to noise which makes it a robust model (Breiman, 2001). In figure 9 the process of the random forest algorithm is visualized.

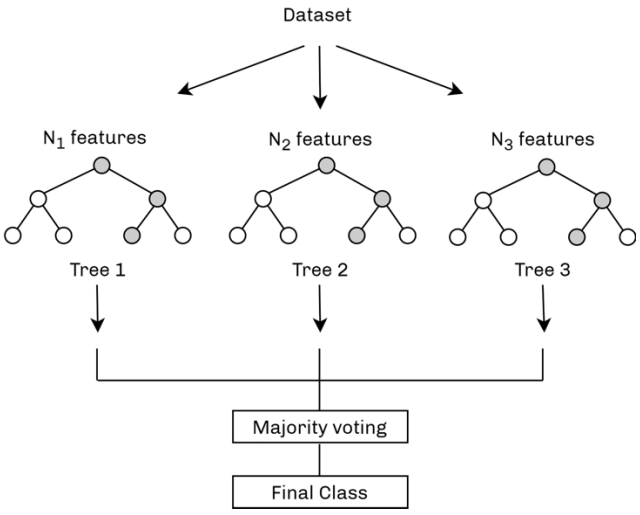

Figure 9
Simplified visualization of Random forest algorithm
Source: Author, based on Dimitriadis & Liparas, 2018

When using random trees two parameters will have to be defined. These are the number of trees and the number of features in the splits of the trees. Breiman (2002) states setting the feature of splits equal to the square root of the total number of features gives the best result. Regarding to the number of trees Liaw & Wiener (2002) argue more trees result in a better outcome of variable importance and proximity. According to Breiman (2001) using a large number of trees can be unnecessary. However, using more trees than required does not harm the model. Thanh Noi & Kappas (2017) recommend using 500 trees with a split of 2, 3 or 4. This is also the number used in this study.

3.6. Selection of training samples

There are various sampling designs that can be adopted. A probability sampling design can be viewed upon as better practice compared to a subjective sampling design. However, a difficult component in sampling ground truth is that the sample units in some probability sampling designs can be distributed in a certain way through space while observations are influenced by the accessibility of the surface and are often close to each other (McRoberts et al., 2014).

The ground truth dataset has been collected by Verhoeve (2019) in February 2019. The polygons in the dataset have been collected based on the classification made by van den Bergh (2016) which means areas for sampling are chosen based on previously defined strata. However, as some areas are difficult to access no objective sampling design has been chosen.

The original dataset consists of 90 polygons, shown in table 4 and figure 10. The class 'urban' has been removed as the classifiers had some difficulty with disguising this class. The urban areas in moduli are relatively small which means they can be added manually.

Class	*Amount*
Grassland	20
Barren	14
Woody Savannah	14
Agriculture	13
Savannah	12
Open Shrubland	7
Forest	4
Water	3
Closed Shrubland	3
Total	90

Table 4
Ground truth polygons per class in original dataset

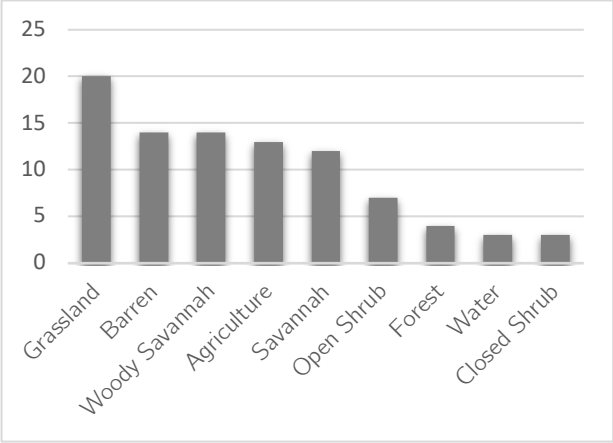

Figure 10
Ground truth polygons per class in original dataset

In table 4 and figure 10 it can be observed for some classes very little ground truth has been collected. As mentioned in earlier chapters an increase in ground truth has a positive influence on the accuracy of classifiers such as random forest (Thanh Noi & Kappas, 2017; Millard & Richardson, 2014). Thus, for this study extra ground truth is collected. The extra polygons are added with the help of Vivid, a high resolution (0.5 meters) satellite data image layer, made of imagery ranging from 2010 to 2018. This imagery layer is used as a reference in combination with Landsat and Sentinel imagery.

Next to a small number of samples collected, the samples in the original dataset are mostly concentrated on the west side of the study area which means the samples are not evenly distributed. It is important the collected samples used for the classification are evenly distributed (Olofsson et al., 2014). Only polygons are added of which the LULC class can be known by looking at the satellite imagery and previously collected samples as it is not possible to verify the classes in the field. This means no objective sampling is used. However, the new polygons are added throughout the whole study area instead of only in the west site in order to make the distribution more equal. Previously defined strata are also taken into account which means for example that for the forest class a large part of the samples are concentrated around the mountains in the middle of the study area as this is where forests are primarily located.

The new dataset consists of 343 polygons, shown in table 5 and figure 11. In figure 11 in darker grey the number of samples in the original dataset are shown. For some classes a larger number of new polygons are collected compared to others as for these classes it has been easier to identify areas from the satellite imagery.

Class	*Amount*
Grassland	38
Barren	38
Woody Savannah	64
Agriculture	47
Savannah	46
Open Shrubland	18
Forest	37
Water	35
Closed Shrubland	20
Total	343

Table 5
Ground truth polygons per class in adjusted dataset

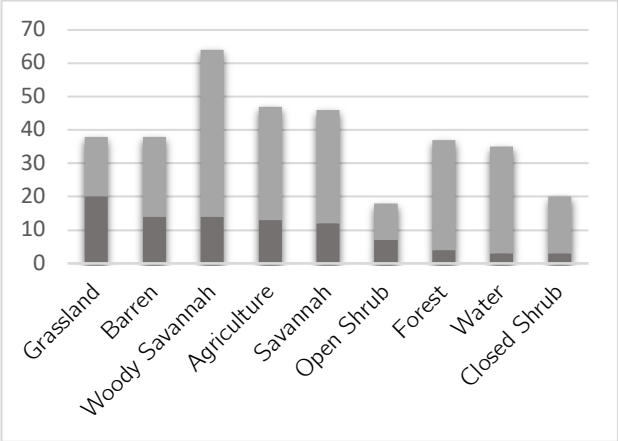

Figure 11
Ground truth polygons per class in adjusted dataset

In figure 12 the location of the original dataset and location of the added samples are visualized.

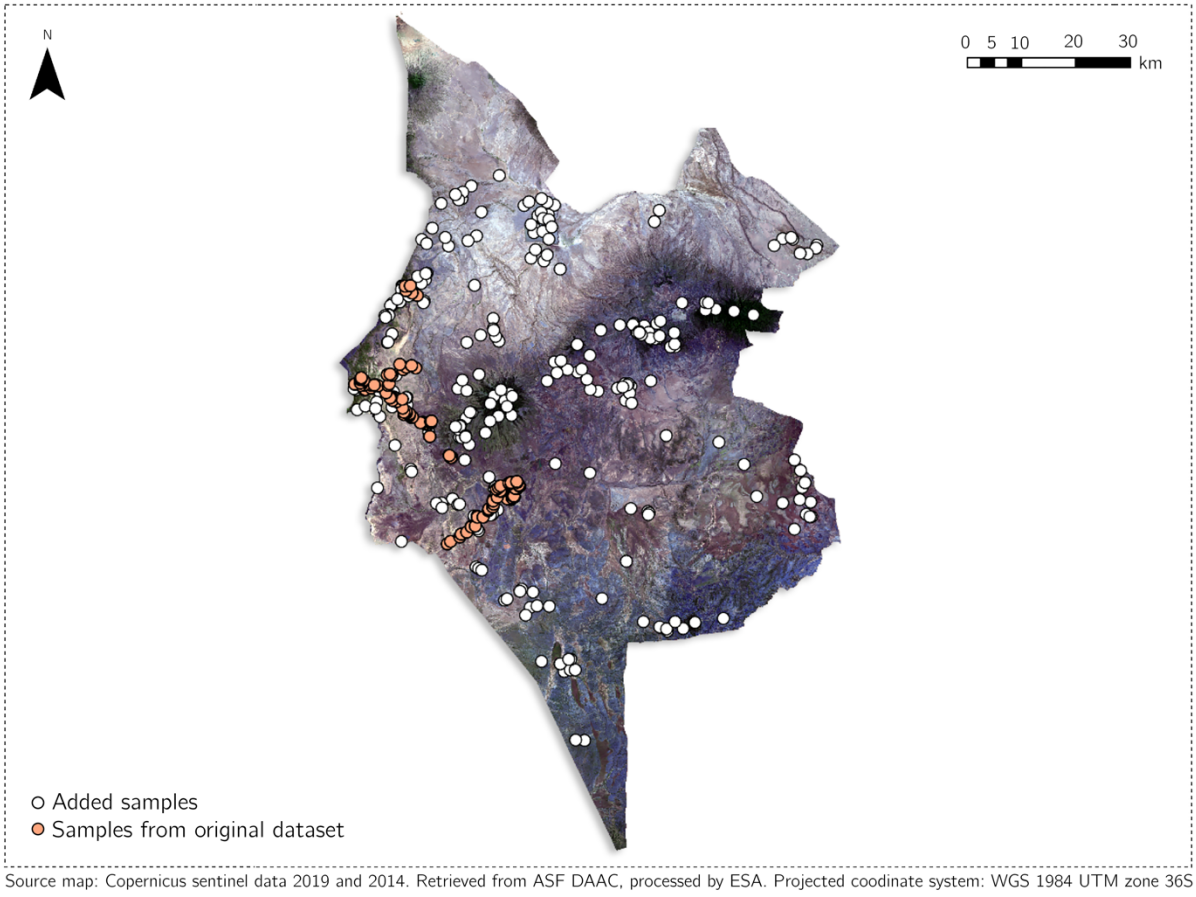

Figure 12
Location of the samples of the two datasets

The new dataset contains more polygons and is more balanced. However, as for some classes more samples are collected compared to others there is still some imbalance. To balance out the dataset and increase the inputs for the classifiers further, points are collected within the polygons

with the use of equalized stratified random sampling. In the classifiers the means of spectral reflectance of the polygons are used, so if 30 polygons are incorporated for a LULC class which contain 3000 pixels, in reality only 30 inputs are used. By sampling random points within the polygons, the amount of ground truth samples used by the classifier can be increased. As the result of some trial and error 3000 points per class have has been chosen to train the classifier as this resulted in the highest accuracy while keeping computation time relatively low. By using equalized stratified random sampling this means each class gets an equal number of points, so the dataset is balanced out.

In previously conducted studies in Monduli (van den Bergh 2016; Verhoeve 2019) the collected ground truth dataset has been used to train the classifier. This classifier has subsequently been applied on all the available imagery. This means the classifier is trained on a different image as it is applied on. With this method differences in atmospheric effects and radiometric characterises of the images have an influence on the outcome of the classification. In this study for each year incorporated in the study the classifier is trained separately to avoid these factors to influence the results. This means the ground truth dataset is adjusted for each year to match the imagery.

3.7. Accuracy assessment

By calculating similar accuracy values for the classifications, it is possible to compare the three methods and use the classifications with the highest accuracy values for the change detection. For the validation of the classifications only a site-specific method is applied as there are not yet any (to be assumed) correct statistical estimates of the quantities of the LULC classes to use for a non-site-specific analysis. As mentioned, it is important the data used as a reference for the error matrix is independent of the data used for the classification. In this study 20% of the ground truth is kept separate from the training data to be used as validation data for the supervised methods. For the sampling of the validation data stratified random sampling is used after which random points are sampled with equalized stratified random sampling. In figure 13 the location of the validation and training samples are visualised

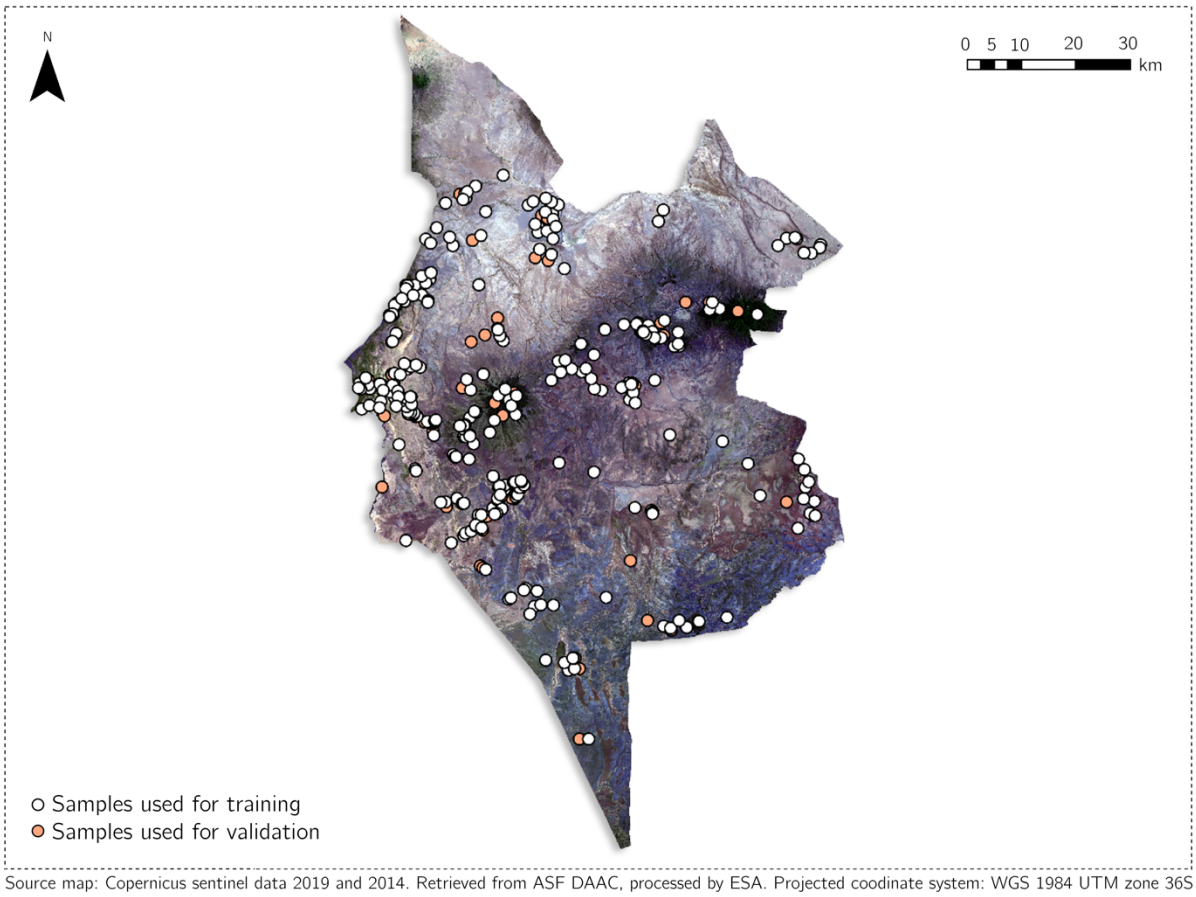

Source map: Copernicus sentinel data 2019 and 2014. Retrieved from ASF DAAC, processed by ESA. Projected coodinate system: WGS 1984 UTM zone 36S

Figure 13
Location of the validation and training samples

For the unsupervised classification 100% of the ground truth samples can be used for validation. In the error matrix of the site-specific validation method the urban class is not included as this class has been added manually.

3.8. Software programs

In this study two GIS software programs are used: ArcGIS PRO and Erdas Imagine. The models used in this study are shown in appendix K. First the clouds have been filtered out, the bands are stacked, and all bands and ancillary data are converted to the same bit size in ArcGIS PRO. Next all the data is stacked in Erdas Imagine (see appendix K1). Both the classification of the imagery in Erdas Imagine and ArcGIS PRO have been explored. In appendix K4 a model to classify the images with a random forest classifier in Erdas Imagine is demonstrated. The MSI has not been added yet here. In Erdas Imagine it is possible to use a random, an equalized random or a stratified random method to sample points within the polygons. With random sampling points are generated randomly and in equalized random sampling it would be possible to sample random points within each feature. Thus, in equalised random sampling it is, for example, possible to collect 30 points within each polygon. This increases the inputs for the classifier but does not balance out the classes. With a stratified random method points are proportionally distributed for each class. However, not necessarily all polygons are included in the sampling. In the final classifications in

this study ArcGIS PRO is used in which the points are generated with an equalized stratified random sampling method. This means the inputs are increased, and an equal number of points is generated for each class. All polygons have been included in the sampling. See appendix K2 and K3 for an illustration of the model and the python script.

3.9. Workflow of the study

In figure 14 the workflow of the study is visualized in a flow chart. The workflow consists of the following steps: 1) data collection and pre-processing, 2) selection of training samples, 3) image classification, 4) accuracy assessment, 5) classification of all the images with the most accurate method, and 6) change detection. In the flow diagram the colours refer to the research questions.

In step 1 the Landsat imagery, Sentinel imagery and ancillary data (SRTM) are collected and derivative data (Slope, NDVI and MSI) are calculated. This data is then pre-processed which includes mosaicking the tiles, filtering out the clouds, converting all the data to the same bit size and stacking the different bands and ancillary and derivative data. In step 2 the dataset collected by Verhoeve (2019) is acquired and the ground truth is improved. The dataset is cut in two parts, one for validation and one for training. For both datasets random points are collected. In step 3 the images are classified. First an unsupervised ISODATA classification is performed to answer RQ1, then a maximum likelihood classification follows to answer RQ2, and lastly random forest is applied to answer RQ3. In step 4 an accuracy assessment follows, and the accuracy and classification results are compared. This will be repeated for both Sentinel and Landsat to answer RQ4. In step 5 the most accurate method is applied on all satellite imagery and the accuracy of the classifications is calculated. Lastly, in step 6 change detection is performed on the most accurate classifications. These last steps are performed to answer RQ5.

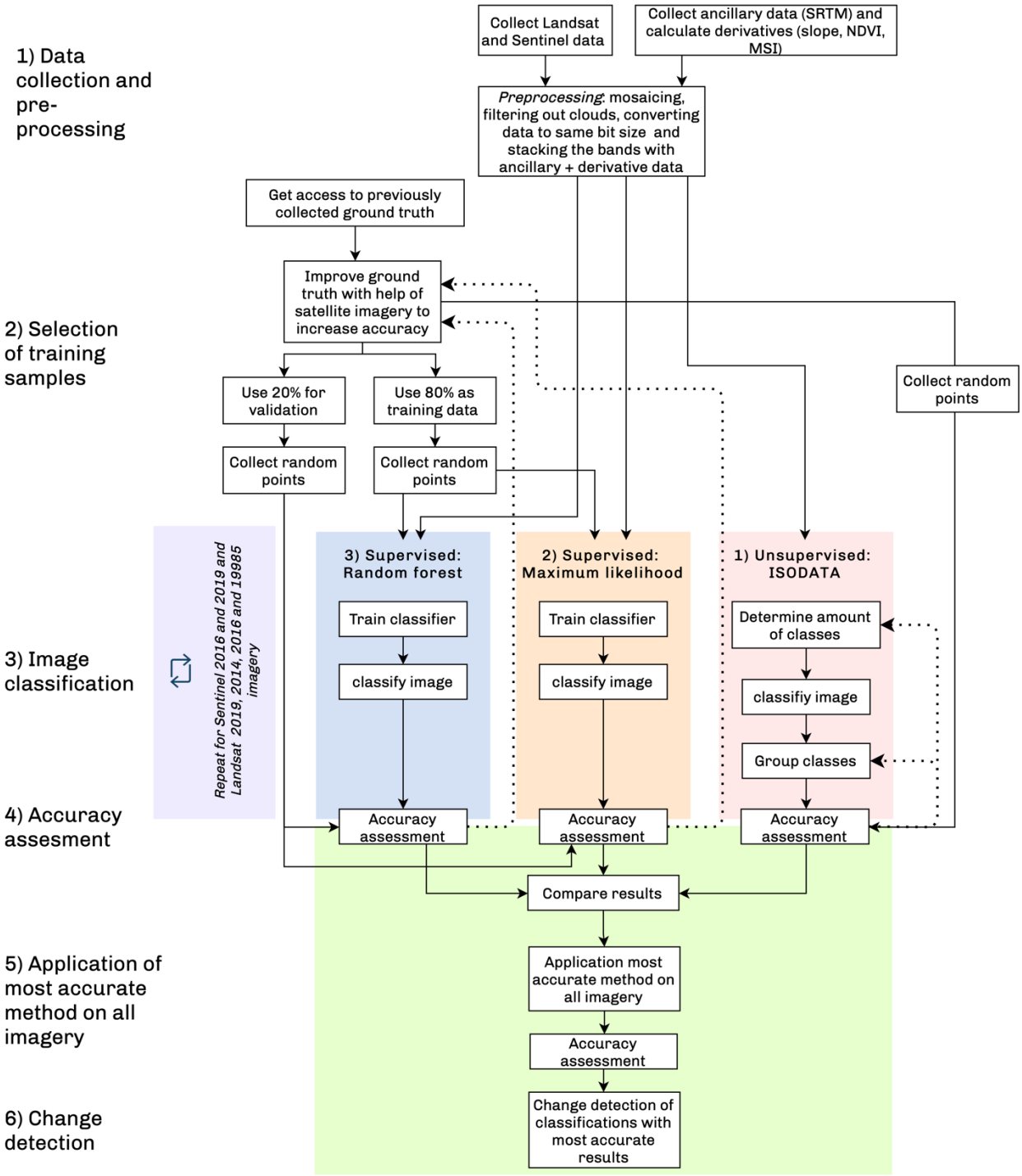

RQ1: How is the Land use and Cover (LULC) classified in Monduli with the use of an unsupervised ISODATA classification method?
RQ2: How is the Land use and Cover (LULC) classified in Monduli with the use of an supervised maximum likelihood classification method?
RQ3: How is the Land use and Cover (LULC) classified in Monduli with the use of an supervised random forest classification method
RQ4: How do the outcomes of the classifications of Landsat imagery compare to Sentinel imagery?
RQ5: How does the land use and cover in Monduli change over multiple years from 1985 to 2019 with the best suited method and imagery?

Figure 14
Workflow of the study

4. Study area

4.1. General description of the study area

The study area is situated in Tanzania, Eastern Africa. Tanzania is divided into 31 regions and 169 districts. Monduli district is located in the Arusha Region in the northern part of the country. The area is just under 7000 km2 in size and in 2012 the population was set at 158,929 people. The average yearly population growth in Arusha is 2.7%, which would mean the population in Monduli can be roughly estimated at around 192,717 in 2019 (National Bureau of Statistics, 2016). In figure 15 the location of the study area is visualized.

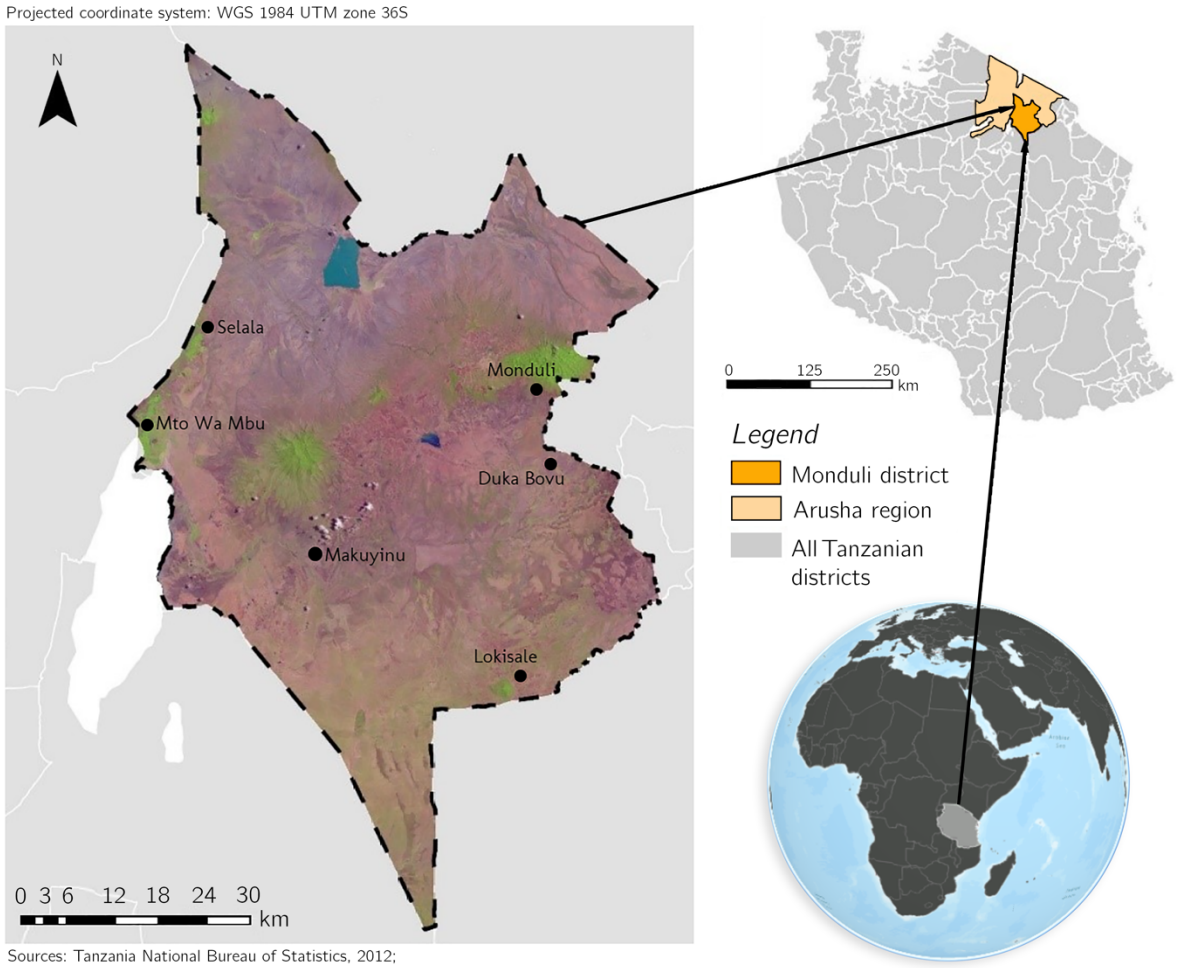

Figure 15
Location of the study area

The landscape of Monduli is shaped by tectonic activity (Iranga, 1992). The East African Rift System, located within the study area, is an active continental rift zone (Loth & Prins, 1986). In the middle and northern part there are a few isolated mountains. Underneath these mountains are Vulcanic rocks (Iranga, 1992) and on the surface they are covered with forest. In figure 15 one can observe a larger lake in the northern part of the study area and a small lake in the middle. However, due to variations in precipitation amounts the lakes in the area can fluctuate in size

(Loth & Prins, 1986). Additionally, there are six villages in the study area called Monduli, Mto wa Mbu, Selala, Makayuni, Lolkisale and Duka Bovu, also visualized in figure 15.

4.2. Climate

As previously mentioned, the climate of the Monduli district is semi-arid. In figure 16 the annual precipitation patterns and temperature are visualized. There can be two wet and two dry seasons distinguished. The first 'long rains' season starts in March and ends in May (MAM) and the second 'short rains' season start in October and ends in December (OND). The dry seasons are in January and February and from June until September (Tanzania Meteorological Authority, 2019).

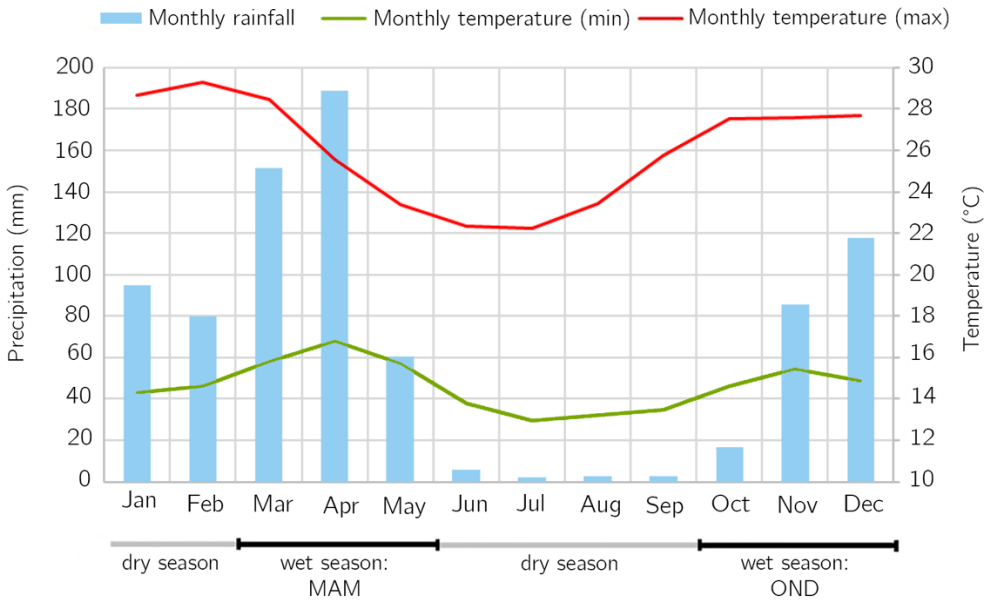

Figure 16
Annual precipitation patterns and temperature variability
Source: Adjusted figure of Verhoeve, 2019

Climate change results in higher temperatures and an increase in rainfall in Tanzania (Luhunga et al., 2018). In Arusha region it has been around 0.75% - 1.0% hotter in 2019 compared to the long-term average (1981-2010) and it has been the fourth warmest year since 1970 in the whole of Tanzania (Tanzania Meteorological Authority, 2019). In Arusha in the MAM season the rainfall accumulation has been similar, however in the OND season the climate has been wetter compared to the normal (Tanzania Meteorological Authority, 2019). There have also been more extreme weather events. In Arusha the meteorological station recorded 126.4 mm of rainfall in 24 hours between 28th and 29th of April 2019 which is the fourth highest amount of rainfall since the implementation of the station in 1949 (Tanzania Meteorological Authority, 2019). The shift of rainfall later in the season seems to be a trend in the Arusha district which results in a shorter growing season (Kihupi, Tarimo, Masika, Boman & Dick, 2015). In the study by van den Bergh (2016) the Maasai mention they experience more frequent periods of drought and a decrease in quality of both the pastures and agricultural fields which could be related to the increase in temperature which results in more evapotranspiration. Furthermore, an increase in wind speeds

is measured in the area which could potentially also be a result of changes to the landscape (Kihupi et al., 2015).

4.3. Land Use and Cover types

The division of the LULC classes is made based on the land-cover definitions used by the International Geosphere-Biosphere Program (IGBP) (Loveland & Belward, 1997; Verhoeve, 2019). The LULC in Monduli is divided into ten classes based on the amount of canopy cover, tree hight and the presence of buildings, water or agriculture (Verhoeve, 2019). In table 6 the classes are described and visualized with an illustration and photograph made in the field by Verhoeve (2019).

Table 6
Land Use and Land Cover Classes

#	*Class name*	*Description*	*Illustration*	*Photograph*
5	Mixed forest	Domination of various types of trees. Trees > 2 meters. Canopy cover > 60%.		
6	Closed shrubland	Low, woody vegetation that cover a large part of the land without high trees. Woody vegetation < 2 meters. Canopy Shrub > 60%		
7	Open shrubland	Low woody vegetation that does not cover the land completely, without large trees. Woody vegetation < 2 meters. Canopy Shrub 10%-60%		
8	Woody savannah	Various grasses and weeds can be observed, together with higher trees. Trees > 2 meters Canopy cover 30%-60%		
9	Savannah	Various grasses and weeds with some canopy cover and higher trees. Trees > 2 meters Canopy cover 10%-30%		

10	Grassland	Land is covered with various types of grasses and weeds. Little number of trees and shrubs. Woody vegetation cover < 10%		
12	Agriculture	Land covered with (seasonal) crops.		
13	Built up / natural vegetation mosaic	Land dominated by buildings. Houses > 40%-60%		 *(source: AirBnB n.d.)*
16	Barren or sparsely vegetated	Soil, sand or rocks are exposed. Vegetation cover < 10%	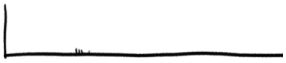	
17	Water bodies	Streams, lakes, rivers, boreholes.		

5. Results

5.1. Unsupervised: ISODATA

With the unsupervised ISODATA classifications of four Landsat images a first impression of the LULC distribution in the study area is provided. With this method the classes are generated based on the spectral signatures of the data itself, and not on the ground truth dataset. Therefore, the quality of the ground truth dataset does not have an impact on the classification. In figure 17 the unsupervised ISODATA classifications are shown, next to the quantity of the classes visualised in a bar chart. For the specific quantities see table G1.

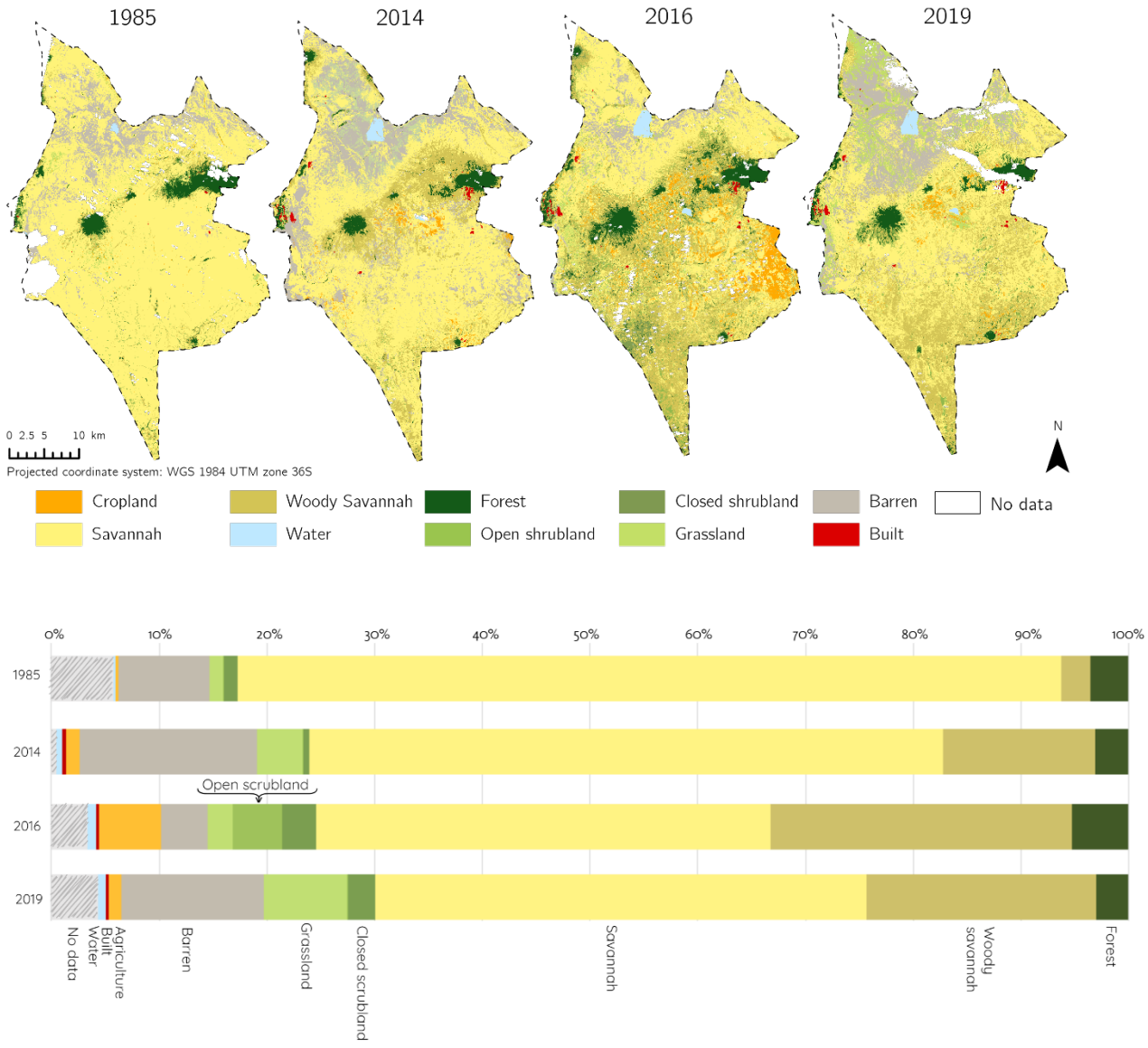

Figure 17
Unsupervised ISODATA classification of four Landsat images with quantities in bar charts

There are quite large differences in the LULC distribution per year. In the classification of 1985 81.1% of the study area is covered in Savannah. This demonstrates the spectral signatures of the surface are very similar in this whole area. The surface above the mountains in the middle and east of the study area is classified as forests (3.8%). Around these forests and in the south some areas are classified as woody savannah (2.9%) and in the north some barren (9.0%) can be observed. Additionally, around the forests some closed shrub can be spotted and around the barren ground in the north some pixels are classified as grassland. The quantities of these classes are all below 1.5%.

In the classification of 2014, there is more variation in the way the surface is classified. A part of the area previously classified as Savannah (now 58.9%) is grouped separately as woody savannah (14.1%). These pixels are primarily located around the forests in the middle and east part of the study area, and in the south. Furthermore, a larger part of the study area in the north and west side is grouped as barren (16.5%) and grassland (4.2%). Lastly, some pixels are classified as agriculture, primarily in the middle of the study area.

In the classification of 2016, the highest amount of variation in LULC classes can be observed. In this classification 42.2% is classified as savannah and 28.0% as woody savannah. Additionally, more pixels are grouped as open shrubland (4.6%) or closed shrubland (3.2%). Grassland (2.4%) and barren (4.3%) decreased in quantity compared to the 2014 classification. In the north areas that were previously grouped as grassland or barren are now classified as savannah. Additionally, in the east and middle of the study area a larger part is classified as agriculture (5.7%). On the east side this was previously classified as either barren or savannah. Lastly, in this classification a larger part around the mountains is classified as forest (5.2%) compared to the other classifications.

In the classification of 2019, most of the pixels classified as open shrubland or closed shrubland in the 2016 classification are now grouped as savannah (47.7%) or woody savannah (22.2%). Woody savannah is primarily located in the south of the study area. Around the forests (3.2%) some pixels are classified as closed shrub (2.6%). In the north pixels classified as savannah in the 2016 classification are now classified as barren (14.8%) and grassland (8.1%). The area in the north covered by grassland in this classification is higher compared to 2014 (+3.9%).

When analysing the classifications, it becomes apparent there are relatively large differences in the LULC groups between 2014, 2016 and 2019. Furthermore, a large part of the study area, which in reality also consists of closed shrub, open shrub, grassland or woody savannah is all classified as savannah in some of the classifications, specifically in 1985.

When looking at table 7 it becomes apparent the ISODATA unsupervised classifications have a relatively low overall accuracy and kappa coefficient. The complete error matrixes of the four years can be found in appendix A.

Table 7
Accuracy of ISODATA classifier

Year	Overall accuracy	Kappa coefficient
1985	0.369	0.290
2014	0.393	0.317
2016	0.457	0.390
2019	0.430	0.359

The classification of 2016 shows the highest amount of variation in LULC classes which would correspond the most to the actual landscape of the study area. This is also represented by the highest overall accuracy and kappa coefficient. In total the overall accuracy of the maps ranges from 0.369 to 0.430 and the kappa coefficient from 0.290 to 0.359. Landis & Koch (1977) mentioned a value of kappa between 0.4 and 0.8 can be regarded as a moderate agreement between the classification and reference data and a value below 0.4 as poor agreement. All values are below 0.4 which means there is a poor correspondence between the classifications and the reference data. When analysing the confusion matrixes, the classes that increase the overall accuracy the most are forest and water while open shrub, closed shrub and grassland in general have the lowest user's and producer's accuracy.

5.2. Supervised: Maximum likelihood

In the supervised methods the ground truth determines the way the pixels are classified. Maximum likelihood is a more traditional supervised classification method that has been around for a long time. In this method the spectral signatures of the ground truth are used to calculate the probability of pixels belonging to a certain class. In figure 18 the results of the maximum likelihood classifications of four Landsat images are demonstrated and the quantities are visualised in a bar chart. For the specific quantities see table G2.

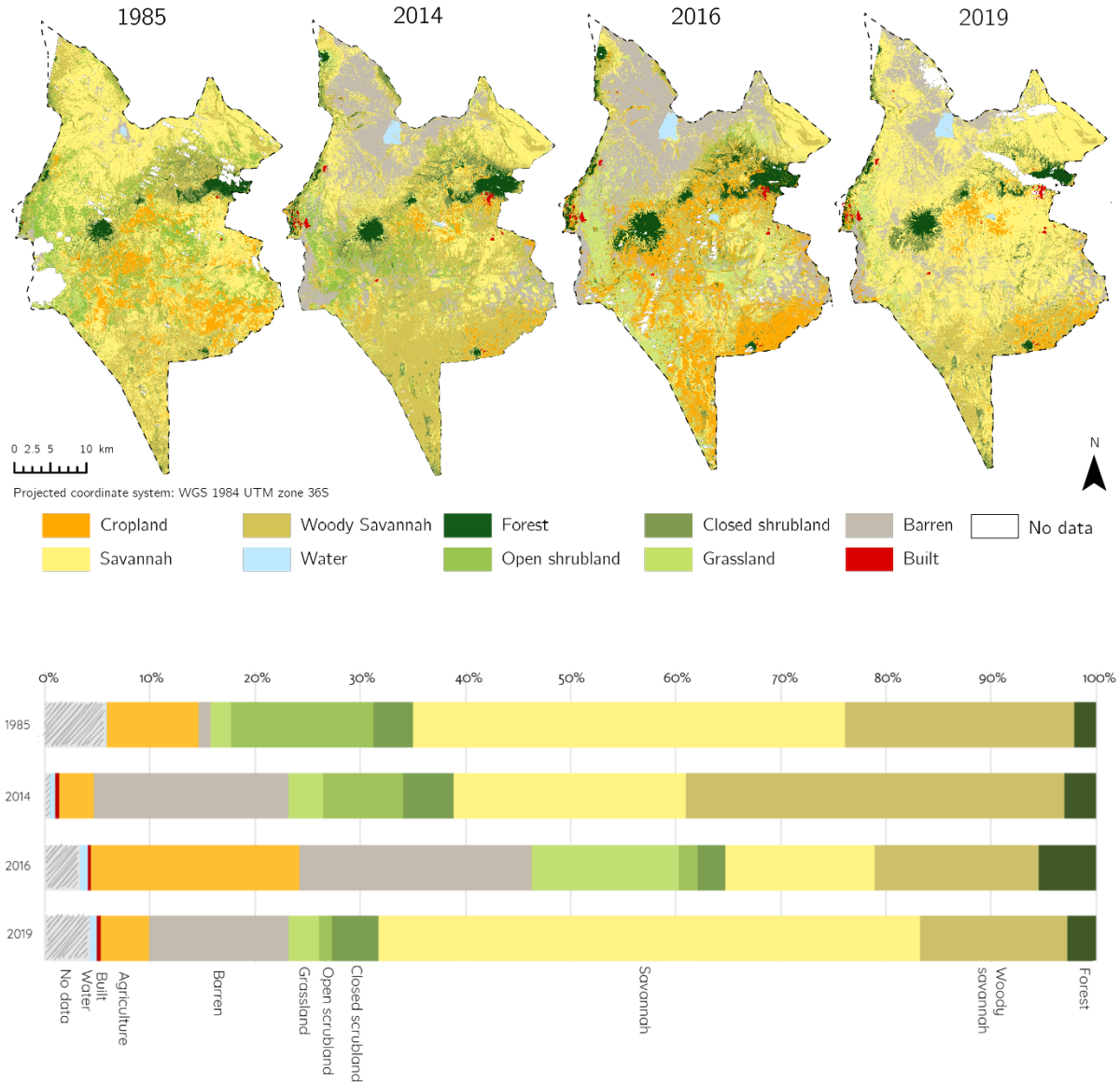

Figure 18

Supervised maximum likelihood classification of four Landsat images with quantities in bar charts

In the classification of 1985 the western half of the study area, all classified as savannah in the unsupervised method, is now primarily covered in savannah (41.1%), woody savannah (21.8%), open shrubland (13.6%) and cropland (8.7%). Around the forest (2.1%) in the east there are some pixels classified as closed shrub (3.8%) and in the middle of the study area some grassland (2.0%) can be observed. In the north, around the lake, much of the pixels are classified as savannah with only a small part classified as barren (1.1%).

In the classification of 2014 much more of the area around the lake in the north, classified as savannah in the 1985 classification, is now classified as barren (18.5%). Additionally, some more barren can be observed in the west and east. The amount of cropland (3.3%) decreased a lot compared to the 1985 classification which would go against expectations. Furthermore, a large part of the south of the study area is classified as woody savannah (36.1%). Savannah (22.1%) decreases in quantity, which seems primarily a result of the increase in woody savannah and barren. The quantity of forests (3.0%) increased slightly with 0.9%. In the middle and east of the study area some open shrubland (7.6%) can be found. Closed shrubland (4.8%) is primarily concentrated under the forest in the west and above the forest in the east. Lastly, grassland (3.3%) is mainly located in the north-west of the study area.

The classification of 2016 seems to differ the most from the other classifications. It is immediately noticeable a much larger part of the southern half of the study area is classified as agriculture (19.8%). A large part around the pixels classified as agriculture is now perceived as grassland (14.0%). These areas seemed to be classified as closed shrubland, savannah or woody savannah in the classification of 2014. In the 2016 classification woody savannah (15.6%) is now primarily located around the forests, in the middle part of the study area. Savannah (14.2%) seems to be located in the middle, east and some in the north-west. Much of the northern half of the study area, around the lake, is classified as barren in the 2016 classification. Additionally, forests increased in size from 2014 to 2016 with 2.5%.

In the classification of 2019, the large number of pixels classified as agriculture in 2016 are perceived as either savannah (51.5%) and some woody savannah (14.0%). Agriculture decreases to 4.6% in 2019. The woody savannah located around the forests in 2016 is classified as savannah in 2019, and woody savanna is located in the south of the study area, similar to 1985 and 2014. Forests decreased with 2.8% from 2016 to 2019. Around these forests much of the pixels are classified as closed shrubland (4.4%). Some areas in the west are still classified as grassland (2.9%), but a large part changed to other classes, such as savannah. Lastly, the number of pixels classified as barren in the north around the lake decreases to 13.3%

The maps and bar charts in figure 18 show relatively large fluctuations in LULC classes where large fluctuations between years are unexpected, such as forests. In table 8 the overall accuracy and kappa coefficient of the classifications is shown. For the error matrixes see appendix B.

Table 8
Accuracy of Maximum Likelihood classifier

Year	Overall accuracy	Kappa coefficient
1985	0.659	0.616
2014	0.616	0.568
2016	0.604	0.555
2019	0.516	0.455

The overall accuracies range from 0.659 to 0.516 and the kappa coefficient from 0.616 to 0.455. The values do not go below 0.4. However, for 2019 the kappa coefficient is only 0.455. When looking at the confusion matrix of 2019 it becomes apparent the user's and producer's accuracy of forest and water are very high which increases the accuracy. Other classes such as closed shrub, open shrub and woody savannah have a very low user's and producer's accuracy and barren, agriculture, grassland and savannah have a more moderate user's and producer's accuracy. For the other classifications a similar pattern can be observed as for 2019, some classes have a high accuracy but other classes very low which results in the overall accuracy to balance out at around 0.6 on average.

5.3. Supervised: Random Forest

With the use of a supervised maximum likelihood classifier the overall accuracy and kappa coefficient increased. However, large fluctuations between years are observed. The supervised random forest classifier is a more advanced, machine learning algorithm which is more robust compared to maximum likelihood. In figure 19 the resulting maps of the random forest classifications of four Landsat images are shown and the quantities of the LULC classes are visualised in a bar chart. For the specific quantities see table G3.

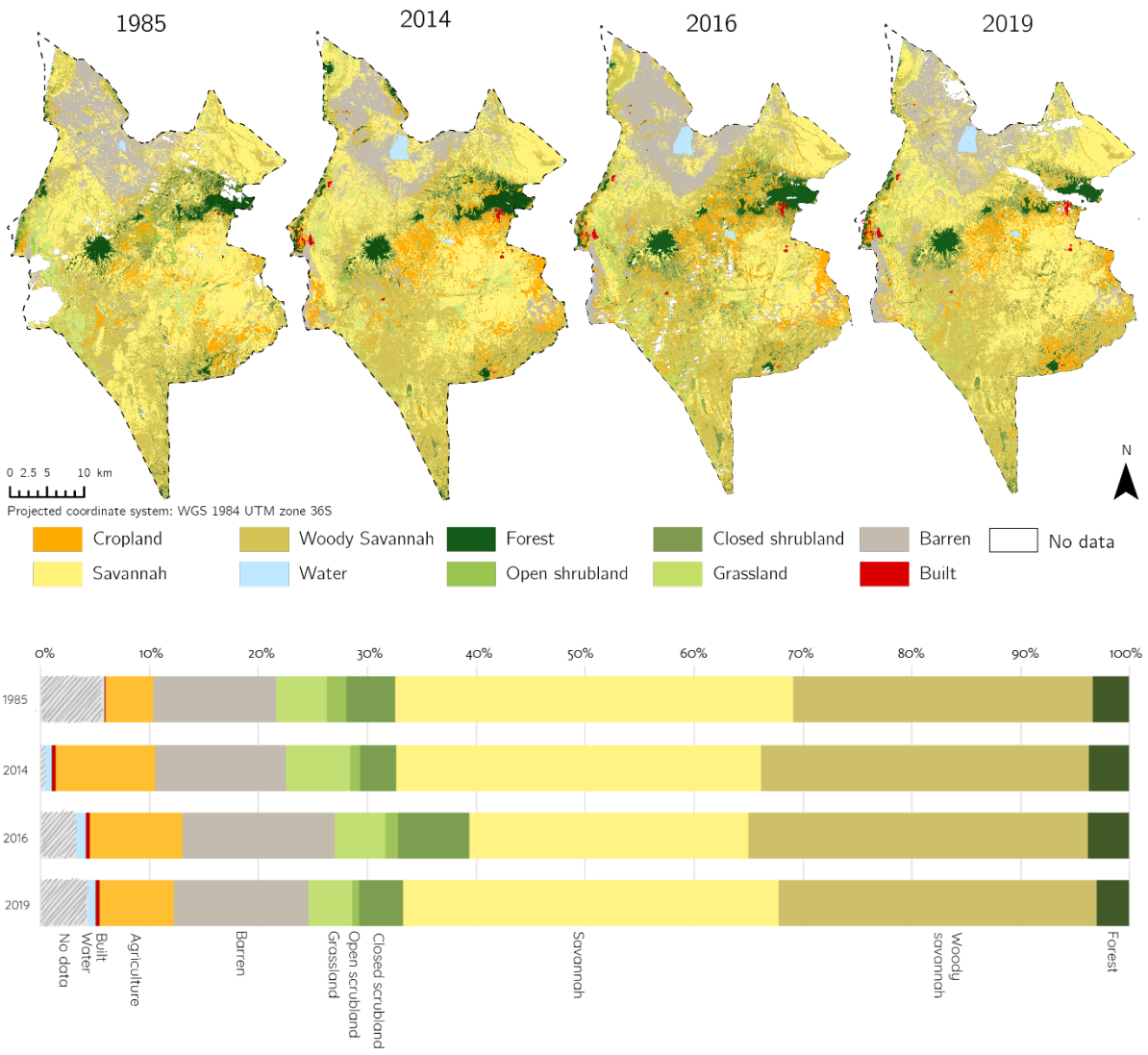

Figure 19
Supervised random forest classification of four Landsat images with quantities in bar charts

In the classification of 1985, most of the study area is covered by savannah (36.5%) and woody savannah (27.5%). Woody savannah is primarily located in the south and south-west side. Some grassland (4.7%) can be observed in the west and middle of the study area, and closed shrub (4.5) and open shrub (1.8%) are mostly situated around the forest (3.4%) in the east. Agriculture (4.4%) is distributed in patches around the northern half of the study area.

In the classification of 2014, a LULC class with a large increase compared to 1985 is agriculture (9.2%). This LULC class is primarily located on the west side, south-east side, around and between the forests, and east side of the study area. The number of pixels in the south and south-east classified as woody savannah also seems to increase, at the expense of savannah. The amount of grassland in the south decreases. However, in total quantity grassland increases slightly from 1985 to 2014 (to 5.9%). The amount of land classified as barren (12.0%) is quite similar. However, in 2016 around the lake in the north more pixels are classified as savannah. Furthermore, in the east and west areas are classified as barren which were either clouds or (woody) savannah in 1985. Similar to 1985 above the forests in the east some pixels are classified as closed shrub (3.3%). Forested areas increase slightly (+0.4%). As the increase is relatively small, this could partly be due to the fact that an area above the forests in the east is covered by clouds in 1985.

In the classification of 2016, an increase in closed shrub (+3.3%) in the middle of the study area under the forest and between areas classified as agriculture can be observed. There is also an increase in woody savannah above the forests, in total woody savannah increases with 1.0% The number of pixels classified as forest stays relatively similar. There seems to be slight differences in pixels classified as agricultural areas (-0.7%), but no major increase or decrease. Lastly in the north more of the area around the lake is classified as barren (14.0%) instead of Savannah.

The classification of 2019 looks very similar to the classification of 2014. In quantity the LULC classes stays relatively similar when comparing these two classifications. There are only some slight differences. Noticeable is a decrease in agriculture (-2.3%) in the south-east, west and middle of the study area. Furthermore, the distribution of the pixels classified as barren or savannah in the north is different. A small area classified as forest and agriculture in the north-west in 2014 is also smaller in 2019 and lastly there is less grassland (4.0%) in the east in 2019 compared to 2014.

When looking at the maps and the quantity of the LULC classes there are much less fluctuations with the use of random forest compared to maximum likelihood. The classifications of 2014, 2016 and 2019 seem relatively similar, specifically 2014 and 2019. In table 9 the overall accuracy and kappa coefficient of the classifications is shown. See appendix C (table C1, C4, C6 and C8) for the error matrixes.

Table 9
Accuracy of random forest classifier

Year	Overall accuracy	Kappa coefficient
1985	0.759	0.729
2014	0.751	0.720
2016	0.652	0.609
2019	0.766	0.736

The accuracies of 1985, 2014 and 2019 are on the higher spectrum of a moderate correspondence between the classification and the reference data. 2019 has the highest accuracy with an overall

accuracy of 0.766 and a kappa coefficient of 0.736. The map of 2016 shows the largest difference in LULC distribution between the three most recent years. From table 9 is becomes clear this classification also has the lowest accuracy. Specifically, savannah decreased quite a lot in 2016. The user's and producer' accuracy of Savannah is also lower in 2016 compared to the other years.

5.4. Comparison Landsat and Sentinel imagery

5.4.1. Unsupervised: ISODATA

First the results of the ISODATA classifications are demonstrated. Classifications of sentinel images from 2016 and 2019 are compared to the 2016 and 2019 Landsat classifications described in the previous chapters. In figure 20 the results are visualised. See table H1 for the specific quantities of the Sentinel classifications and table G1 for the specific quantities of the Landsat classifications.

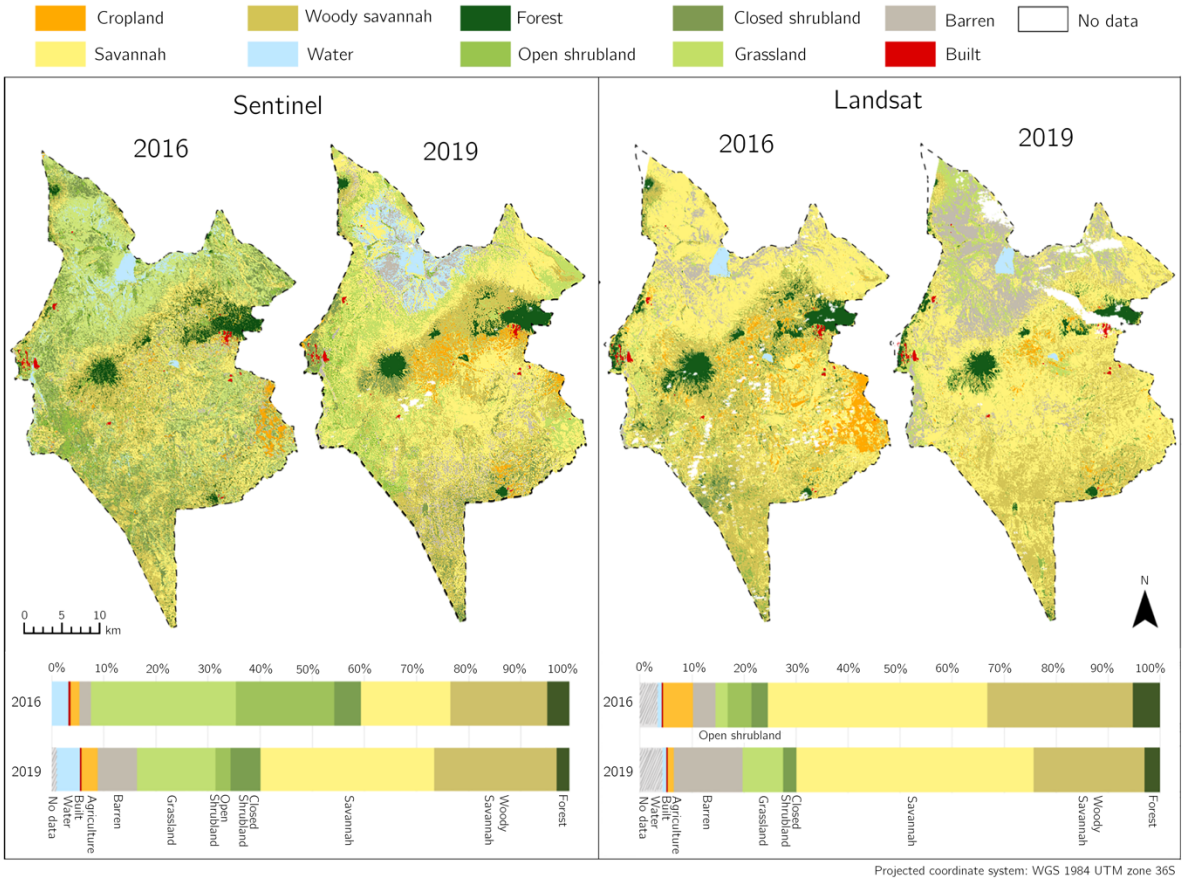

Figure 20
Unsupervised ISODATA classification of Sentinel and Landsat imagery

When comparing the maps of 2016 immediately noticeable is the inability of the classifier to detect the difference between the lake in the north and the land surrounding it in the Sentinel classification. A lot of pixels around this lake are classified as water, while for Landsat they are classified as either barren, grassland or savannah. Furthermore, a lot of the surface is classified as either open shrub (18.9%) or grassland (27.8%). 'Only' 17.2% is classified as savannah and 18.5% as woody savannah while in the Landsat classification the quantity of these classes is much higher.

When comparing the maps of 2019, a similar complication is encountered with the surface around the lake, while for the Landsat classifications there are no issues. Additionally, the small lake in the middle of the study area, which can be observed in the Sentinel 2016 and the Landsat 2016

and 2019 classifications, is not recognized as water in the Sentinel 2019 classification, but as forest. Furthermore, in the Sentinel 2019 classification the amount of area classified as grassland (15%) and open shrub (3.0%) is smaller compared to 2016. However, the quantity of grassland is still higher compared to the Landsat classification. For sentinel the increase in grassland is primarily located in the west side. There are also more areas classified as agriculture (3.1%) in the Sentinel classification compared to the Landsat classification. Additionally, the number of pixels classified as forests decreases from 2016 to 2019 for both Landsat and Sentinel classifications. Around these forests a large area is classified as woody savannah for Sentinel 2019, while this is classified as savannah in the Landsat classification.

In the unsupervised Sentinel classifications large areas are covered in one class, such as grassland, while in reality this area is also made up of other classes, such as savannah. However, this has also been an issue in the Landsat classifications where this resulted in a large area to be covered with savannah. Additionally, for the Sentinel classifications there are issues with the distinction of the lake in the north. In table 10 the accuracies of the ISODATA classifications are shown next to the Landsat accuracy results. See appendix D for the error matrixes of the Sentinel classifications and appendix A (table A3 and A4) for the error matrixes of the Landsat classifications.

Table 10
Comparison of accuracy of ISODATA classification of Sentinel and Landsat imagery

	Sentinel		***Landsat***	
Year	*Overall accuracy*	*Kappa coefficient*	*Overall accuracy*	*Kappa coefficient*
2016	0.373	0.295	0.457	0.390
2019	0.385	0.309	0.430	0.359

For both Sentinel and Landsat, the accuracies show a poor correspondence between the classifications and the reference data. However, for sentinel the accuracy results are even lower with an average overall accuracy of 0.379 and kappa coefficient of 0.302.

5.4.2. Supervised: Maximum Likelihood

The unsupervised ISODATA classification demonstrated there are some issues with distinguishing classes with the Sentinel imagery. In order to see how the classifications can be improved with a supervised method, Sentinel maximum likelihood classifications are compared with the Landsat classifications. In figure 21 the results are visualised. See table H2 for the specific quantities of the Sentinel classifications and table G2 for the specific quantities of the Landsat classifications.

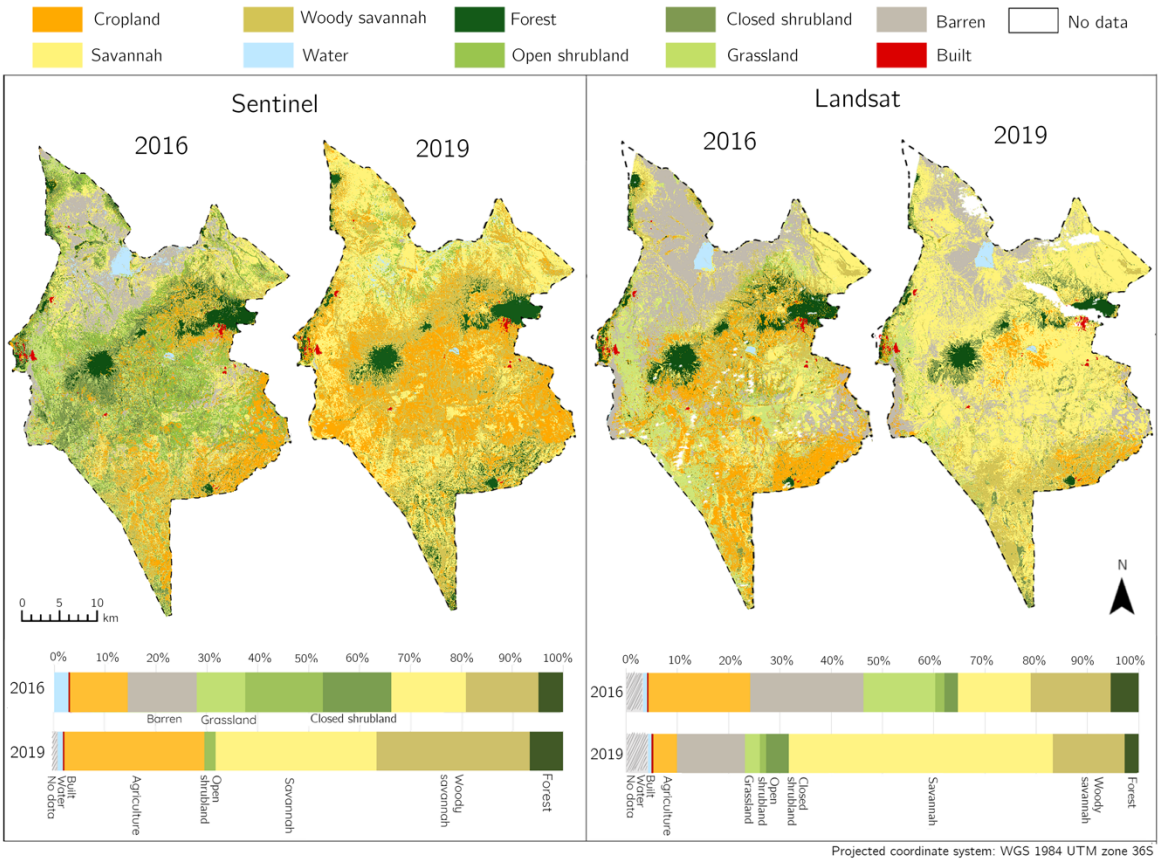

Figure 21
Supervised maximum likelihood classification of Sentinel and Landsat imagery

The Sentinel classification of 2016 is classified in a very different way compared to the Landsat classification of the same year. Similar to the Landsat classification the Sentinel classification has a lower number of pixels classified as savannah (14.6%) and woody savannah (14.3%). However, the amount of barren (13.6%) is lower and closed shrubland (13.5%) and open shrubland (15.2%) higher compared to the Landsat classification. Closed shrubland is mostly situated around the forests. Grassland and open shrubland can be found in the middle and western part of the study area. The north, around the lake is classified as barren. A lot less pixels are classified as water around the lake compared to the unsupervised classification, however there are still some areas misclassified. Furthermore, in the sentinel classification there is not as much surface classified as agriculture compared to the Landsat classification. Most of the agricultural areas (11.3%) are located around the forest in the east, north-east and south of the study area.

In the Sentinel classification of 2019, it is immediately noticeable a large part is covered in agriculture (27.4%) and the lake in the north is not present in the map anymore. Furthermore, the amount of open shrub, grassland and barren decreased a lot. In the Landsat classification of 2019, a large part of the study area is covered by savannah. Compared to the Sentinel 2019 classification, the Landsat 2019 classification looks a lot more balanced.

Similar to the Landsat classification there seem to be some issues with large fluctuations in classes for the Sentinel classifications. However, for Sentinel different fluctuations are observed. It seems unlikely an additional 16.1% of the study area would be turned into agriculture from 2016 to 2019. This also does not correspond to the satellite imagery. Additionally, issues with

misclassification of water bodies are encountered while in the Landsat classifications this class can be accurately mapped.

In table 11 the accuracy of the maximum likelihood classifier of Sentinel imagery are shown next to the accuracies of the Landsat classifications. See appendix E for the error matrixes of the Sentinel classifications and appendix B (table B3 and B4) for the error matrixes of the Landsat classifications.

Table 11
Comparison of accuracy of maximum likelihood classification of Sentinel and Landsat imagery

	Sentinel		***Landsat***	
Year	*Overall accuracy*	*Kappa coefficient*	*Overall accuracy*	*Kappa coefficient*
2016	0.620	0.573	0.604	0.555
2019	0.385	0.309	0.516	0.455

The overall accuracy and kappa coefficient of the Sentinel 2016 classification is much higher compared to the Sentinel classification of 2019. The 2019 classification has a poor agreement between the classification and the reference data, while 2016 has a moderate agreement. For 2019 closed shrub, open shrub and grassland lower the accuracy the most. These classes are barely present in the map which consequently means for these classes there is zero agreement between the reference data and the 2016 classification. The accuracy of the Sentinel classification of 2016 is similar to the Landsat classification. However, they differ a lot in the way the surface is classified, and both do not seem to be a correct representation.

5.4.3. Supervised: Random Forest

Sentinel maximum likelihood classifications did not result in a much higher accuracy compared to the Landsat classifications. To analyse the influence of the random forest algorithm on the accuracy in figure 22 the results of the random forest classifications of the Sentinel imagery are visualised next to the Landsat classifications. See table H3 for the specific quantities of the Sentinel classifications and table G3 for the specific quantities of the Landsat classifications.

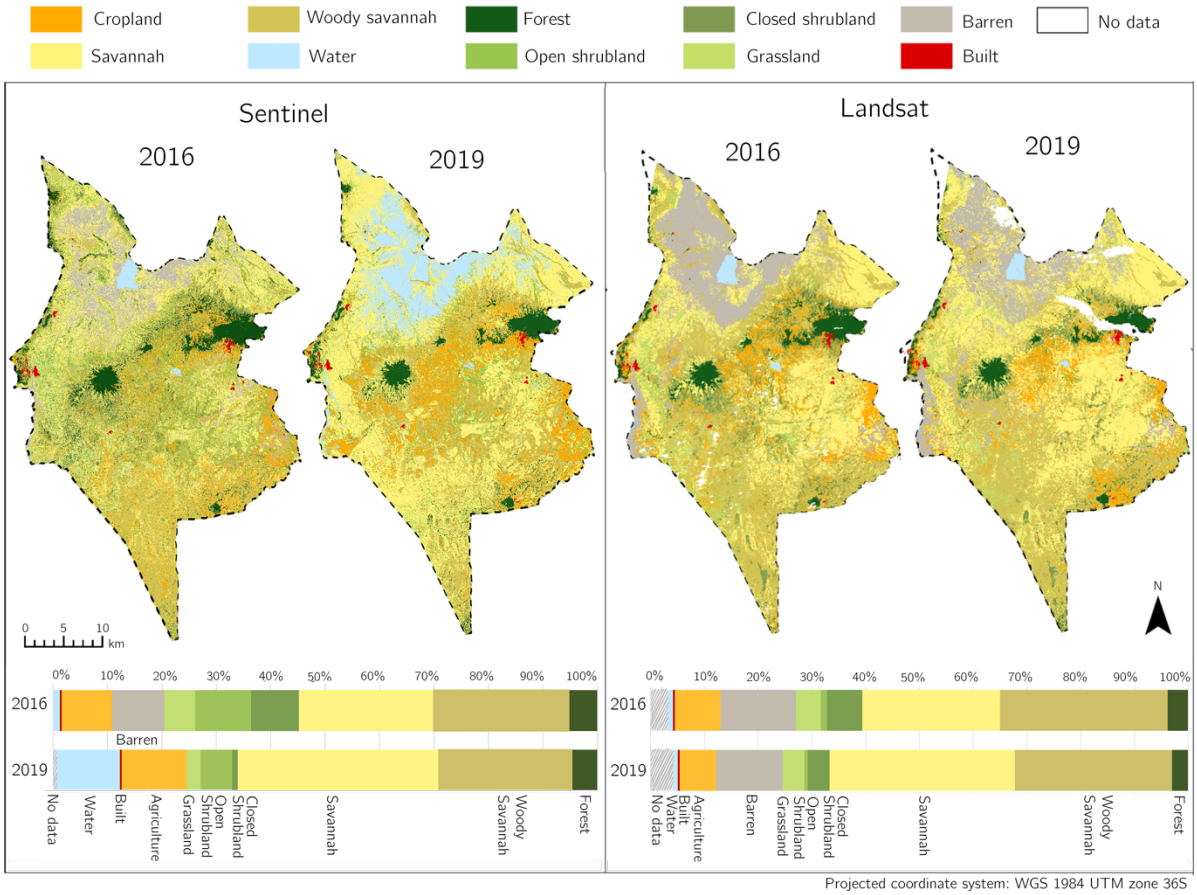

Figure 22

Supervised random forest classification of Sentinel and Landsat imagery

In the classification of 2016 with sentinel imagery there seem to be less issues with the water in the north compared to the Sentinel ISODATA and Sentinel maximum likelihood classifications. Furthermore, a lower amount of the area in the north around the lake is covered with barren compared to the Landsat imagery. Additionally, compared to the Landsat classification a larger quantity of the middle of the study area is covered in open shrub (10.3%) or closed shrub (8.7%). The pixels classified as agriculture seem less concentrated as in the Landsat classification. Lastly, agriculture (9.3%) is more spread throughout the northern half of the study area and around the forests.

In the classification of 2019 of Sentinel imagery there are again, complications with the water in the north. The area classified as barren in the Landsat classification is now completely covered with water (11.6%). Furthermore, there is an increase in pixels classified as agriculture (11.9%) compared to the Landsat classifications. Similar to the Landsat classification savannah (36.8%) increases in size. However, the increase in the Sentinel classification is concentrated around the forest in the east side of the study area and in the Landsat classification in the west side. Additionally, more areas are classified as open shrub (5.8%) compared to the Landsat classifications. These areas seem primarily classified as savannah in the Landsat classification.

In table 12 the accuracies of the classifications are demonstrated. See appendix F for the error matrixes of the Sentinel classifications and appendix C (table C6 and C8) for the error matrixes of the Landsat classifications.

Table 12
Comparison of accuracy of random forest classification of Sentinel and Landsat imagery

	Sentinel		***Landsat***	
Year	*Overall accuracy*	*Kappa coefficient*	*Overall accuracy*	*Kappa coefficient*
2016	0.596	0.546	0.652	0.609
2019	0.452	0.384	0.766	0.736

The random forest algorithm did not increase the accuracy results for both Sentinel classifications. The accuracies for the random forest classifications of Landsat imagery are much higher compared to Sentinel. The classification of Sentinel 2019 with random forest does have a higher accuracy compared to the maximum likelihood classification of Sentinel 2019. However, regardless of the increase in accuracy, there still seems to be a poor agreement between the classification and the reference data. For the classification of 2016 there seems to be a moderate agreement, however, the accuracy is still lower compared to the Landsat classification.

5.5. Most accurate method applied on all the available imagery

5.5.1. Short review of the accuracy of the applied methods

In the previous chapters the results of three classification methods have been demonstrated. The unsupervised ISODATA classifications gave some insights into the spectral reflections in the study area. For some images a large area is grouped into one class due to the characteristics of the data. This indicates a large part of the study area has a similar spectral reflection which corresponds to potential issues in remote sensing previously described in chapter 2.4. This has resulted in a low accuracy for the unsupervised classifications.

For the maximum likelihood classifications of Landsat imagery, the overall accuracy is 0.599 and kappa coefficient 0.549. This indicates a moderate correspondence between the classification and the reference data. However, with the maximum likelihood method fluctuations in the LULC distribution between years seem relatively high. Between the random forest classifications of Landsat imagery less fluctuations can be observed. LULC classes such as forest seem relatively stable through the years, which is not the case for the maximum likelihood classifications. The average overall accuracy of the random forest classifications is 0.732 and the kappa coefficient 0.699. This demonstrates a moderate to high agreement between the reference data and the classifications.

Contrary to expectations Sentinel imagery did not provide higher accuracies compared to the Landsat imagery. For Sentinel the highest general accuracy achieved is an overall accuracy of 0.524 and kappa coefficient 0.441 for the random forest classifications. In particular for the 2019 classification the accuracies are higher for Landsat compared to Sentinel.

5.5.2. Random forest classifications of 1985 to 2019 of Landsat imagery

As random forest with Landsat imagery resulted in the most accurate classifications this classifier is used to classify all the available images to analyse how the LULC classes change throughout the years. The resulting maps and LULC quantities are shown in figure 23. Additionally, in figure 24 the quantities of the LULC classes are visualised in a line graph.

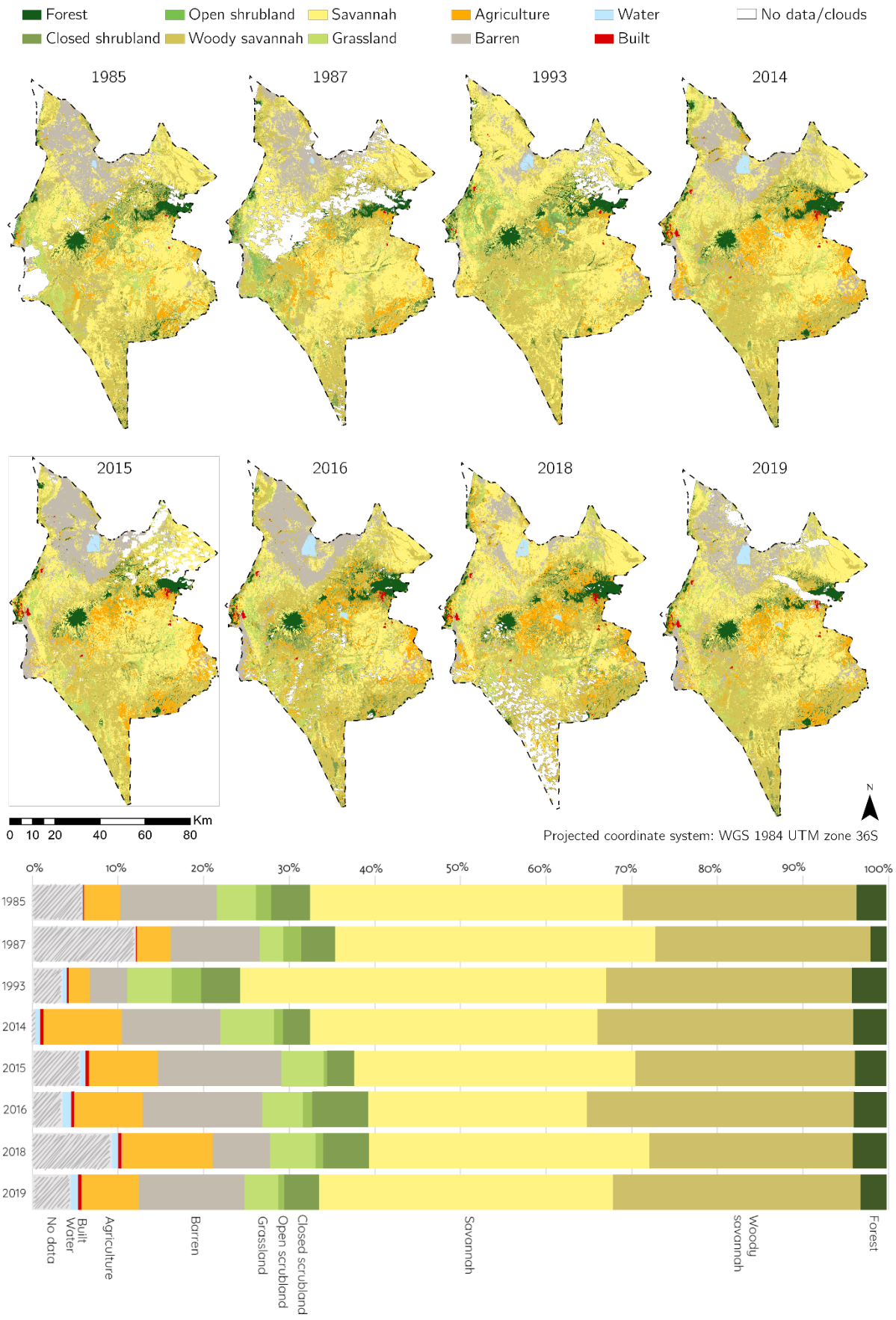

Figure 23

Results of random forest classification on all available Landsat imagery from 1985 to 2019

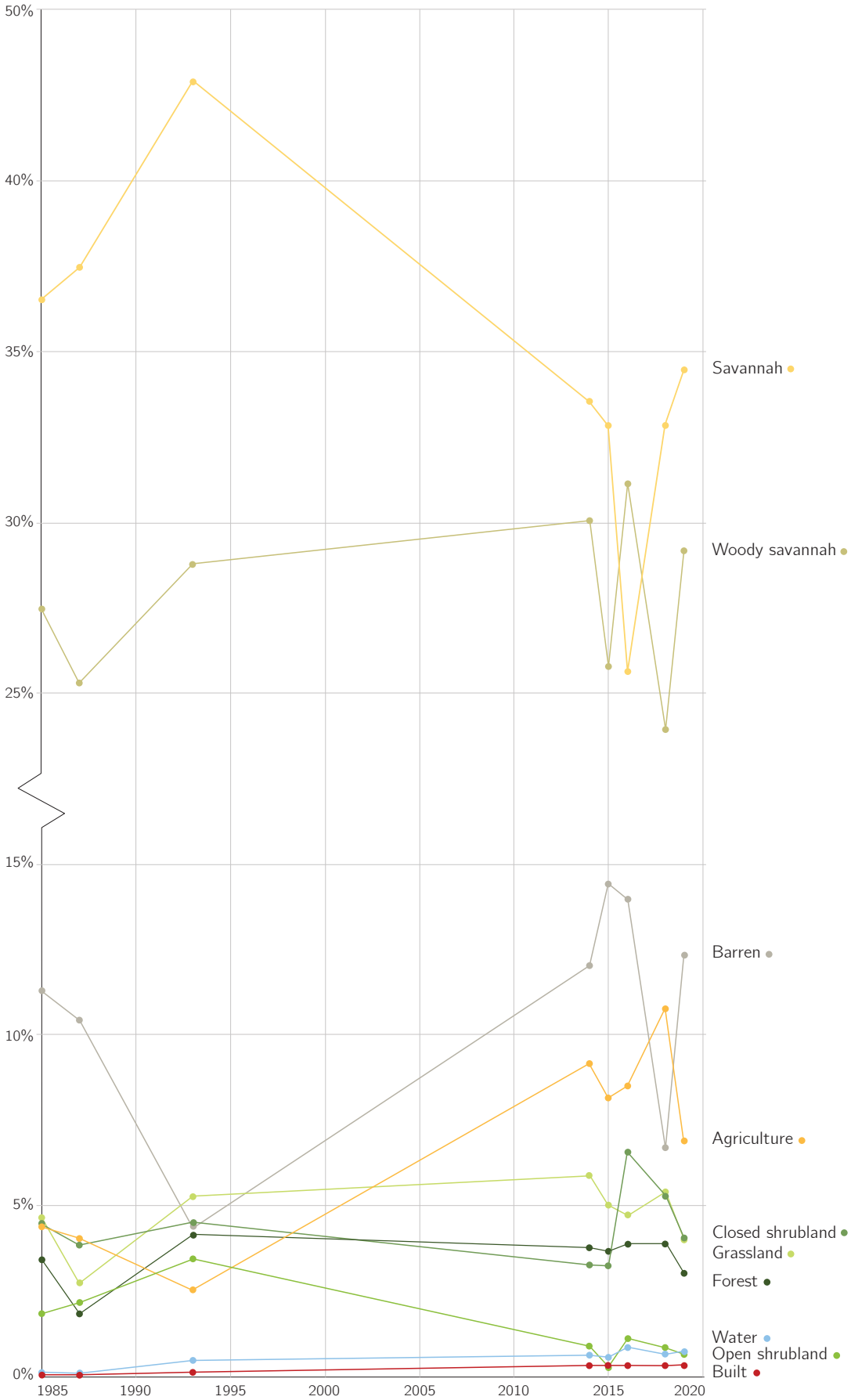

Figure 24

Results of random forest classification on all available Landsat imagery from 1985 to 2019 displayed in a Line graph

In the classifications forested areas seem to stay relatively constant. However, for some years some smaller and larger decreases can be observed. In 1985 forests covered 3.4% of the study area, in 1987 1.8% and in 2019 3.0%, while on average 3.8% is covered with forests for the other years. However, these fluctuations are most likely for a large part due to clouds covering the locations of the forests in some imagery, as can be observed in figure 23.

In all the classifications savannah and woody savannah cover most of the surface. These areas are located throughout the study area with woody savannah primarily covering the south, middle-west side and around the forests. There are quite come fluctuations in these classes throughout the years. Furthermore, there seems to be some movement in regard to pixels that are classified as savannah in some classifications and woody savannah in others. Specifically, in the northern half of the study area this can be observed.

For grassland, open and closed shrub, all vegetation types with little to no tree cover, the quantities are around the same percentage as the forested areas. These three classes are primarily located around the forests, in the west and middle of the study area. However, the specific locations seem to differ quite a lot for each year. Additionally, over the years some fluctuations in these classes can be observed. Grassland demonstrates a decrease from 1985 to 1987 with 2.0% and increases again from 1987 to 1993. From 1993 to 2014 grassland increases a little bit, but decreases from 2015 to 2019 with 1.0%, with a small increase in 2018. Open shrubland increases from 1985 to 1993 with 1.6% but decreases again with 2.5% in 2014. From 2014 to 2019 the quantity of open shrubland stays relatively stable. Closed shrubland stays relatively similar in quantity from 1985 to 2015, with some small increases and decreases, and mainly has as a large increase to 2016 with 3.4%, after which it decreases again in size.

Barren is primarily located in the north of the study area. The quantity of this class fluctuates quite a lot between years with a coverage of 11.3% in 1985, 4.4% in 1993 and 14.4% in 2015. Specifically, in 1993 and 2018 the amount of barren is much lower compared to the other imagery. In these years savannah increases as most of the barren land seems to turn into savannah during the years of a decrease.

Agriculture is located in the middle of the study area, under the forest in the east around Monduli (the village), in the south-east around Lokisale and west side of the study area around Mto Wa Mbu. A clear increase can be observed in the amount of agriculture between the classifications of 1985 to 1993 and 2014 to 2019. From 1985 to 1993 on average the amount of agriculture is 3.6% and from 2014 to 2019 6.9%. However, there are some fluctuations in the specific amounts throughout the years.

The two smallest classes in quantity are water and built environment. These two classes also increase. In the classification of 1985 and 1987 the amount of water is very low (0.1%), in 1993 one can already see an increase in the water in the north (0.5%) and from 2014 to 2019 the amount of water is on average 0.7%. Built environment increases in and around all the village in the study area. In 1985 only Monduli and Mto Wa Mbu and some buildings close to Duka Bovu are large enough to be observed in the classification. In the classifications of 2014 to 2019 all the villages in total have increased six times in size when comparing them to the classification of 1985.

In table 13 the accuracies of the classifications are demonstrated. The classifications with the highest accuracies are highlighted. See appendix C for the error matrixes.

Table 13
Accuracy of random forest classifier on all Landsat imagery from 1985 to 2019

Year	Overall accuracy	Kappa coefficient
1985	0.759	0.729
1987	0.705	0.668
1993	0.746	0.714
2014	0.751	0.720
2015	0.730	0.696
2016	0.652	0.609
2018	0.639	0.594
2019	0.766	0.736

On average the overall accuracy of the classifications is 0.719 and the kappa coefficient 0.683. This means there is a moderate agreement between the classifications and the reference data. When analysing the specific accuracies, the classifications of 1987, 2015, 2016 and 2018 have the lowest accuracy and 1985, 1993, 2014 and 2019 the highest accuracy. These last four all have an overall accuracy of 0.746 and kappa coefficient of 0.714 or higher. For 2019 the highest accuracy is achieved with an overall accuracy of 0.766 and the kappa coefficient 0.739. This is on the higher end of the moderate agreement spectrum, as a kappa coefficient of above 0.8 would indicate a high agreement.

5.7. Change detection

The four random forest classifications with the highest accuracy are used for the change detection analysis. In appendix I the maps are displayed in a large format. In figure 25 it can be observed that when the quantities of the classes of the most accurate classifications are visualised in a graph less fluctuations are observed compared to the graph in figure 24, specifically for vegetation classes such as woody savannah, closed shrub, grassland and for forests.

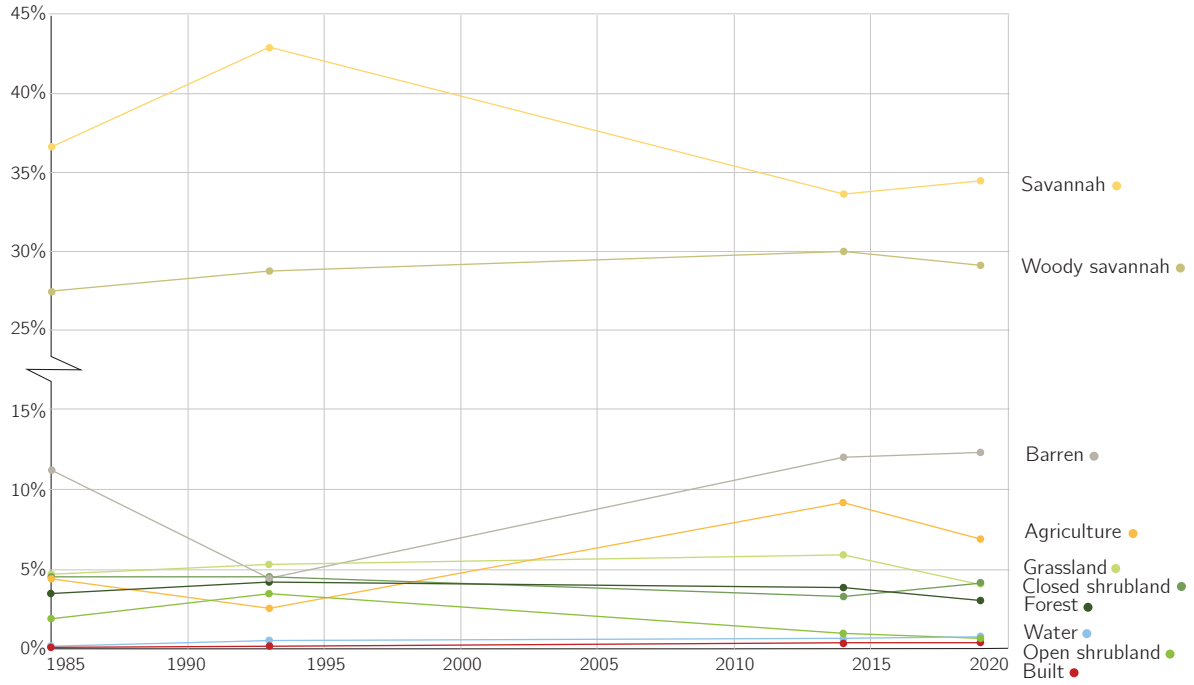

Figure 25

Graph with LULC quantities in percentages of the most accurate RF classifications

From these four classified images a change detection matrix and Sankey diagram have been produced. See appendix J for the change detection matrixes. In table 14 the quantity of the LULC classes for the initial classified raster and the percentage of change are shown. In figure 26 the change detection matrixes are visualized in a Sankey diagram. The bigger the lines in the diagram the larger the quantity of the change.

Table 14

Summary of change detection matrices

	1985 - 1993		*1993 - 2014*		*2014 - 2019*		
	Total 1985	Changed	Total 1993	Changed	Total 2014	Changed	*Total 2019*
	%	*%*	*%*	*%*	*%*	*%*	*%*
Forest	3.4	1.0	4.1	1.7	3.8	1.3	3.0
Woody Savannah	27.5	14.3	28.8	14.6	30.1	9.8	29.2
Savannah	36.5	17.1	42.9	23.9	33.6	10.7	34.5
Closed shrubland	4.5	3.6	4.5	4.1	3.2	1.9	4.0
Open shrubland	1.8	1.6	3.4	3.4	0.9	0.8	0.6
Grassland	4.7	3.7	5.3	4.5	5.9	4.7	4.0
Barren	11.3	9.3	4.4	1.9	12.0	4.5	12.3
Agriculture	4.4	4.0	2.5	1.6	9.2	5.0	6.9
Built	0.0	0.0	0.1	0.0	0.3	0.0	0.3
Water	0.1	0.1	0.5	0.5	0.6	0.0	0.7
No data/clouds	5.8	5.8	3.4	3.4	0.4	0.1	4.5
Totals	100	60.5	100	59.5	100	38.8	100

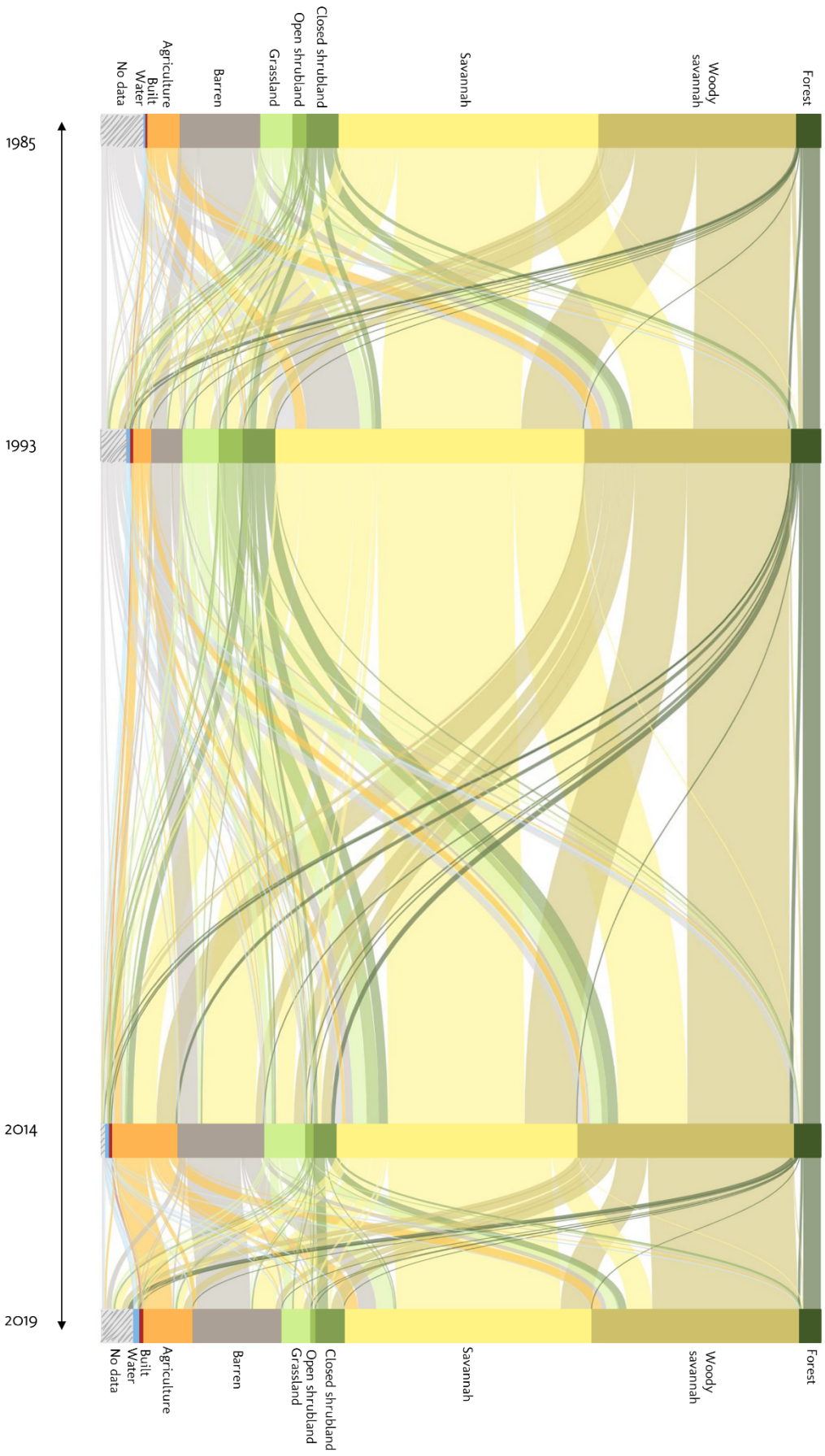

Figure 26
Sankey diagram of LULC changes from 1985, 1993, 2014, to 2019

As mentioned, classes show less fluctuations in quantity in figure 25 compared to figure 24. However, from table 14 and figure 26 it can be concluded that there are some fluctuations in the way pixels are classified. From 2014 to 2019 the least pixel change can be observed, while the area changed to and from 1993 is the largest. The two classes with the highest absolute number of pixels changed between years are savannah and woody savannah. Woody savannah mostly changes to savannah. From 1993 to 2014 this is followed by crops and from 2014 to 2019 by closed shrubland. Savannah also primarily changes to woody savannah. From 1985 to 1993 this is followed by barren, grass or open or closed shrub. From 1993 to 2014 savannah also changes quite a lot to barren followed by agriculture and grassland and from 2014 to 2019 next to woody savannah mainly to barren. The amount of savannah that turns into woody savannah is around the same amount that turns from woody savannah to savannah.

Pixels classified as barren, closed shrub, open shrub, grassland and agriculture shift the most between years in relative terms. From 1985 to 1993 closed shrubland primarily turns into either (woody) savannah, forest, open shrub or crops. From 1993 to 2014 closed shrublands turns into (woody) savannah, crops or grass and from 2014 to 2019 there is primarily a shift to woody savannah. Open shrub follows a similar pattern with changes to closed shrub, savannah and woody savannah. Grassland mainly shifts to savannah or woody savannah over the years. From 1993 to 2014 pixels also move from grassland to barren or agriculture. The decrease of barren in figure 26 in 1993 are primarily pixels changing from barren to savannah. Lastly, pixels classified as agriculture do not stay classified as agriculture throughout the years. The classes that have primarily been turned into agriculture are savannah, woody savannah, closed shrubland and forest. In figure 27 an example of an area previously covered by these classes and turned into agriculture is shown.

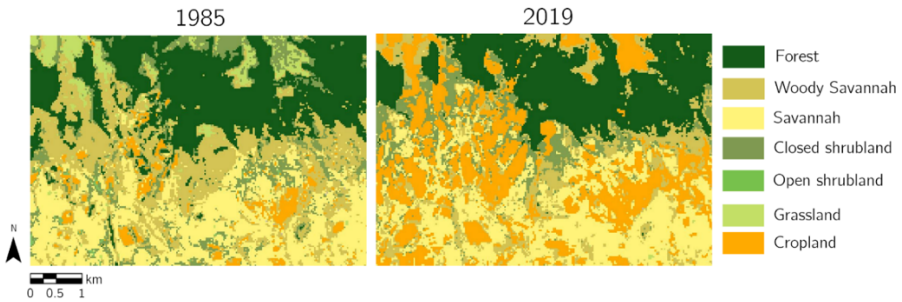

Figure 27
Visualisation of an area turned into agriculture around the forest in the east, close to Monduli (the village)

Forests primarily shift from and to no data, which is related to cloud cover above the mountains. Next to no data, pixels formerly classified as forest also move to woody savannah, followed by agriculture and close shrubland. From 1985 to 0.4% of the surface changes from forest to woody savannah, from 1993 to 2014 this number was 0.5% and from 2014 to 2019 0.3%. The shift to either closed shrub or agriculture mainly took place from 1993 to 2014. During this period 0.5% of the surface changed from forest to closed shrubland and 0.3% to agriculture.

Water and built environment both have a relatively constant increase. Built environment increased in and round the 6 villages. Savannah has been the primary LULC class to turn into built environment over the years, however other LULC classes also decrease as a result of an increase

in built environment. In figure 28 an example of an area where this process occurred is demonstrated.

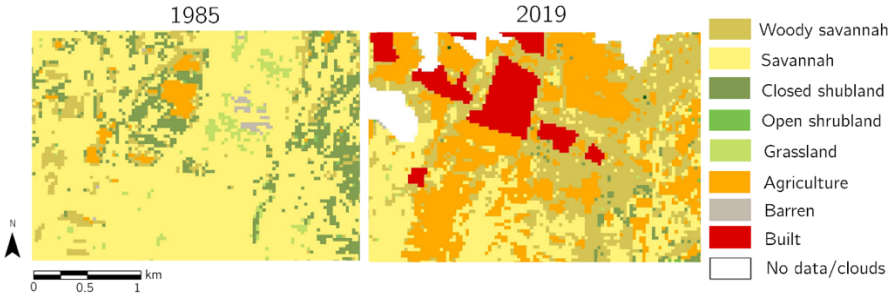

Figure 28
Visualisation of an area turned into built environment around Monduli (the village)

Water also shows a constant increase throughout the years. The primary class to be turned into water is barren. In figure 29 the lake in the north is demonstrated in 1985 and 2019.

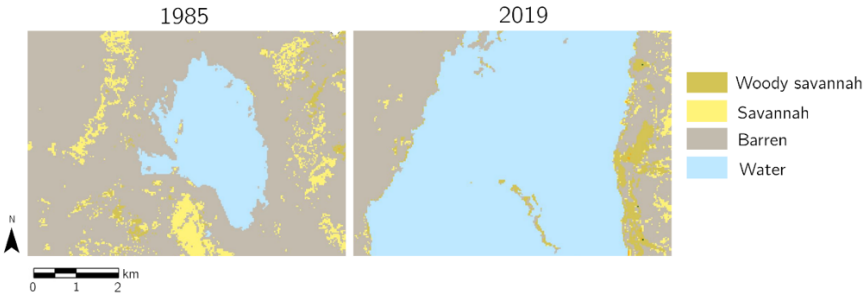

Figure 29
Visualisation of the increase of the lake in the north of the study area

6. Discussion

6.1. Reflection and relation to other studies

Monduli contains several components that make the landscape difficult to map with remote sensing, which resulted in complications in previously conducted studies (van den Bergh, 2016; Verhoeve, 2019). This study has attempted to combat these issues and increase the accuracy of the classifications. In total three classification methods have been applied on Landsat and Sentinel imagery: ISODATA, maximum likelihood and random forest, and the most accurate classifications are used for a post-classification change detection analysis.

To answer the first sub research question '*How is the land use and cover classified in Monduli with the use of an unsupervised ISODATA classification method?'* four unsupervised ISODATA classifications have been produced. In these classifications the data is grouped based on the characteristics of the data itself and independent of the ground truth. The ISODATA classifications only reached an overall accuracy of 0.368 to 0.430. This means there is a moderate to poor agreement. Classes that increase the overall accuracy are forest and water, followed by savannah, barren and agriculture, while other classes primarily have a user´s and producer´s accuracy close to zero. The classifications demonstrated there is a difference in the way the savannah landscape is grouped per image. In some images a large area is grouped into one class and in others there is more variation. Specifically, in 2016 more LULC groups can be observed. This indicates there are differences in the spectral reflectance of the savannah landscape between images, which demonstrates the difficulty of choosing imagery with a similar phenology in the study area. It is important imagery originates from the same season, in order to prevent that conclusions are drawn as a result of differences in phenology. Consequently, in this study only imagery in and around the same month the ground truth is collected in has been used. However, because of the dry and wet seasons, there can be differences in precipitation patterns throughout the year in the study area, which results in variations in reflectance values. The imagery in this study is taken during the months January to March, which is after the 'short rains' or at the beginning of the 'long rains'. In hind side, the short rains might be less reliable compared to the long rains which means there is a higher chance of differences in precipitation patterns between years. Therefore, images are more likely to have differing reflectance values. Furthermore, a shift in precipitation seems to have occurred. This means there has been an increase in rainfall during the shorter OND (October, November, December) rain season. As the used imagery ranges from January to March, higher rainfall during the OND season in the past few years could have potentially influenced the amount of green vegetation in more recent imagery. Additionally, as mentioned, in some classifications large areas are grouped into one class. This last issue is related to the similarity of the spectral reflectance of the savannah landscape, which is also mentioned in other studies (Meerman & Sabido, 2001; Stuart et al., 2006). The similarity of the classes for the visible part of the electromagnetic spectrum can also be observed in the photographs of the land use and cover classes in chapter 4.3. This similarity in spectral reflectance of some vegetation classes also caused issues for the supervised classifications.

To answer the second sub research question '*How is the land use and cover classified in Monduli with the use of a supervised maximum likelihood classification method?'* four maximum likelihood classifications have been produced. The classifications reached an overall accuracy of 0.659 to

0.516 and kappa coefficient of 0.616 to 0.455 which, although higher compared to the unsupervised classifications, also indicates a moderate to poor agreement between the classification and the reference data. Open shrub, closed shrub, woody savannah and savannah are the classes with the lowest user's and producer's accuracy. Regardless, the issue with the separation of the LULC class 'water' encountered by van den Bergh (2016), demonstrated in chapter 2.8, is not present in these classifications. This could be due to the fact that the classifier is trained separately for the 1985 classification and by the inclusion of a moisture index (MSI). The supervised maximum likelihood classifications resemble the landscape more compared to the unsupervised classifications and have slightly higher accuracies. However, they demonstrate relatively large fluctuations in the distribution of the LULC classes. For example, there are some unlikely fluctuations in forested areas, also encountered by Verhoeve (2019). Between 1985 and 2014 some differences in the LULC distribution are expected, while from 2014 to 2016 and 2019, the distribution should be relatively similar as some classes cannot increase and decrease within one or two years. The low accuracy and high fluctuations in classes for the maximum likelihood classification in this study raises further questions about the accuracy of the classifications by van den Bergh (2016), who also used a maximum likelihood method. In the study by van den Bergh (2016), an accuracy of 0.935 has been reached for the 2016 classification, while in this study the overall accuracy is 0.604 for 2016. However, the higher accuracy achieved by van den Bergh (2016) could be related to the amount of classes used. In the classification and accuracy assessment by van den Bergh (2016) different vegetation types (open shrub, closed shrub, woody savannah and savannah), which decreased the overall accuracy in this study, are all grouped into one savannah class. If these classes would have been grouped together is this study the accuracy would have most likely also been high. Regardless, relatively high fluctuations in forested areas are observed which makes the results of the maximum likelihood classifications questionable and not accurate enough to draw conclusions about the LULC change in Monduli.

To answer the third sub research question '*How is the land use and cover classified in Monduli with the use of a supervised random forest classification method?'* four random forest classifications have been produced. The accuracy rates of the classifications reach an average overall accuracy of 0.732 and kappa coefficient of 0.699. The classifications still show some fluctuations, nonetheless, much less compared to the maximum likelihood classification. Furthermore, no large, unexpected fluctuations in classes such as forest are observed, and the different vegetation classes have a higher accuracy compared to the maximum likelihood classifications. The accuracy is difficult to compare to Verhoeve (2019), who also used a random forest method, as the training and validation data had not been kept separate in the study by Verhoeve (2019) which results in a large positive bias. Additionally, in the final maps and error matrix by Verhoeve (2019) the different savannah and shrubland vegetation classes are all merged into one savannah class, which increases the accuracy. Regardless of the higher accuracy of the classifications by Verhoeve (2019), issues were encountered with classifying forest and water correctly. As these issues are not present in this study the accuracies of the classifications produced are believed to be higher.

From previous research (Fisher et al. 2018; Karlson et al. 2020) it was expected Sentinel imagery could improve the ability to classify more precise LULC classes and distinguish smaller agricultural areas because of the higher spatial resolution. This is why an answer to the following sub research question has been sought: '*How do the outcomes of the land use and cover classifications of Landsat imagery compare to Sentinel imagery?*' In total six sentinel classifications are compared

to Landsat. Unfortunately, Sentinel imagery did not result in higher accuracies compared to Landsat. Relatively large, unlikely differences in the way the landscape is mapped between 2016 and 2019 are observed. Additionally, something that seemed difficult to distinguish in all of the Sentinel classifications is the shallow water in the north of the study area and the land surrounding it. The inability of the classifiers applied on the Sentinel imagery to recognize differences between LULC classes could be related to the lower number of spectral bands. The SWIR bands are not available in a 10-meter resolution for Sentinel, which means there are less inputs for the classifier to be used to distinguish between classes. The water in the north is the same area that caused issues for the classification of 1985 with Landsat imagery by van den Bergh (2016) and Verhoeve (2019). However, Landsat imagery has a higher number of spectral bands available compared to Sentinel which means the ability to distinguish water should be increased. By also adding a moisture index (MSI), the water could be mapped accurately with Landsat imagery in this study.

As with random forest on Landsat imagery the highest accuracy and least unlikely fluctuations could be achieved in total eight Landsat images have been classified from 1985 to 2019 with the random forest method. The four most accurate classifications reach an overall accuracy of at least 0.746 and kappa coefficient of 0.714. These classifications are used to answer the last sub research questions: *'How does the land use and cover in Monduli change over multiple years from 1985 to 2019 with the best suited method and imagery'* Similar to the maximum likelihood classifications, the classes that decrease the accuracy are open shrub, closed shrub, woody savannah, savannah and grassland. Together, the average producer's accuracy of these classes for the 2019 classification is 0.648 and user's accuracy 0.744, while for forest, barren, agriculture and water the average producer's accuracy is 0.913 and user's accuracy 0.875. From the error matrixes it can be concluded the accuracy for the vegetation classes is lower because these classes are sometimes mixed up. Additionally, from observing the change detection matrixes and maps it can be concluded there is quite some movement of pixels from one vegetation class to another. Specifically, in absolute terms the classification of pixels shifts a lot between savannah and woody savannah. This can be the result of difficulties in mapping the classification of fuzzy boundaries of areas where the number of trees is around the dividing line of 30%.

All the vegetation classes (savannah, open shrubland, closed shrubland and grassland) decreased, except for woody savannah. However, because of fluctuations in the vegetation classes and the lower accuracy, it is difficult to make definitive conclusions about a specific increase or decrease of these areas from 1985 to 2019. Still, what can be concluded with more certainty is that the vegetation classes in total decreased with 2.7%. This decrease can be related to the increase of agriculture, built environment, water and barren. Another class that decreased are forests. From the change detection matrixes, it can be concluded most of this change is related to cloud cover. However, there is also some movement of pixels from forests to other classes. This is mainly woody savannah, followed by agriculture and closed shrubland. The shift from forest to agriculture or closed shrubland is primarily present from 1993 to 2014. Within these years 0.3% of the study area changed from forest to agriculture and 0.5% to closed shrubland. The shift between forest and woody savannah can be the result of the extraction of wood described by Butz (2013). This would correspond to studies in other regions in Africa such as Congo which demonstrate deforestation as forests are turned into woody savannahs (Oliveras & Malhi 2016). However, the area change is relatively small and what should be kept it mind is that some level of misclassifications of fuzzy boundaries could potentially also play a role. In some images, areas

with a number of trees around the boundary line of 60% might be classified as forests and in others as woody savannah.

Thus, classes that increased are agriculture, built environment, water and barren. Despite expected issues with mapping agriculture accurately as a result of small heterogenous agricultural systems in countries in Africa (Burke & Lobell, 2017), the producer's and user's accuracy of this class have been relatively high. There are however quite a lot of fluctuations in pixels classified as agriculture. This could be related to changes in pasture use which means not all fields are covered with crops at the same time. The overall increase in agriculture and built environment has been expected and can be connected to changes in the lifestyle of the Maasai and population growth (Fratkin, 2001; National Bureau of Statistics, 2016; Schmidt, 1997). Additionally, the amount of water has grown from 1985 to 2019. This corresponds to an increase in rainfall in the study area and can also be related to a shift in precipitation to the OND season (Kihupi et al. 2015; Tanzania Meteorological Authority 2019). Barren also increase in size, in total from 1985 to 2019 an increase of 1.0% has been found. This can be a result of grazing pressures (Blake et al. 2018; Kiunsi & Meadows 2006) and an increase in agricultural areas which results in less vegetation cover (Schmidt, 1997). An increase in barren land can be problematic as these areas are prone to soil erosion because less vegetation is present to hold the soil. However, there are large fluctuations in the quantity of barren land. Between the four most accurate classifications (1985, 1993, 2014 and 2019) the biggest difference is observed in 1993. Specifically, barren in the north of the study area decreases and savannah increases 1985 to 1993. The increase in barren from 1985 to 1993 can possibly be related to an increase in rainfall, as from 1987 to 1993 the amount of water in the study area increases from 0.1% to 0.5% while from 1993 to 2014 water only increases to 0.6%. The decrease of barren in 1993 raises questions about the resilience of the landscape and the influence of precipitation patterns on the LULC distribution in Monduli.

The findings in this study have differed from the findings by Kiuni & Meadows (2006) in which LULC changes from 1960 to 1999 are analysed. However, no information on the classification method or accuracy have been given in this study which make the results less well grounded. Additionally, as already mentioned, the higher accuracy results achieved by Bergh (2016) have been the result of the merging of vegetation classes. In this study it has been demonstrated the maximum likelihood method used by van den Bergh (2016) provided less accurate results in Monduli compared to the random forest method used for the final classifications in this study. Verhoeve (2019) also used a random forest method, however the ground truth and training datasets had not been kept independent of each other and the samples were only located in the west of the study area. This has not been the case in this study which makes the accuracy result of much more reliable. However, there are still some remarks to make on the validation process in this study. Ideally an objective sampling method would have been applied in the collection of the ground truth. As no objective sampling has taken place, there could still be some level of positive bias in the accuracy results. Even though the samples were collected throughout the whole study area, some accuracy and training samples could still be relatively close to each other. By using objective sampling first and consequently collecting the ground truth at the sample locations with a combination of high spatial resolution satellite imagery and analysis of the LULC classes in the field, the accuracy results would be the most solid.

Some additional comments can be made about the collection of the ground truth. Certain steps have been taken in order to balance out the original dataset collected by Verhoeve (2019), and to increase the inputs for the classifiers. Extra ground truth is collected with the use of high

spatial resolution satellite imagery and points are sampled within the polygons to increase the inputs for the classifier and further balance out the ground truth classes. Additionally, the dataset has been adjusted for each year and the classifier is trained separately. With this method there is a higher chance of faults in the newly collected ground truth dataset as it has not been possible to verify the polygons in the field. Furthermore, the adjustments of the dataset for the imagery before 2016 can be less accurate compared to recent years as no sentinel imagery with a 10-meter resolution is available to use as a reference. However, these steps still seem to have a positive influence on the accuracy of the classifications when comparing them to Verhoeve (2019) and van den Bergh (2016) as in these studies it had not been possible to accurately classify classes with distinctive spectral signatures, such as water, in all the classifications. Additionally, no large, unlikely, fluctuations in forested areas are observed for the random forest classifications in this study.

6.2. Recommendations for further research

In hind side it could be argued imagery during the long rain season (MAM) might be better suited for the study area as this season produces the most reliable rains. Additionally, the highest spectral variation can be recorded during the long rains which might increase the ability to differentiate between different types of savannah. However, a downside is the high probability of cloud cover in this season. Additionally, during the long rain season there could still be differences in rainfall quantities observed. When images from the longer dry season (June to September) are chosen there is less spectral variation, which is needed to differentiate between vegetation classes, however it is most likely images have a similar phenology. This means there could be a higher chance changes recorded in the study are actually the result of changes to the landscape and not because of differences in phenology. This is something that should be taken into account in further research. Additionally, something to keep in mind is that Sentinel has a higher temporal resolution which means there is a higher chance of the availability of low cloud cover in images. Thus, using Sentinel in a 30-meter resolution with all the available spectral bands for more recent years, in combination with Landsat 30 meter for the other years, could be useful.

Moreover, in this study there have still been some complications with the classification of fuzzy boundaries, specifically between savannah and woody savannah. Further research in the study area can try to combat this by using a fuzzy or continuous classification method. Maps created with a fuzzy classification technique are more difficult to present and to use for change detection, however they can contain a higher amount of information and will represent the surface more accurately. An example of a study which applies a fuzzy classification and gradient technique for mapping vegetation is performed by Feilhauer et al. (2020).

Furthermore, in this study an increase in the ability to map the agriculture in the heterogeneous system in Monduli has been sought by using sentinel imagery. It was expected Sentinel is more capable at mapping detailed classes and smaller patches of LULC classes because of the higher spatial resolution. However, because of the lower number of spectral bands available less distinctions could be made between the classes. Regardless of the lower resolution of the Landsat imagery in the classifications the accuracy of agriculture has been high in this study. However, potentially a lower amount of small agricultural areas have been included in the study area as they are not recognized in the satellite imagery and have therefore not been included in the

training and validation datasets. In future research a further increase of the accuracy of agriculture and ability to map other classes could be sought by combining Landsat and Sentinel imagery. This technique is called image fusion (Xie et al. 2008). Crnojevic et al., (2014) applied this method on landsat-8 and RapidEye imagery to map small agricultural areas in Serbia and improved the overall accuracy of the classifications of small and large agricultural fields.

Additionally, improvements of classifications in arid regions such as Monduli could possibly be achieved with deep learning algorithms. For this study the possibilities of this method have also been explored. The method has existed for a relatively short period of time but gained attention in recent years in relation to LULC classifications. With this method patterns can be detected without applying a segmentation process. This could potentially solve issues in cases where classes are difficult to distinguish from each other because of their similarity (Stoian et al. 2019). One of the deep learning models are Convolutional Neural Networks (CNN). In a CNN network an architecture is used in which image patches are extracted and ran through a hierarchy of filters. In a CNN there is an automatic feature extraction from labelled images. It has originally been used for images that had to be classified into one single class label (Ronneberger, Fischer & Brox 2015). However, in LULC classifications in the output each pixel should get a class label. For land cover classification two CNN approaches can be used. The first category are patch-based approaches which label the centre pixel of an image patch. Second are approaches that use a specific network architecture to be able to classify every pixel of an image (Stoian et al. 2019). One of the second approaches is U-net. The first application of U-net has been for the semantic segmentation of biomedical images in 2015 (Ronneberger et al. 2015). U-net solves issues with localization by performing the classification on each pixel which means the input and output are the same size (Ronneberger et al. 2015). Furthermore, approaches like U-net are computationally more efficient compared to patch-based approaches, and they also learn spatial dependencies between classes (Stoian et al. 2019). Something to take into consideration when applying deep learning is that in GIS software such as Erdas Imagine, Qgis and ArcGIS LULC classification with deep learning is momentarily only available (with U-net) in ArcGIS PRO. Most CNN architectures need a large number of classified images to train the classifier. U-net claims to be able to be trained from a small amount of images (Ronneberger et al. 2015) and in Arcgis PRO it is even possible to use 'sparse training data' which means only a part of the training image has to be classified ("Land Cover Classification Using Sparse Training Data", n.d.). However, it is only possible to use 8bit RGB images and it is not possible to choose differing image patch sizes. It would however be possible to build a new CNN architecture in deep learning architectures such as pytorch or keras. What should be taken into account is that, as mentioned, for most CNN architectures a large number of fully classified images is needed to achieve a high accuracy. For Europe a dataset of 24000 labelled Sentinel-2 images is available (German Research Center for Artificial Intelligence, 2019). In order to use a CNN architecture for classifications in Africa such a dataset needs to be available to use.

Lastly, this study demonstrates barren ground in Monduli fluctuates in quantity. The decrease of barren during an increase in water indicates that precipitation patterns have a large influence on the distribution of the LULC classes. It shows barren ground regenerates again after period of more drought. Further research into the resilience of the landscape and relationship between the LULC distribution and precipitation patterns would be needed to increase understanding of the landscape.

7. Conclusion

This study has sought to answer the following research question: *How has the land use and land cover (LULC) in the Monduli district in Tanzania changed over time from 1985 to 2019?*

Three classification methods have been applied on Landsat and Sentinel imagery: an unsupervised ISODATA method, a supervised maximum likelihood method and a supervised random forest method. Sentinel 2 has a higher spatial resolution compared to Landsat 4, 5 and 8, however, unfortunately Sentinel 2 classifications did not offer a higher accuracy. This can be related to the lower number of spectral bands available which makes distinguishing classes with similar spectral signatures more complicated. Regardless, with the Landsat imagery relatively high accuracies could be achieved with the random forest classification algorithm. The classifications produced in this study show less unrealistic fluctuations in LULC classes over the years compared to previously conducted studies and the accuracies are believed to be higher. In total, eight land use and cover classifications of the study area with a random forest method have been produced of which four achieved an overall accuracy above 0.747. This means there is a moderate to high correspondence between the classifications and the reference data. These classifications have been used for the post-classification change detection method.

From 1985 to 2019 savannah, grassland, closed shrub and open shrub decrease, and woody savannah, barren, agriculture, water and built environment increase. The specific quantities are shown in table 15. If an increase has occurred in comparison to the previous year the number is visualised in a green box and if the class decreased the number is visualised in an orange box. On the right side the increase or decrease from 1985 to 2019 is shown.

Table 15
LULC quantities in percentages of 1985, 1993, 2014 and 2019

	Total 1985 %	*Total 1993 %*	*Total 2014 %*	*Total 2019 %*	*1985 > 2019*	
Forest	3.4	4.1	3.8	3.0	- 0.4%	
Woody Savannah	27.5	28.8	30.1	29.2	+ 1.7%	
Savannah	36.5	42.9	33.6	34.5	- 2.0%	
Closed shrubland	4.5	4.5	3.2	4.0	- 0.5%	- 2.7%
Open shrubland	1.8	3.4	0.9	0.6	- 1.2%	
Grassland	4.7	5.3	5.9	4.0	- 0.7%	
Barren	11.3	4.4	12.0	12.3	+ 1.0%	
Agriculture	4.4	2.5	9.2	6.9	+ 2.5%	
Built	0.0	0.1	0.3	0.3	+ 0.3%	
Water	0.1	0.5	0.6	0.7	+ 0.6%	
No data/clouds	5.8	3.4	0.4	4.5		

The different vegetation types (savannah, woody savannah, grassland and open and closed shrubland) show some fluctuations. Furthermore, the user's and producer's accuracy of these classes is lower compared to the other classes, as one vegetation class is sometimes misclassified as another. This can be related to similarities in spectral signatures, complications in classifying fuzzy boundaries and differences in phenology between the imagery, which makes a definitive

conclusion of an increase or decrease from 1985 to 2019 of the specific vegetation classes less reliable compared to other LULC classes. However, when the different vegetation classes are grouped together as one class, the amount decreased with 2.7% in total from 1985 to 2019.

The decrease in forests seems to be primarily the result of cloud cover in certain images. However, there are also some pixels previously classified as forests that turned into woody savannah and a small amount that changed to closed shrubland and agriculture. Other LULC classes that changed to agriculture have been savannah, woody savannah and closed shrubland. Agriculture is located primarily in the middle of the study area, under the forest in the east around Monduli (the village), in the south-east around Lokisale and in the west side around Mto Wa Mbu. Other classes that increased are barren, built environment and water. The increase in barren land from 1985 to 2019 is primarily located in the north of the study area and seems to be at the expense of savannah. However, over the years some fluctuations in barren can be observed. From the four most accurate classifications the largest decrease can be observed in 1993 which mainly results in an increase in savannah. The increase in built environment from 1985 to 2019 is primarily located in and around the 6 villages in the study area. Savannah has been the main class to turn into built environment. Lastly, a consistent increase in water in the study area is detected throughout the years. The primary class that has turned into water is barren land.

Thus, in moduli an increase in agriculture, barren, water and built environment can be observed at the expense of vegetation ((woody) savannah, shrubland and grassland). However, the amount of barren does show some fluctuation over the years. Lastly a decrease in forests is detected. Next to cloud cover this seems to be primarily the result of an increase in woody savannah followed by closed shrub and agriculture.

8. Acknowledgements

I would like to express my appreciation to several people for their involvement in the development of this thesis. First of all, Maarten Zeylmans van Emmichoven for his help with technical components and continuous support and meetings, and Steven de Jong for his overall guidance and for steering me into the right directions. Additionally, I would greatly like to thank IMAGEM for their help and specifically Wim Bozelie for the advice and assistance in the development of a model for random forest classifications in Erdas Imagine. Lastly, I also want to thank Geert Sterk for the input in meetings and Steye Verhoeve for his involvement and by providing me his ground truth dataset and photographs.

9. Bibliography

Abbas, A. W., Minallh, N. Ahmad, N. Abid, S. A. R. & Khan. M. A. A. (2016). K-Means and ISODATA Clustering Algorithms for Landcover Classification Using Remote Sensing. *Sindh University Research Journal - SURJ (Science Series)* 48(2):315–18.

AirBnB. (n.d.). *AirBnB Image Monduli*. Retrieved january 25th 2021 from https://www.airbnb.co.uk/rooms/25925747/photos?adults=1&federated_search_id=56885079-3dbf-40f5-8e9c-7aecf10fe594&source_impression_id=p3_1611939446_WbspfUoIwVCz5%2F14&guests=1

Al-doski, J., Mansor S. B. & Shafri. H. Z. M. (2013). Change Detection Process and Techniques. *Civil and Environmental Research* 3(10):37–46.

Almutairi, A., & Warner, T. A. (2010). Change Detection Accuracy and Image Properties: A Study Using Simulated Data. *Remote Sensing* 2(6):1508–29. doi: 10.3390/rs2061508.

Bashir, S., Javed, A. & Bibi. I. (2018). Soil and Water Conservation. *In: Sabir M, Akhtar J, Hakeem KR (Eds) Soil Science Concepts and Applications. University of Agriculture, Faisalabad* 57(10):708–11. doi: 10.1029/EO057i010p00708.

Bayala, J., Sanou, J., Teklehaimanot, Z., Ouedraogo, S. J., Kalinganire, A. Coe, R. & van Noordwijk, M. (2015). Advances in Knowledge of Processes in Soil-Tree-Crop Interactions in Parkland Systems in the West African Sahel: A Review. *Agriculture, Ecosystems and Environment* 205:25–35. doi: 10.1016/j.agee.2015.02.018.

Bégué, A., Arvor, D., Bellon, B., Betbeder, J., de Abelleyra, D., Ferraz, R. P. D., Lebourgeois, V., Lelong, C., Simões, M. & Santiago Verón, R. (2018). Remote Sensing and Cropping Practices: A Review. *Remote Sensing* 10(1):1–32. doi: 10.3390/rs10010099.

Blake, W. H., Rabinovich, A., Wynants, M., Kelly, C., Nasseri, M., Ngondya, I., Patrick, A., Mtei, K., Munishi, L., Boeckx, P., Navas, A., Smith, H. G., Gilvear, D., Wilson, G., Roberts, N. & Ndakidemi, P. (2018). Soil Erosion in East Africa: An Interdisciplinary Approach to Realising Pastoral Land Management Change. *Environmental Research Letters* 13(12):124014. doi: 10.1088/1748-9326/aaea8b.

Breiman, L. (2001). Random Forests. *Machine Learning* 45(1):5–32. doi: 10.1023/A:1010933404324.

Breiman, L. (2002). *Manual On Setting Up, Using, And Understanding Random Forests V3.1.* https://www.stat.berkeley.edu/~breiman/Using_random_forests_V3.1.pdf

Brodley, C. E., and Mark A. Friedl. (1997). Decision Tree Classification of Land Cover from Remotely Sensed Data. *Remote Sensing of Environment* 61(3):399–409. doi: 10.1016/S0034-4257(97)00049-7.

Burke, M., & Lobell, D. B. (2017). Satellite-Based Assessment of Yield Variation and Its Determinants in Smallholder African Systems. *Proceedings of the National Academy of Sciences of the United States of America* 114(9):2189–94. doi: 10.1073/pnas.1616919114.

Butz, R. J. (2013). Changing Land Management: A Case Study of Charcoal Production among a Group of Pastoral Women in Northern Tanzania. *Energy for Sustainable Development* 17(2):138–45. doi: 10.1016/j.esd.2012.11.001.

Campbell, J. B. (2002). *Introduction to Remote Sensing*. 3rd ed. Guilford Press, New York.

Chuvieco, E., & Congalton, R. G. (1988). Using Cluster Analysis to Improve the Selection of Training Statistics in Classifying Remotely Sensed Data. *Photogrammetric Engineering and Remote Sensing* (54):1275–1281.

Clark, B. J. F., & Pellikka, P. K. E. (2009). Landscape Analysis Using Multi-Scale Segmentation and Object-Oriented Classification. *Recent Advances in Remote Sensing and Geoinformation Processing for Land Degradation Assessment* 323–41. doi: 10.1201/9780203875445.ch21.

Cohen, J. (1960). A Coefficient of Agreement for Nominal Scales. *Educational and Psychological Measurement* 20:37–46. doi: 10.1177/001316446002000104

Congalton, R. (2001). Accuracy Assessment and Validation of Remotely Sensed and Other Spatial Information. *International Journal of Wildland Fire* 10(3–4):321–28. doi: 10.1071/wf01031.

Congalton, R., and Green, K. (2019). *Assessing the Accuracy of Remotely Sensed Data: Principles and Practices.*. Londen: Routledge.

Cortes, C., & Vapnik, V. (1995). Support-Vector Networks. *Machine Learning* 20:273–97. doi: 10.1007/BF00994018.

Crnojevic, V., Lugonja, P., Brkljac, B., & Brunet, B. (2014). Classification of Small Agricultural Fields Using Combined Landsat-8 and RapidEye Imagery: Case Study of Northern Serbia. *Journal of Applied Remote Sensing* 8(1):083512. doi: 10.1117/1.jrs.8.083512.

Dimitriadis, S. I., & Liparas, D. (2018). How Random Is the Random Forest? Random Forest Algorithm on the Service of Structural Imaging Biomarkers for Alzheimer's Disease: From Alzheimer's Disease Neuroimaging Initiative (ADNI) Database. *Neural Regeneration Research* 13(6):962–70. doi: 10.4103/1673-5374.233433.

Duda, T., and Canty, M. (2002). Unsupervised Classification of Satellite Imagery: Choosing a Good Algorithm. *International Journal of Remote Sensing* 23(11):2193–2212. doi: 10.1080/01431160110078467.

Eiumnoh, A., & Shrestha, R. P. (2000). Application of DEM Data to Landsat Image Classification: Evaluation in a Tropical Wet-Dry Landscape of Thailand. *Photogrammetric Engineering and Remote Sensing* 66(3):297–304.

Land Cover Classification Using Sparse Training Data. (n.d.) Retrieved September 28, 2020 from https://developers.arcgis.com/python/sample-notebooks/land-cover-classification-using-sparse-training-data/

Feilhauer, H., Zlinszky, A., Kania, A., Foody, G. M., Doktor, D., Lausch, A. & Schmidtlein, S. (2020). Let Your Maps Be Fuzzy!—Class Probabilities and Floristic Gradients as Alternatives to Crisp Mapping for Remote Sensing of Vegetation. *Remote Sensing in Ecology and Conservation* 1–14. doi: 10.1002/rse2.188.

Fisher, J. R. B., Acosta, E. A., Dennedy-Frank, P. J., Kroeger, T. & Boucher, T. M. (2018). Impact of Satellite Imagery Spatial Resolution on Land Use Classification Accuracy and Modeled Water Quality. *Remote Sensing in Ecology and Conservation* 4(2):137–49. doi: 10.1002/rse2.61.

Fratkin, E. (2001). East African Pastoralism in Transition: Maasai, Boran, and Rendille Cases. *African Studies Review* 44(3):1–25. doi: 10.2307/525591.

German Research Center for Artificial Intelligence. (2019). *Multimedia Analysis & Data Mining: Downloads*. Retrieved from http://madm.dfki.de/downloads

Homewood, K., Kristjanson, P. & Trench, P. C. (2009). Changing Land Use, Livelihoods and Wildlife Conservation in Maasailand. Chapter 1 in Homewood K, Kristjanson P, Chenevix Trench P. 2009. '*Staying Maasai? Livelihoods, Conservation and Development in East African Rangelands'*. Springer Press, New York.

Huerte, A. R. (2004). Remote Sensing for Environmental Monitoring. In *Environmental Monitoring and Characterization*: 183-206. doi: 10.1016/B978-012064477-3/50013-8

Iranga, M. D. (1992). Seismicity of Tanzania: Distribution in Time, Space, Magnitude, and Strain Release. *Tectonophysics* 209(1–4):313–20. doi: 10.1016/0040-1951(92)90040-D.

Jensen, J. R. (2004). *Introductory Digital Image Processing; A Remote Sensing Perspective*. New Jersey: Prentice Hall.

De Jong, S. M., Van der Meer, F. D. & Clevers. J. (2004). *Remote Sensing Image Analysis: Including the Spatial Domain*. Vol. 5. London, UK: Dordrecht.

Karlson, M., Ostwald, M., Bayala, J., Bazié, H. R., Ouedraogo, A., S., Soro, B., Sanou, J. & Reese. H. (2020). The Potential of Sentinel-2 for Crop Production Estimation in a Smallholder Agroforestry Landscape, Burkina Faso. *Frontiers in Environmental Science* 8(June):1–13. doi: 10.3389/fenvs.2020.00085.

Kihupi, N. I., Tarimo, A. K. P. R., Masika, R. J., Boman, B., & Dick, W. A. (2015). Trend of Growing Season Characteristics of Semi-Arid Arusha District in Tanzania. *Journal of Agricultural Science* 7(9). doi: 10.5539/jas.v7n9p45.

Kiunsi, R. B., & Meadows, M. E. (2006). Assessing Land Degradation in the Monduli District, Northern Tanzania. *Land Degradation and Development* 17(5):509–25. doi: 10.1002/ldr.733.

Landis, J., & Koch, G. (1977). The Measurement of Observer Agreement for Categorical Data. *Biometrics* 33:159–174. doi: 10.2307/2529310

Lein, J. K. (2011). *Environmental Sensing: Analytical Techniques for Earth Observation*. Springer Science & Business Media.

Level-2. (n.d.). Retrieved February 15, 2021 from https://sentinels.copernicus.eu/web/sentinel/user-guides/sentinel-2-msi/processing-levels/level-2

Li, M., Zang, S., Zhang, B. Li, S. & Wu, C. (2014). A Review of Remote Sensing Image Classification Techniques: The Role of Spatio-Contextual Information. *European Journal of Remote Sensing* 47(1):389–411. doi: 10.5721/EuJRS20144723.

Liaw, A., & M. Wiener. (2002). Classification and Regression by RandomForest. *R News* 2(3):18–22.

Lillesand, T., & Kiefer. W. R. (2015). *Remote Sensing and Image Interpretation*. Hoboken, New Jersey: Wiley

Loth, P. E., & Prins, H. (1986). Spatial Patterns of the Landscape and Vegetation of Lake

Manyara National Park. *ITC Journal* 2:115–30.

Loveland, T. R., & Belward, A. S. (1997). The IGBP-DIS Global 1km Land Cover Data Set, DISCover: First Results. *International Journal of Remote Sensing* 18(15):3289. doi 10.1080/014311697217099

Lu, D., Mausel, P., Brondízio, E. & E. Moran. (2004). Change Detection Techniques. *International Journal of Remote Sensing* 25(12):2365–2401. doi: 10.1080/0143116031000139863.

Luhunga, P. M., Kijazi, A. L., Chang'a, L., Kondowe, A., Ng'ongolo, H. & Mtongori, H. (2018). Climate Change Projections for Tanzania Based on High-Resolution Regional Climate Models from the Coordinated Regional Climate Downscaling Experiment (CORDEX)-Africa. *Frontiers in Environmental Science* 6(OCT):1–20. doi: 10.3389/fenvs.2018.00122.

Macleod, R. D., & Congalton, R. G. (1998). A Quantitative Comparison of Change-Detection Algorithms for Monitoring Eelgrass from Remotely Sensed Data. *Photogrammetric Engineering and Remote Sensing* 64(3):207–16.

Maisongrande, P., Kuhlmann, J., Boulet, G., Lobo, A., Henry, P. & Hafeez, M. (2007). ENSO Impact on the Australian Vegetation: A Satellite Diagnostic from 1998-2006. *MODSIM07 - Land, Water and Environmental Management: Integrated Systems for Sustainability, Proceedings* (December):2583–89.

McRoberts, R. E., Tomppo, E. O. & Czaplewski, R. L. (2014). Sampling Designs for National Forest Assessments: Knowledge Reference for National Forest Assessments. *Food and Agricultural Organisation of the UN (FAO)* 23–40.

Meerman, J. C., & Sabido, W. (2001). *Central American Ecosystems: Belize*. Programme for Belize, Belize City. 2 volumes 50 + 88 pp.

Millard, K., & Richardson, M. (2015). On the Importance of Training Data Sample Selection in Random Forest Image Classification: A Case Study in Peatland Ecosystem Mapping. *Remote Sensing* 7:8489–8515.

Millard, K., &. Richardson, M. (2015). On the Importance of Training Data Sample Selection in Random Forest Image Classification: A Case Study in Peatland Ecosystem Mapping. *Remote Sensing* 7(7):8489–8515. doi: 10.3390/rs70708489.

Msoffe, F. U., Kifugo, S. C., Said, M. Y., Neselle, M. O., van Gardingen, P., Reid, R. S., Ogutu, J. O., Herero, M., and de Leeuw, J. (2011). Drivers and Impacts of Land-Use Change in the Maasai Steppe of Northern Tanzania: An Ecological, Social and Political Analysis. *Journal of Land Use Science* 6(4):261–81. doi: 10.1080/1747423X.2010.511682.

Mtui, D. T., Lepczyk, C. A., Chen, Q., Miura, T. and Cox, L. J. (2017). Change in Two Wildlife Protected Areas in Tanzania Using Landsat Imagery. *PLoS ONE* 12(9):1–20. doi: 10.1371/journal.pone.0185468

National Bureau of Statistics. (2016). *Arusha Region, Basic Demographic and Socio-Economic Profile, 2012 Population and Housing Census*.

Navulur, K. (2006). *Multispectral Image Analysis Using the Object-Oriented Paradigm.* New York: Taylor and Francis.

Van Niel, T. G., McVicar, T. R & Datt., B. (2005). On the Relationship between Training

Sample Size and Data Dimensionality: Monte Carlo Analysis of Broadband Multi-Temporal Classification. *Remote Sensing of Environment* 98(4):468–80. doi: 10.1016/j.rse.2005.08.011.

Observing in infrared. (2014, Mar 4). Retrieved January 25, 2020 from https://earthobservatory.nasa.gov/features/FalseColor/page5.php

Oliveras, I., & Malhi, Y. (2016). Many Shades of Green: The Dynamic Tropical Forest–Savannah Transition Zones. *Philosophical Transactions of the Royal Society B: Biological Sciences* 371(1703). doi: 10.1098/rstb.2015.0308.

Olofsson, P., C. E. Woodcock, C. Holden, M. A. Friedl, and D. Sulla-Menashe. (2014). "Good Practices for Estimating Area and Assessing Accuracy of Land Change." *Remote Sensing of Environment* 148:42–57. doi: 10.1016/j.rse.2014.02.015.

Pilon, P.G., Howarth, P.J., Bullock, R.A., and Adeniyi, P.O. (1988). An enhanced classification approach to change detection in semi- arid environments, Photogrammetric Engineering b Remote Sensing, 54(12):1709-1716

Pimentel, D. (2006). Soil Erosion: A Food and Environmental Threat. *Environment, Development and Sustainability* 8(1):119–37. doi: 10.1007/s10668-005-1262-8.

Reese, H. M., Lillesand, T. M., Nagel, D. E., Stewart, J. S., Goldmann, R. A., Simmons, T. Chipman, E. J. W. and Tessar, P. A. (2002). Statewide Land Cover Derived from Multi-Seasonal Landsat TM Data: A Retrospective of the WISCLAND Project. 1699:37–55.

Robertson, L. D., & King, D. J. (2011). Comparison of Pixel-and Object-Based Classification in Land Cover Change Mapping. *International Journal of Remote Sensing* 32(6):1505–29. doi: 10.1080/01431160903571791.

Rock, B. N., Vogelmann, J. E., Williams, D. L., Vogelmann, A. F. & Hoshizaki, T. (1986). Remote Detection of Forest Damage: Plant Response to Stress May Have Spectral 'signatures' That Could Be Used to Map, Monitor, and Measure Forest Damaga." *BioScience* 36(7):439–45.

Ronneberger, O., Fischer, P. & Brox, T. (2015). U-Net: Convolutional Networks for Biomedical Image Segmentation. *Lecture Notes in Computer Science (Including Subseries Lecture Notes in Artificial Intelligence and Lecture Notes in Bioinformatics)* 9351:234–41. doi: 10.1007/978-3-319-24574-4_28.

Rozenstein, O. F., & Karnieli, A. (2011). Comparison of Methods for Land-Use Classification Incorporating Remote Sensing and GIS Inputs. *Applied Geography* 31(2):533–44. doi: 10.1016/j.apgeog.2010.11.006.

Schmidt, P. R. (1997). Archaeological Views on a History of Landscape Change in East Africa. *Journal of African History* 38(3):393–421. doi: 10.1017/S002185379700697X.

Sen2Cor (n.d.). Retrieved December 1, 2020 from http://step.esa.int/main/third-party-plugins-2/sen2cor/

Sheykhmousa, M., Mahdianpari, M., Ghanbari, H., Mohammadimanesh, F., Ghamisi, P. & Homayouni, S. (2020). Support Vector Machine Versus Random Forest for Remote Sensing Image Classification: A Meta-Analysis and Systematic Review. *IEEE Journal of Selected Topics in Applied Earth Observations and Remote Sensing* 13:6308–25. doi: 10.1109/JSTARS.2020.3026724.

Stoian, A., Poulain, V., Inglada, J., Poughon, V. & Derksen, D. (2019). Land Cover Maps Production with High Resolution Satellite Image Time Series and Convolutional Neural Networks: Adaptations and Limits for Operational Systems. *Remote Sensing* 11(17):1–26. doi: 10.3390/rs11171986.

Story, M., & Congalton, R. (1986). Accuracy Assessment: A User's Perspective. *Photogrammetric Engineering and Remote Sensing* 52:397–399.

Stuart, N., Barratt, T. & Place, C. (2006). Classifying the Neotropical Savannas of Belize Using Remote Sensing and Ground Survey. *Journal of Biogeography* 33(3):476–90. doi: 10.1111/j.1365-2699.2005.01436.x.

Tanzania Meteorological Authority. (2019). "Statement on the Status of Tanzania Climate in 2019."

Thanh Noi, P., & Kappas, M. (2017). Comparison of Random Forest, k-Nearest Neighbor, and Support Vector Machine Classifiers for Land Cover Classification Using Sentinel-2 Imagery. *Sensors (Basel, Switzerland)* 18(1):18. doi: 10.3390/s18010018.

Landsat Collection 2: Level 2 Science Products (n.d.). Retrieved December 1, 2020 from https://www.usgs.gov/core-science-systems/nli/landsat/landsat-collection-2-level-2-science-products

van den Bergh, H. A. J. (2016). *The Impacts of Maasai Settlement on Land Cover, Meteorological Conditions and Wind Erosion Risk in Northern Tanzania*. Utrecht University.

Verhoeve, S. L. (2019). *Satellite Based Analysis of Environmental Changes in the Monduli and Longido Districts, Tanzania. Utrecht University*.

Xie, Y., Sha, Z. & Yu, M. (2008). Remote Sensing Imagery in Vegetation Mapping: A Review. *Journal of Plant Ecology* 1(1):9–23. doi: 10.1093/Jpe/Rtm005.

Xu, M., Watanachaturaporn, P., Varshney, P. K. & Arora, M. K. (2005). Decision Tree Regression for Soft Classification of Remote Sensing Data. *Remote Sensing of Environment* 97(3):322–36. doi: 10.1016/j.rse.2005.05.008.

Zhang, C., Liu, C., Zhang, X. & Almpanidis, G. (2017). An Up-to-Date Comparison of State-of-the-Art Classification Algorithms. *Expert Systems with Applications* 82:128–50. doi: 10.1016/j.eswa.2017.04.003.

9. Appendices

Appendix A

Error matrixes ISODATA Landsat imagery

A1. Error matrix ISODATA Landsat 1985

Class	*Forest*	*Closed shrub*	*Open shrub*	*Woody savannah*	*Savannah*	*Grassland*	*Agriculture*	*Barren*	*Water*	***Total***	***User Accuracy***
Forest	3335	976	0	197	7	67	192	0	0	4774	0.699
Closed shrub	9	124	230	185	0	61	0	0	0	609	0.204
Open shrub	0	0	0	0	0	0	0	0	0	0	0.000
Woody savannah	402	1392	0	193	0	116	17	0	0	2120	0.091
Savannah	0	1008	3500	2961	3241	3183	3229	1933	0	19055	0.170
Grassland	0	245	0	126	0	0	8	177	0	556	0.000
Agriculture	0	4	0	1	24	0	301	0	4	334	0.901
Barren	0	1	20	29	478	208	3	1640	22	2401	0.683
Water	0	0	0	0	0	0	0	0	3476	3476	1.000
Total	3746	3750	3750	3692	3750	3635	3750	3750	3502	33325	0.000
Producer Accuracy	0.890	0.033	0.000	0.052	0.864	0.000	0.080	0.437	0.993	0.000	0.369

A2. Error matrix ISODATA Landsat 2014

Class	*Forest*	*Closed shrub*	*Open shrub*	*Woody savannah*	*Savannah*	*Grassland*	*Agriculture*	*Barren*	*Water*	***Total***	***User Accuracy***
Forest	3039	510	5	2	0	47	100	0	0	3703	0.821
Closed shrub	4	0	0	15	0	153	158	0	0	330	0.000
Open shrub	0	0	20	9	0	14	44	0	0	87	0.230
Woody savannah	675	2954	200	983	119	335	1030	22	1	6319	0.156
Savannah	25	257	2772	2504	2584	1951	786	1042	145	12066	0.214
Grassland	0	0	0	0	167	0	0	279	0	446	0.000
Agriculture	0	0	0	0	18	2	985	66	28	1099	0.896
Barren	0	29	753	237	862	1248	582	2341	224	6276	0.373
Water	0	0	0	0	0	0	65	0	3257	3322	0.980
Total	3743	3750	3750	3750	3750	3750	3750	3750	3655	33648	0.000
Producer Accuracy	0.812	0.000	0.005	0.262	0.689	0.000	0.263	0.624	0.891	0	0.393

A3. Error matrix ISODATA Landsat 2016

Class	*Forest*	*Closed shrub*	*Open shrub*	*Woody savannah*	*Savannah*	*Grassland*	*Agriculture*	*Barren*	*Water*	***Total***	***User Accuracy***
Forest	3401	1143	117	120	20	101	124	0	0	5026	0.677
Closed shrub	126	268	117	177	218	264	181	0	0	1351	0.198
Open shrub	58	53	649	465	118	154	196	0	0	1693	0.383
Woody savannah	156	2003	713	1802	671	741	957	320	0	7363	0.245
Savannah	0	256	1751	1158	2160	1601	569	1311	31	8837	0.244
Grassland	0	0	8	22	284	754	0	67	1	1136	0.664
Agriculture	0	27	395	0	98	109	1723	956	0	3308	0.521
Barren	0	0	0	5	181	26	0	1096	136	1444	0.759
Water	0	0	0	0	0	0	0	0	3577	3577	1.000
Total	3741	3750	3750	3749	3750	3750	3750	3750	3745	33735	0.000
Producer Accuracy	0.909	0.071	0.173	0.481	0.576	0.201	0.459	0.292	0.955	0.000	0.457

A4. Error matrix ISODATA Landsat 2019

Class	*Forest*	*Closed shrub*	*Open shrub*	*Woody savannah*	*Savannah*	*Grassland*	*Agriculture*	*Barren*	*Water*	***Total***	***User Accuracy***
Forest	3389	1570	102	1	0	0	308	0	0	5370	0.631
Closed shrub	98	586	359	109	21	0	8	0	0	1181	0.496
Open shrub	0	0	0	0	0	0	0	0	0	0	0.000
Woody savannah	240	618	664	976	466	604	612	41	16	4237	0.230
Savannah	12	929	2290	2323	2120	2180	1113	1689	35	12691	0.167
Grassland	3	43	294	20	397	835	73	621	23	2309	0.362
Agriculture	0	4	35	0	0	0	1630	29	0	1698	0.960
Barren	0	0	6	321	746	131	6	1370	74	2654	0.516
Water	0	0	0	0	0	0	0	0	3596	3596	1.000
Total	3742	3750	3750	3750	3750	3750	3750	3750	3744	33736	0.000
Producer Accuracy	0.906	0.156	0.000	0.260	0.565	0.223	0.435	0.365	0.960	0.000	0.430

Appendix B

Error matrixes Maximum Likelihood Landsat imagery

B1. Error matrix Maximum Likelihood Landsat 1985

Class	*Forest*	*Closed shrub*	*Open shrub*	*Woody savannah*	*Savannah*	*Grassland*	*Agriculture*	*Barren*	*Water*	***Total***	***User Accuracy***
Forest	585	0	0	0	0	0	0	0	0	585	1.000
Closed shrub	68	428	0	47	0	0	0	0	0	543	0.788
Open shrub	4	305	577	19	54	392	0	1	0	1352	0.427
Woody savannah	73	17	86	572	125	0	6	0	0	879	0.651
Savannah	0	0	82	109	552	276	8	315	251	1593	0.347
Grassland	20	0	5	0	0	78	0	0	0	103	0.757
Agriculture	0	0	0	3	19	0	736	0	0	758	0.971
Barren	0	0	0	0	0	4	0	434	15	453	0.958
Water	0	0	0	0	0	0	0	0	484	484	1.000
Total	750	750	750	750	750	750	750	750	750	6750	0.000
Producer Accuracy	0.780	0.571	0.769	0.763	0.736	0.104	0.981	0.579	0.645	0.000	0.659

B2. Error matrix Maximum Likelihood Landsat 2014

Class	*Forest*	*Closed shrub*	*Open shrub*	*Woody savannah*	*Savannah*	*Grassland*	*Agriculture*	*Barren*	*Water*	***Total***	***User Accuracy***
Forest	534	0	0	0	0	0	0	0	95	629	0.849
Closed shrub	175	669	58	156	0	0	55	0	0	1113	0.601
Open shrub	0	0	391	1	26	194	18	71	0	701	0.558
Woody savannah	41	62	227	507	119	0	178	0	0	1134	0.447
Savannah	0	0	66	67	432	134	103	204	0	1006	0.429
Grassland	0	0	8	10	0	227	5	4	0	254	0.894
Agriculture	0	19	0	9	0	0	391	0	107	526	0.743
Barren	0	0	0	0	173	195	0	471	11	850	0.554
Water	0	0	0	0	0	0	0	0	537	537	1.000
Total	750	750	750	750	750	750	750	750	750	6750	0.000
Producer Accuracy	0.712	0.892	0.521	0.676	0.576	0.303	0.521	0.628	0.716	0.000	0.616

B3. Error matrix Maximum Likelihood Landsat 2016

Class	*Forest*	*Closed shrub*	*Open shrub*	*Woody savannah*	*Savannah*	*Grassland*	*Agriculture*	*Barren*	*Water*	***Total***	***User's Accuracy***
Forest	644	309	0	12	0	0	27	0	5	997	0.646
Closed shrub	1	4	10	57	0	0	4	0	0	76	0.053
Open shrub	0	98	304	0	22	0	5	6	0	435	0.699
Woody savannah	42	94	9	139	29	2	4	0	0	319	0.436
Savannah	0	0	0	39	259	12	1	53	108	472	0.549
Grassland	0	188	240	169	42	736	22	23	0	1420	0.518
Agriculture	63	57	187	334	19	0	687	0	0	1347	0.510
Barren	0	0	0	0	379	0	0	668	0	1047	0.638
Water	0	0	0	0	0	0	0	0	637	637	1.000
Total	750	750	750	750	750	750	750	750	750	6750	0.000
Producer's Accuracy	0.859	0.005	0.405	0.185	0.345	0.981	0.916	0.891	0.849	0.000	0.604

B4. Error matrix Maximum Likelihood Landsat 2019

Class	*Forest*	*Closed shrub*	*Open shrub*	*Woody savannah*	*Savannah*	*Grassland*	*Agriculture*	*Barren*	*Water*	***Total***	***User's Accuracy***
Forest	637	112	0	0	0	0	0	0	2	751	0.848
Closed shrub	68	136	62	138	0	0	99	0	0	503	0.270
Open shrub	0	186	88	1	0	0	74	4	0	353	0.249
Woody savannah	43	246	226	143	21	0	0	0	0	679	0.211
Savannah	2	0	187	457	621	292	107	259	29	1954	0.318
Grassland	0	65	187	11	10	432	0	63	0	768	0.563
Agriculture	0	5	0	0	0	0	387	0	105	497	0.779
Barren	0	0	0	0	98	26	83	424	0	631	0.672
Water	0	0	0	0	0	0	0	0	614	614	1.000
Total	750	750	750	750	750	750	750	750	750	6750	0.000
Producer's Accuracy	0.849	0.181	0.117	0.191	0.828	0.576	0.516	0.565	0.819	0.000	0.516

Appendix C

Error matrixes Random Forest Landsat imagery

C1. Error matrix Random Forest Landsat 1985

Class	*Forest*	*Closed shrub*	*Open shrub*	*Woody savannah*	*Savannah*	*Grassland*	*Agriculture*	*Barren*	*Water*	***Total***	***User Accuracy***
Forest	748	0	0	0	0	0	0	0	0	748	1.000
Closed shrub	0	546	0	16	0	25	0	0	0	587	0.930
Open shrub	0	12	286	1	9	64	0	0	0	372	0.769
Woody savannah	2	16	289	583	165	30	3	4	0	1092	0.534
Savannah	0	9	0	139	485	254	0	142	0	1029	0.471
Grassland	0	0	175	9	30	375	0	0	0	589	0.637
Agriculture	0	166	0	0	0	0	747	0	0	913	0.818
Barren	0	1	0	2	61	2	0	604	0	670	0.901
Water	0	0	0	0	0	0	0	0	750	750	1.000
Total	750	750	750	750	750	750	750	750	750	6750	0.000
Producer Accuracy	0.997	0.728	0.381	0.777	0.647	0.500	0.996	0.805	1.000	0.000	0.759

C2. Error matrix Random Forest Landsat 1987

Class	*Forest*	*Closed shrub*	*Open shrub*	*Woody savannah*	*Savannah*	*Grassland*	*Agriculture*	*Barren*	*Water*	***Total***	***User Accuracy***
Forest	730	0	0	0	0	0	0	0	0	730	1.000
Closed shrub	2	355	0	50	0	0	0	0	0	407	0.872
Open shrub	0	64	271	6	1	26	0	0	0	368	0.736
Woody savannah	0	275	0	500	236	0	10	0	0	1021	0.490
Savannah	0	33	242	122	349	371	0	0	0	1117	0.312
Grassland	0	23	237	69	66	253	0	0	0	648	0.390
Agriculture	18	0	0	0	0	0	740	0	0	758	0.976
Barren	0	0	0	3	15	100	0	750	0	868	0.864
Water	0	0	0	0	0	0	0	0	750	750	1.000
Total	750	750	750	750	667	750	750	750	750	6667	0.000
Producer Accuracy	0.973	0.473	0.361	0.667	0.523	0.337	0.987	1.000	1.000	0.000	0.705

C3. Error matrix Random Forest Landsat 1993

Class	*Forest*	*Closed shrub*	*Open shrub*	*Woody savannah*	*Savannah*	*Grassland*	*Agriculture*	*Barren*	*Water*	***Total***	***User Accuracy***
Forest	702	3	0	11	0	0	0	0	0	716	0.980
Closed shrub	0	495	0	0	0	0	0	0	0	495	1.000
Open shrub	0	0	216	0	95	0	0	0	0	311	0.695
Woody savannah	48	161	184	475	147	0	0	0	0	1015	0.468
Savannah	0	0	324	158	453	197	6	101	0	1239	0.366
Grassland	0	91	21	81	36	553	0	0	0	782	0.707
Agriculture	0	0	5	25	0	0	742	0	0	772	0.961
Barren	0	0	0	0	19	0	2	649	0	670	0.969
Water	0	0	0	0	0	0	0	0	750	750	1.000
Total	750	750	750	750	750	750	750	750	750	6750	0.000
Producer Accuracy	0.936	0.660	0.288	0.633	0.604	0.737	0.989	0.865	1.000	0.000	0.746

C4. Error matrix Random Forest Landsat 2014

Class	*Forest*	*Closed shrub*	*Open shrub*	*Woody savannah*	*Savannah*	*Grassland*	*Agriculture*	*Barren*	*Water*	***Total***	***User Accuracy***
Forest	673	67	0	3	0	0	9	0	0	752	0.895
Closed shrub	72	678	0	15	0	0	19	0	0	784	0.865
Open shrub	0	0	335	0	0	0	0	14	0	349	0.960
Woody savannah	5	5	309	623	186	32	21	0	0	1181	0.528
Savannah	0	0	17	5	491	335	0	30	0	878	0.559
Grassland	0	0	89	20	19	276	15	35	0	454	0.608
Agriculture	0	0	0	84	1	0	686	14	97	882	0.778
Barren	0	0	0	0	53	107	0	657	0	817	0.804
Water	0	0	0	0	0	0	0	0	653	653	1.000
Total	750	750	750	750	750	750	750	750	750	6750	0.000
Producer Accuracy	0.897	0.904	0.447	0.831	0.655	0.368	0.915	0.876	0.871	0.000	0.751

C5. Error matrix Random Forest Landsat 2015

Class	*Forest*	*Closed shrub*	*Open shrub*	*Woody savannah*	*Savannah*	*Grassland*	*Agriculture*	*Barren*	*Water*	***Total***	***User Accuracy***
Forest	741	0	0	12	0	0	4	0	0	757	0.979
Closed shrub	8	464	0	4	0	4	0	0	0	480	0.967
Open shrub	0	0	220	0	0	11	0	0	0	231	0.953
Woody savannah	1	47	495	564	99	58	19	0	0	1283	0.440
Savannah	0	17	0	102	476	238	15	93	0	941	0.506
Grassland	0	74	35	63	97	412	0	0	0	681	0.605
Agriculture	0	148	0	5	2	4	642	0	0	801	0.801
Barren	0	0	0	0	76	23	70	657	0	826	0.795
Water	0	0	0	0	0	0	0	0	750	750	1.000
Total	750	750	750	750	750	750	750	750	750	6750	0.000
Producer Accuracy	0.988	0.619	0.293	0.752	0.635	0.549	0.856	0.876	1.000	0.000	0.730

C6. Error matrix Random Forest Landsat 2016

Class	*Forest*	*Closed shrub*	*Open shrub*	*Woody savannah*	*Savannah*	*Grassland*	*Agriculture*	*Barren*	*Water*	***Total***	***User Accuracy***
Forest	653	155	0	21	0	0	5	0	0	834	0.783
Closed shrub	66	460	0	146	0	49	24	0	0	745	0.617
Open shrub	0	12	215	0	0	15	1	0	0	243	0.885
Woody savannah	31	76	341	423	305	128	55	0	0	1359	0.311
Savannah	0	15	168	78	353	237	31	93	0	975	0.362
Grassland	0	16	26	42	83	321	44	19	0	551	0.583
Agriculture	0	16	0	40	2	0	590	0	0	648	0.910
Barren	0	0	0	0	7	0	0	638	0	645	0.989
Water	0	0	0	0	0	0	0	0	750	750	1.000
Total	750	750	750	750	750	750	750	750	750	6750	0.000
Producer Accuracy	0.871	0.613	0.287	0.564	0.471	0.428	0.787	0.851	1.000	0.000	0.652

C7. Error matrix Random Forest Landsat 2018

Class	*Forest*	*Closed shrub*	*Open shrub*	*Woody savannah*	*Savannah*	*Grassland*	*Agriculture*	*Barren*	*Water*	***Total***	***User Accuracy***
Forest	697	107	0	64	0	0	50	0	0	918	0.759
Closed shrub	52	340	0	4	0	31	6	0	0	433	0.785
Open shrub	0	2	254	0	0	86	0	0	0	342	0.743
Woody savannah	1	111	442	391	72	0	70	0	0	1087	0.360
Savannah	0	108	0	108	300	274	5	84	0	879	0.341
Grassland	0	3	54	125	221	359	0	3	0	765	0.469
Agriculture	0	79	0	58	37	0	614	0	0	788	0.779
Barren	0	0	0	0	120	0	5	663	57	845	0.785
Water	0	0	0	0	0	0	0	0	693	693	1.000
Total	750	750	750	750	750	750	750	750	750	6750	0.000
Producer Accuracy	0.929	0.453	0.339	0.521	0.400	0.479	0.819	0.884	0.924	0.000	0.639

C8. Error matrix Random Forest Landsat 2019

Class	*Forest*	*Closed shrub*	*Open shrub*	*Woody savannah*	*Savannah*	*Grassland*	*Agriculture*	*Barren*	*Water*	***Total***	***User Accuracy***
Forest	699	149	0	0	0	0	54	0	0	902	0.775
Closed shrub	40	530	0	31	0	0	1	0	0	602	0.880
Open shrub	0	0	281	0	0	0	1	0	0	282	0.996
Woody savannah	9	60	282	652	171	18	19	1	0	1212	0.538
Savannah	2	0	0	47	463	107	1	116	0	736	0.629
Grassland	0	0	187	15	32	503	0	8	0	745	0.675
Agriculture	0	11	0	0	1	0	665	0	0	677	0.982
Barren	0	0	0	5	83	122	9	625	0	844	0.741
Water	0	0	0	0	0	0	0	0	750	750	1.000
Total	750	750	750	750	750	750	750	750	750	6750	0.000
Producer Accuracy	0.932	0.707	0.375	0.869	0.617	0.671	0.887	0.833	1.000	0.000	0.766

Appendix D

Error matrixes ISODATA Sentinel imagery

D1. Error matrix ISODATA Sentinel 2016

Class	*Forest*	*Closed shrub*	*Open shrub*	*Woody savannah*	*Savannah*	*Grassland*	*Agriculture*	*Barren*	*Water*	***Total***	***User Accuracy***
Forest	2614	471	0	136	49	15	121	0	0	3406	0.767
Closed shrub	198	920	136	197	216	235	210	5	0	2117	0.435
Open shrub	27	362	742	592	1040	1400	401	196	0	4760	0.156
Woody savannah	692	1565	186	1510	330	212	520	0	0	5015	0.301
Savannah	201	398	1536	1100	433	540	569	25	0	4802	0.090
Grassland	1	34	1048	202	1525	1344	241	1234	217	5846	0.230
Agriculture	17	0	0	0	30	0	1061	537	0	1645	0.645
Barren	0	0	102	9	118	0	627	443	0	1299	0.341
Water	0	0	0	4	9	4	0	1310	3533	4860	0.727
Total	3750	3750	3750	3750	3750	3750	3750	3750	3750	33750	0.000
Producer Accuracy	0.697	0.245	0.198	0.403	0.115	0.358	0.283	0.118	0.942	0.000	0.373

D2. Error matrix ISODATA Sentinel 2019

Class	*Forest*	*Closed shrub*	*Open shrub*	*Woody savannah*	*Savannah*	*Grassland*	*Agriculture*	*Barren*	*Water*	***Total***	***User Accuracy***
Forest	2439	1	0	26	0	0	1	0	1392	3859	0.767
Closed shrub	1158	2481	336	387	33	467	535	10	93	5500	0.435
Open shrub	7	402	760	35	384	1217	103	96	19	3023	0.156
Woody savannah	135	771	1258	1972	423	246	1130	62	26	6023	0.301
Savannah	8	36	525	665	1496	956	429	879	358	5352	0.090
Grassland	1	1	871	602	1065	516	656	1342	218	5272	0.230
Agriculture	0	56	0	9	3	0	892	0	1	961	0.645
Barren	2	2	0	35	261	180	4	913	173	1570	0.341
Water	0	0	0	19	85	0	0	448	1470	2022	0.727
Total	3750	3750	3750	3750	3750	3582	3750	3750	3750	33582	0.000
Producer Accuracy	0.697	0.245	0.198	0.403	0.115	0.358	0.283	0.118	0.942	0.000	0.373

Appendix E

Error matrixes Maximum Likelihood Sentinel imagery

E1. Error matrix Maximum Likelihood Sentinel 2016

Class	*Forest*	*Closed shrub*	*Open shrub*	*Woody savannah*	*Savannah*	*Grassland*	*Agriculture*	*Barren*	*Water*	***Total***	***User Accuracy***
Forest	724	80	0	9	0	0	35	0	0	848	0.854
Closed shrub	12	529	26	207	3	0	66	0	0	843	0.628
Open shrub	0	56	351	41	123	102	91	0	0	764	0.459
Woody savannah	4	3	181	309	11	1	271	0	0	780	0.396
Savannah	0	2	102	25	236	39	16	5	14	439	0.538
Grassland	3	80	90	104	95	531	26	0	0	929	0.572
Agriculture	0	0	0	55	4	1	243	105	0	408	0.596
Barren	7	0	0	0	278	76	2	625	96	1084	0.577
Water	0	0	0	0	0	0	0	15	640	655	0.977
Total	750	750	750	750	750	750	750	750	750	6750	0.000
Producer Accuracy	0.965	0.705	0.468	0.412	0.315	0.708	0.324	0.833	0.853	0.000	0.620

E2. Error matrix Maximum Likelihood Sentinel 2019

Class	*Forest*	*Closed shrub*	*Open shrub*	*Woody savannah*	*Savannah*	*Grassland*	*Agriculture*	*Barren*	*Water*	***Total***	***User Accuracy***
Forest	739	285	0	113	0	0	63	0	0	1200	0.616
Closed shrub	0	0	0	0	0	0	0	0	0	0	0.000
Open shrub	0	0	0	0	33	2	0	34	0	69	0.000
Woody savannah	7	270	338	475	247	33	34	64	13	1481	0.321
Savannah	3	16	200	68	285	551	3	347	214	1687	0.169
Grassland	0	0	0	0	0	0	0	0	0	0	0.000
Agriculture	1	179	212	94	185	164	650	199	101	1785	0.364
Barren	0	0	0	0	0	0	0	31	0	31	1.000
Water	0	0	0	0	0	0	0	75	422	497	0.849
Total	750	750	750	750	750	750	750	750	750	6750	0.000
Producer Accuracy	0.985	0.000	0.000	0.633	0.380	0.000	0.867	0.041	0.563	0.000	0.385

Appendix F

Error matrixes Random Forest Sentinel imagery

F1. Error matrix Random Forest Sentinel 2016

Class	*Forest*	*Closed shrub*	*Open shrub*	*Woody savannah*	*Savannah*	*Grassland*	*Agriculture*	*Barren*	*Water*	***Total***	***User Accuracy***
Forest	732	127	8	14	1	0	20	0	0	902	0.812
Closed shrub	11	404	7	149	1	3	109	0	0	684	0.591
Open shrub	0	19	395	20	78	113	68	0	0	693	0.570
Woody savannah	3	115	172	410	102	7	214	10	0	1033	0.397
Savannah	0	3	41	114	375	336	39	66	116	1090	0.344
Grassland	0	74	57	23	51	274	12	0	0	491	0.558
Agriculture	4	8	70	20	15	13	249	20	0	399	0.624
Barren	0	0	0	0	124	4	39	651	98	916	0.711
Water	0	0	0	0	3	0	0	3	536	542	0.989
Total	750	750	750	750	750	750	750	750	750	6750	0.000
Producer Accuracy	0.976	0.539	0.527	0.547	0.500	0.365	0.332	0.868	0.715	0.000	0.596

F2. Error matrix Random Forest Sentinel 2019

Class	*Forest*	*Closed shrub*	*Open shrub*	*Woody savannah*	*Savannah*	*Grassland*	*Agriculture*	*Barren*	*Water*	***Total***	***User Accuracy***
Forest	741	358	0	20	0	0	41	0	0	1160	0.639
Closed shrub	0	0	9	0	1	0	0	0	0	10	0.000
Open shrub	0	0	0	3	45	48	3	24	4	127	0.000
Woody savannah	7	172	317	476	127	4	27	11	0	1141	0.417
Savannah	1	22	235	239	397	436	20	225	3	1578	0.252
Grassland	1	198	156	5	0	250	106	22	0	738	0.339
Agriculture	0	0	33	7	19	9	553	184	107	912	0.606
Barren	0	0	0	0	0	0	0	0	0	0	0.000
Water	0	0	0	0	161	3	0	284	636	1084	0.587
Total	750	750	750	750	750	750	750	750	750	6750	0.000
Producer Accuracy	0.988	0.000	0.000	0.635	0.529	0.333	0.737	0.000	0.848	0.000	0.452

Appendix G

Quantities of the LULC change per method of Landsat imagery

G1. Quantity LULC change ISODATA Landsat

	1985		*2014*		*2016*		*2019*	
	km2	*%*	*km2*	*%*	*km2*	*%*	*km2*	*%*
Forest	247	3.5	214	3.1	366	5.2	214	3.2
Woody Savannah	89	1.3	35	0.5	220	3.2	174	2.6
Savannah	5	0.1	9	0.1	324	4.6	8	0.1
Closed Shrubland	192	2.8	986	14.1	1951	28.0	1484	22.2
Open Shrubland	5331	76.4	4105	58.9	2944	42.2	3184	47.7
Grassland	88	1.3	295	4.2	164	2.4	538	8.1
Barren	19	0.3	86	1.2	399	5.7	81	1.2
Agriculture	589	8.4	1150	16.5	298	4.3	921	13.8
Built	10	0.1	41	0.6	57	0.8	50	0.7
Water	3	0.0	23	0.3	23	0.3	23	0.3
No data/clouds	403	5.8	30	0.4	231	3.3	301	4.5

G2. Quantity LULC change Maximum Likelihood Landsat

	1985		*2014*		*2016*		*2019*	
	km2	*%*	*km2*	*%*	*km2*	*%*	*km2*	*%*
Forest	144	2.1	210	3.0	383	5.5	192	2.7
Woody Savannah	1526	21.8	2517	36.1	1093	15.6	982	14.0
Savannah	2873	41.1	1540	22.1	995	14.2	3604	51.5
Closed Shrubland	263	3.8	335	4.8	181	2.6	306	4.4
Open Shrubland	948	13.6	528	7.6	127	1.8	90	1.3
Grassland	137	2.0	229	3.3	979	14.0	200	2.9
Barren	80	1.1	1291	18.5	1551	22.2	933	13.3
Agriculture	612	8.7	233	3.3	1383	19.8	321	4.6
Built	3	0.0	23	0.3	23	0.3	23	0.3
Water	6	0.1	41	0.6	54	0.8	46	0.7
No data/clouds	403	5.8	30	0.4	231	3.3	301	4.3

G3. Quantity LULC change of the first four Random Forest Landsat

	1985		2014		2016		2019	
	km2	%	km2	%	km2	%	km2	%
Forest	239	3.4	264	3.8	271	3.9	212	3.0
Woody Savannah	1921	27.5	2104	30.1	2178	31.1	2042	29.2
Savannah	2554	36.5	2348	33.6	1794	25.6	2413	34.5
Closed Shrub	313	4.5	228	3.3	459	6.6	282	4.0
Open Shrub	129	1.8	62	0.9	78	1.1	45	0.6
Grassland	326	4.7	412	5.9	330	4.7	281	4.0
Barren	789	11.3	841	12.0	978	14.0	864	12.3
Agriculture	307	4.4	641	9.2	595	8.5	482	6.9
Built	3	0.0	23	0.3	23	0.3	23	0.3
Water	8	0.1	44	0.6	60	0.9	52	0.7
No data/clouds	403	5.8	30	0.4	231	3.3	301	4.3

G4. Quantity LULC change of all the Random Forest Landsat imagery

	1985		1987		1993		2014	
LULC class:	km2	%	km2	%	km2	%	km2	%
Forest	239	3.4	128	1.8	290	4.1	264	3.8
Closed Shrub	313	4.5	270	3.9	315	4.5	228	3.3
Open Shrub	129	1.8	152	2.2	241	3.4	62	0.9
Woody Savannah	1921	27.5	1771	25.3	2014	28.8	2104	30.1
Savannah	2554	36.5	2621	37.5	3001	42.9	2348	33.6
Grassland	326	4.7	192	2.7	369	5.3	412	5.9
Agriculture	307	4.4	283	4.0	177	2.5	641	9.2
Barren	789	11.3	730	10.4	305	4.4	841	12.0
Water	8	0.1	7	0.1	33	0.5	44	0.6
Built	3	0.0	3	0.0	8	0.1	23	0.3
No data + clouds	405	5.8	840	12.0	242	3.5	30	0.4

	2015		2016		2018		2019	
LULC class:	km2	%	km2	%	km2	%	km2	%
Forest	257	3.7	271	3.9	271	3.9	212	3.0
Closed Shrub	228	3.2	459	6.6	370	5.3	282	4.0
Open Shrub	19	0.3	78	1.1	59	0.8	45	0.6
Woody Savannah	1812	25.8	2178	31.1	1675	23.9	2042	29.2
Savannah	2307	32.8	1794	25.6	2298	32.9	2413	34.5
Grassland	353	5.0	330	4.7	377	5.4	281	4.0
Agriculture	572	8.1	595	8.5	753	10.8	482	6.9
Barren	1013	14.4	978	14.0	469	6.7	864	12.3
Water	40	0.6	60	0.9	46	0.7	52	0.7
Built	23	0.3	23	0.3	23	0.3	23	0.3
No data + clouds	400	5.7	231	3.3	654	9.3	301	4.3

Appendix H

Quantities of the LULC change per method of Sentinel imagery

H1. Quantity LULC change ISODATA Sentinel

	2016		*2019*	
	km2	*%*	*km2*	*%*
Forest	349	5.0	223	3.2
Closed Shrub	352	5.0	399	5.7
Open Shrub	1325	18.9	207	3.0
Woody Savannah	1296	18.5	1639	23.4
Savannah	1203	17.2	2333	33.3
Grassland	1941	27.8	1048	15.0
Agriculture	123	1.8	214	3.1
Barren	155	2.2	532	7.6
Water	226	3.2	328	4.7
Built	23	0.3	23	0.3
No data/clouds	1.0	0.0	51.0	0.7

H2. Quantity LULC change Maximum Likelihood Sentinel

	2016		*2019*	
	km2	*%*	*km2*	*%*
Forest	346	4.9	459	6.6
Closed Shrub	1013	14.3	2105	30.1
Open Shrub	1035	14.6	2213	31.6
Woody Savannah	956	13.5	0	0.0
Savannah	1077	15.2	161	2.3
Grassland	681	9.6	0	0.0
Agriculture	962	13.6	3	0.0
Barren	799	11.3	1918	27.4
Water	23	0.3	23	0.3
Built	196	2.8	65	0.9
No data/clouds	1	0.0	51.0	0.7

H3. Quantity LULC change Random Forest Sentinel

	2016		*2019*	
	km2	***%***	***km2***	***%***
Forest	366	5.2	328	4.7
Closed Shrub	610	8.7	72	1.0
Open Shrub	719	10.3	407	5.8
Woody Savannah	1747	25.0	1718	24.5
Savannah	1728	24.7	2578	36.8
Grassland	399	5.7	178	2.5
Agriculture	650	9.3	833	11.9
Barren	670	9.6	1	0.0
Water	85	1.2	809	11.6
Built	23	0.3	23	0.3
No data/clouds	1	0.0	51.0	0.7

Appendix I

Four most accurate maps in larger format

I1. Random forest map Landsat 1985

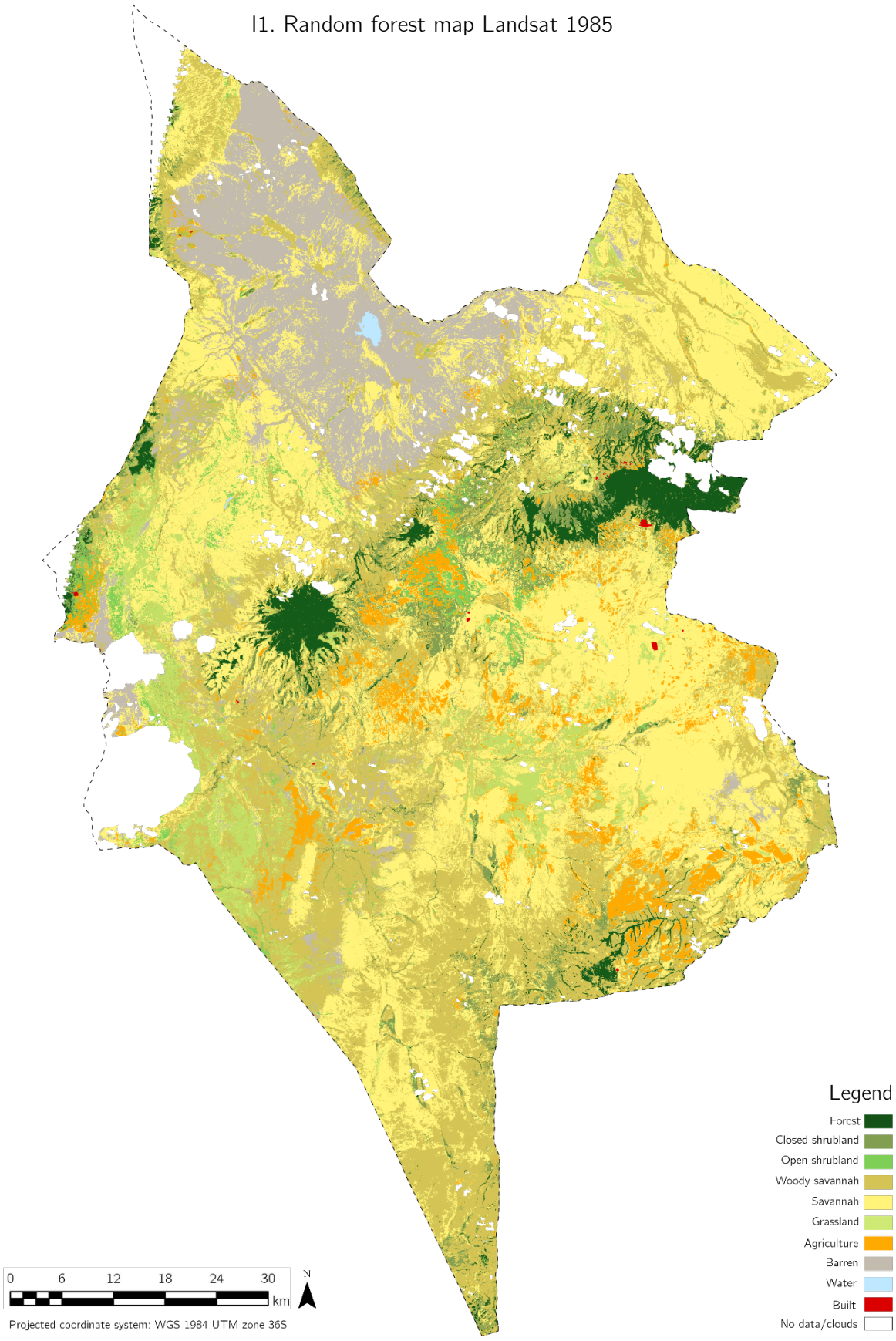

I2. Random forest map Landsat 1993

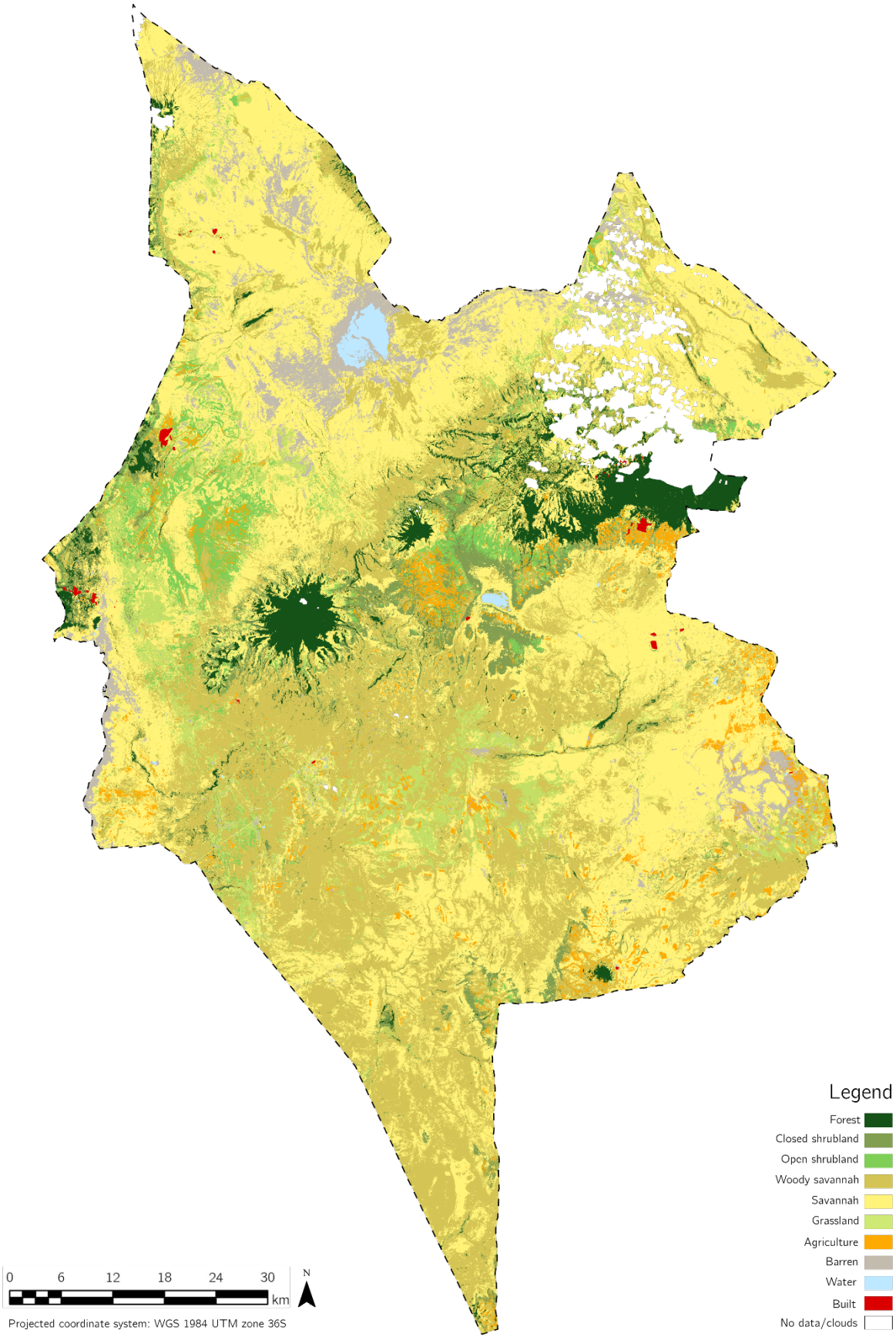

I3. Random forest map Landsat 2014

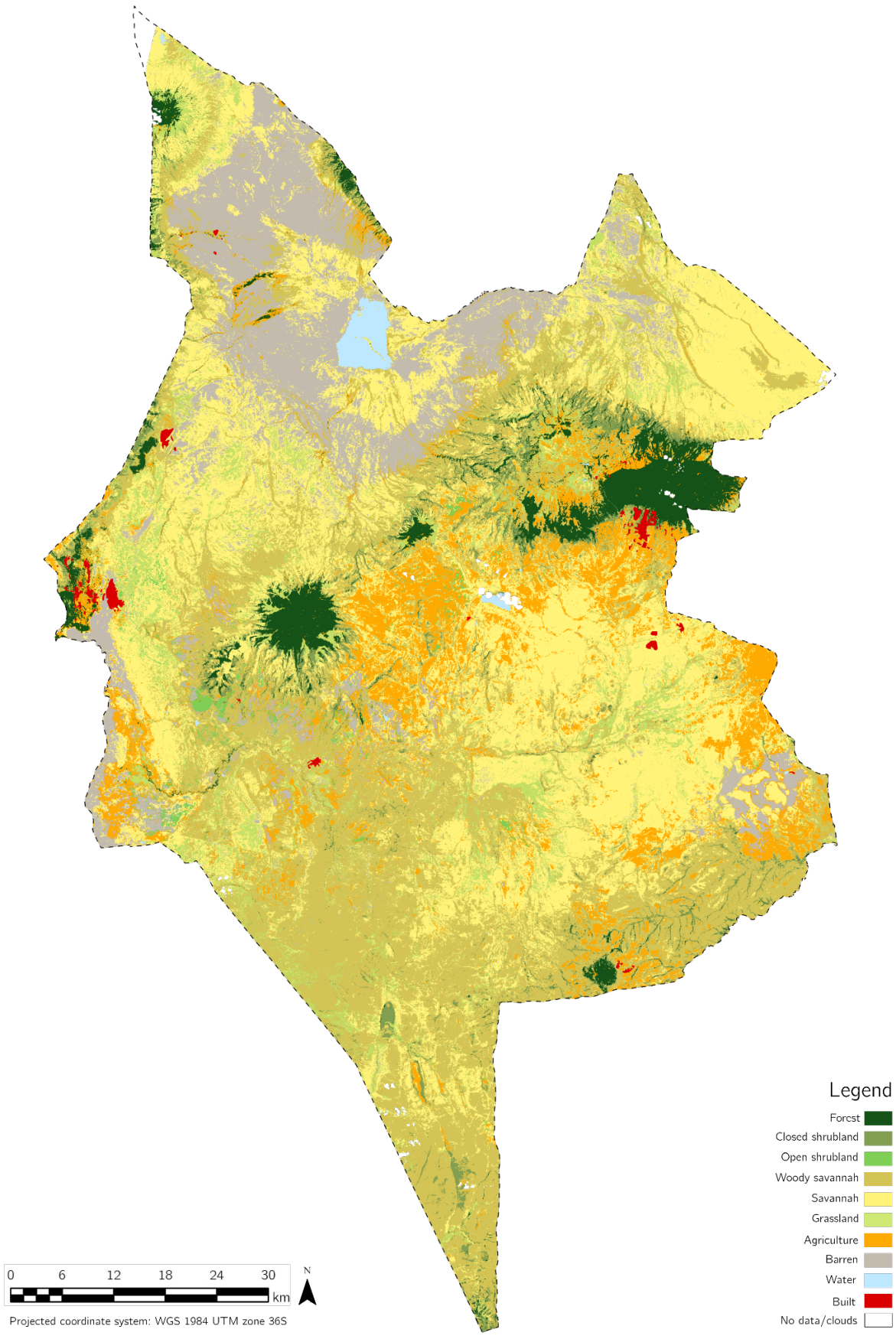

I4. Random forest map Landsat 1993

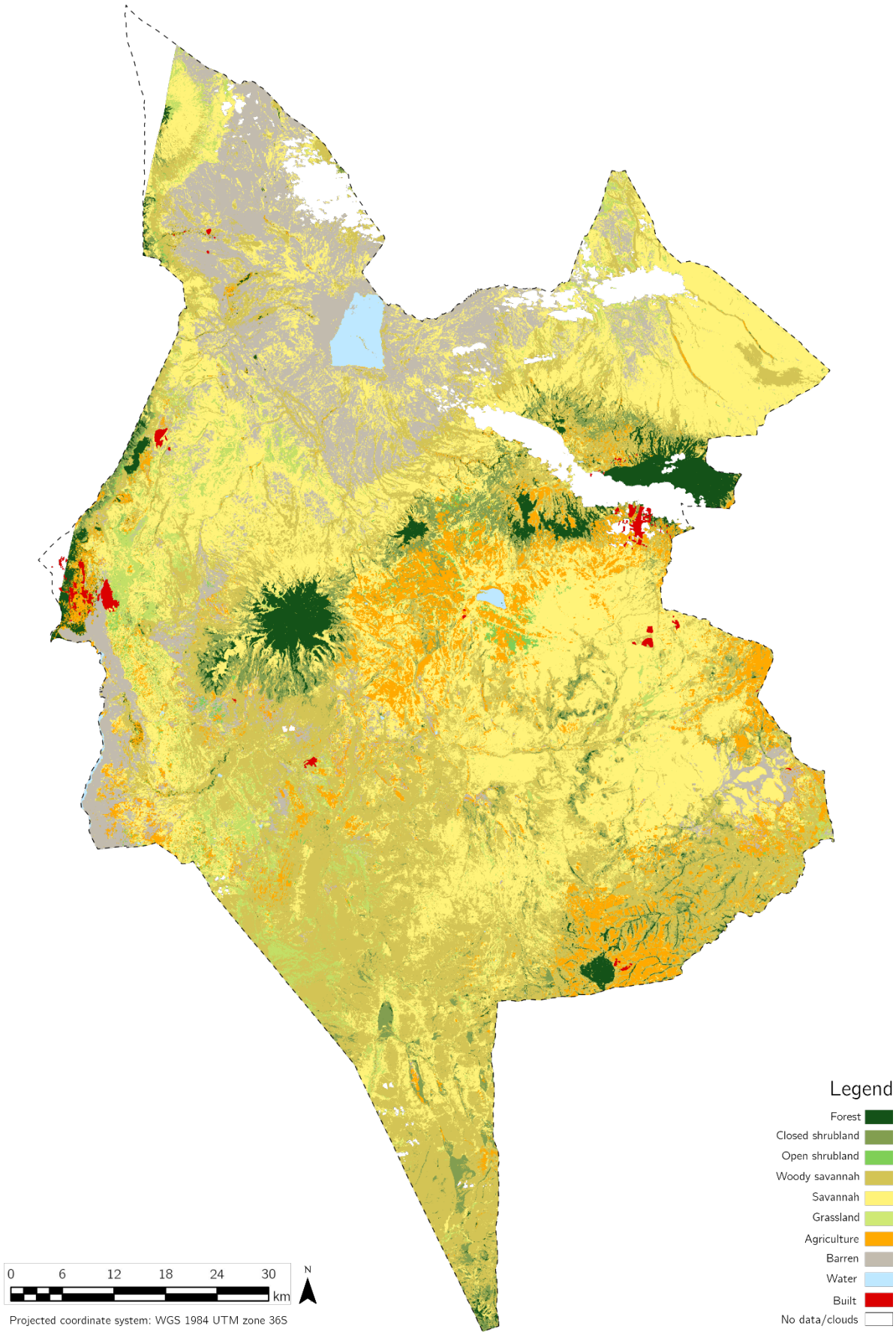

Appendix J

Change detection matrixes

J1. Change detection matrix 1985 to 1993

		1985 classification											
		Barren	*Built*	*ClosedShr.*	*Crops*	*Forest*	*Grass*	*NoData*	*OpenShr.*	*Sav.*	*Water*	*WoodySav.*	*Total*
1993 classification	*Barren*	136	0	3	3	0	4	23	1	105	0	30	305
	Built	1	2	0	1	0	0	0	0	2		1	8
	ClosedShr.	3	0	59	22	9	9	13	24	96	0	80	315
	Crops	4	0	12	30	3	4	12	9	52	0	51	176
	Forest	2	0	38	7	169	4	13	4	11	0	43	290
	Grass	24	0	7	9	1	66	11	8	153	0	89	369
	NoData	4		21	3	24	4	53	2	74	0	57	241
	OpenShr.	8	0	20	5	0	22	7	19	113	0	48	241
	Sav.	519	0	59	114	7	114	195	34	1359	0	598	3000
	Water	18		1	0	0	0	0	0	4	7	3	33
	WoodyS.	71	0	95	113	25	98	77	29	585	0	920	2013
	Total	789	3	313	307	239	326	405	129	2553	8	1920	6991
	Change	653	0	254	277	69	259	352	111	1194	5	1000	

J2. Change detection matrix 1993 to 2014

		1993 classification											
		Barren	*Built*	*ClosedShr.*	*Crops*	*Forest*	*Grass*	*NoData*	*OpenShr.*	*Sav.*	*Water*	*WoodySav.*	*Total*
2014 classification	*Barren*	175	0	3	9	2	26	16	10	520	1	79	840
	Built	1	8	1	2	2	0	0	0	7	0	2	23
	ClosedShr.	0	0	30	4	38	5	18	3	35	0	93	227
	Crops	15	0	61	67	24	25	16	18	227	1	187	641
	Forest	0	0	9	2	172	1	49	0	10	0	20	263
	Grass	9	0	16	7	10	55	17	26	173	0	99	412
	NoData	0	0	2	0	1	0	6	0	11	1	5	28
	OpenShr.	0	0	6	2	1	5	1	6	13	0	28	62
	Sav.	74	0	88	34	5	132	62	119	1328	0	505	2347
	Water	10	0	0	0	0	0	0	0	3	29	2	44
	WoodyS.	20	0	99	48	35	119	55	59	672	1	995	2103
	Total	305	8	315	176	290	369	241	241	3000	33	2013	6991
	Change	130	0	285	109	288	314	235	235	1672	4	1019	

J3. Change detection matrix 2014 to 2019

		2014 classification											
		Barren	*Built*	*ClosedShr.*	*Crops*	*Forest*	*Grass*	*NoData*	*OpenShr.*	*Sav.*	*Water*	*WoodySav.*	*Total*
2019 classification	*Barren*	525	0	0	40	0	9	0	9	222	1	58	864
	Built	0	23	0	0	0	0	0	0	0	0	0	23
	ClosedShr.	0	0	97	23	7	8	0	3	27	0	115	281
	Crops	18	0	5	287	6	9	2	11	64	0	79	481
	Forest	1	0	24	7	171	1	0	0	1	0	6	212
	Grass	20	0	0	5	1	86	0	2	100	0	67	281
	NoData	49	0	13	20	53	22	22	1	63	1	57	301
	OpenShr.	1	0	2	7	0	2	0	5	22	0	5	45
	Sav.	174	0	10	142	1	167	3	19	1597	0	299	2412
	Water	5	0	0	1	0	0	1	0	2	41	1	52
	WoodyS.	48	0	75	109	24	107	1	13	249	1	1415	2041
	Total	840	23	227	641	263	412	30	62	2347	44	2103	6992
	Change	316	0	130	353	92	326	30	62	750	3	688	

Appendix K

Models

K1. Graphic illustration of the stack models for Landsat and Sentinel in Erdas Imagine

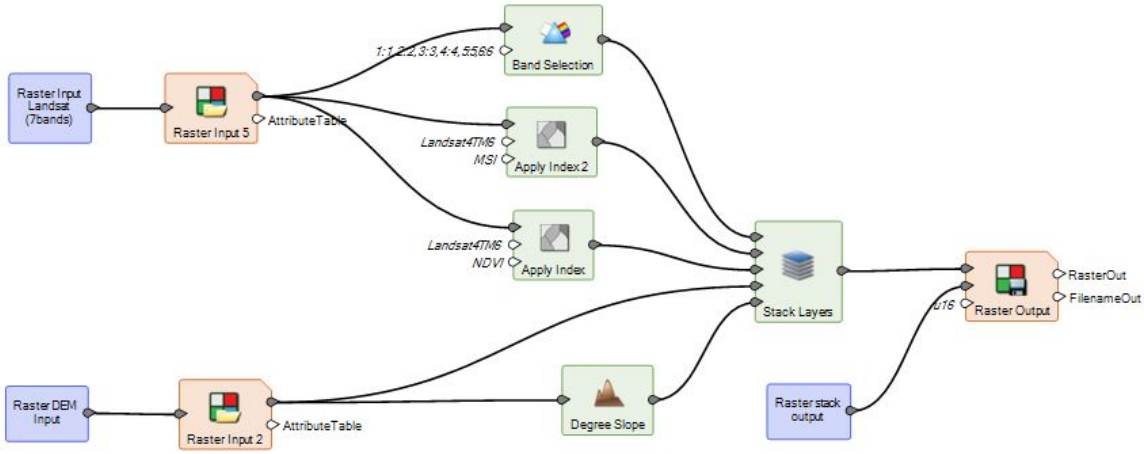

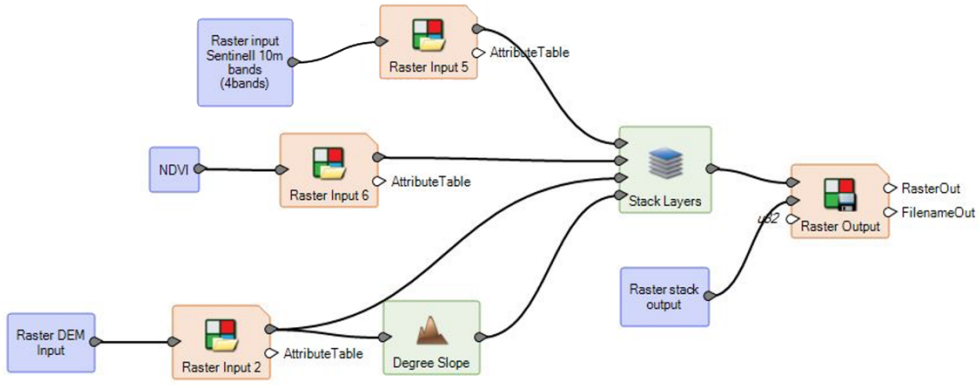

K2. Graphic illustration of RF and ML classification model ArcGIS PRO

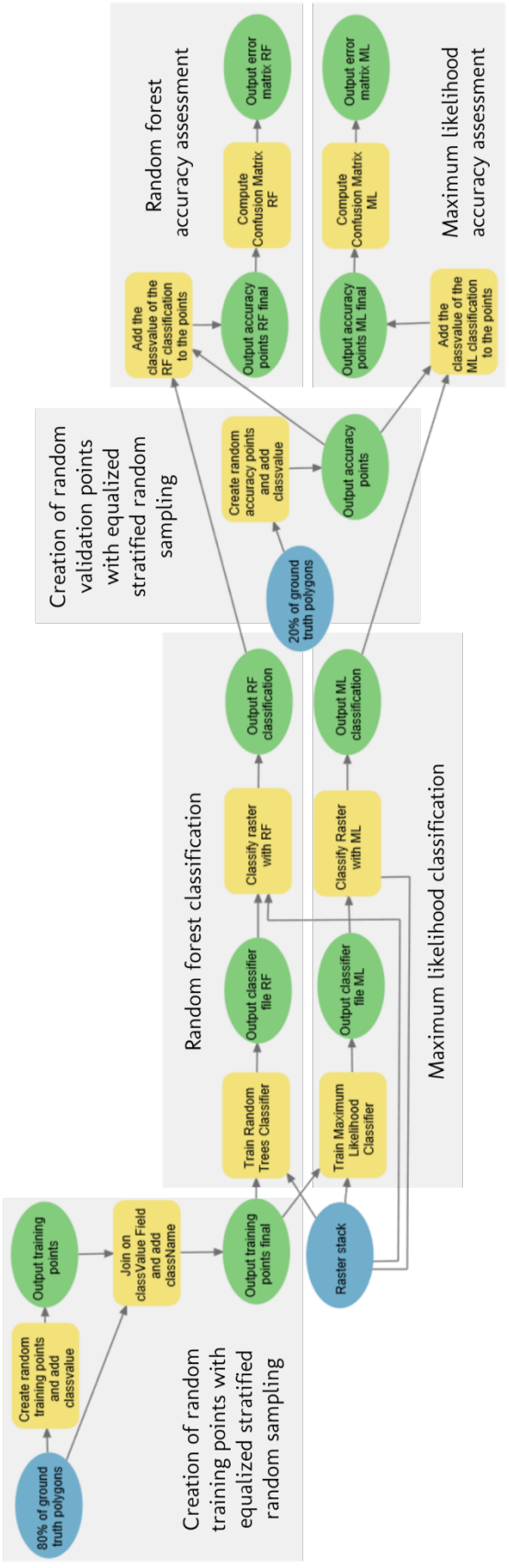

K3. Python code RF and ML classification model ArcGIS PRO

```
# -*- coding: utf-8 -*-
"""
Generated by ArcGIS ModelBuilder on : 2021-02-07 18:20:17
"""
import arcpy

def Model():  # Model

    # To allow overwriting outputs change overwriteOutput option to True.
    arcpy.env.overwriteOutput = False

    # Check out any necessary licenses.
    arcpy.CheckOutExtension("spatial")
    arcpy.CheckOutExtension("ImageAnalyst")

    # Model Environment settings
    with arcpy.EnvManager(scratchWorkspace=r"C:\Users\model.gdb",
workspace=r"C:\Users\[redacted].gdb"):
        Raster_stack = arcpy.Raster("C:\\[redacted]l2019_stack.tif")
        _80_of_ground_truth_polygons = "C:\\[redacted]\\dataset6_80p.shp"
        _20_of_ground_truth_polygons = "C:\\[redacted]\\dataset6_20p.shp"

        # Process: Create random training points and add classvalue (Create Accuracy Assessment Points) (ia)
        Output_training_points = "C:\\[redacted]\\output_accuracyp.shp"
        with arcpy.EnvManager(scratchWorkspace=r"C:\Users\[redacted]\model.gdb",
workspace=r"C:\Users\[redacted]\model.gdb"):
            arcpy.ia.CreateAccuracyAssessmentPoints(in_class_data=_80_of_ground_truth_polygons,
out_points=Output_training_points, target_field="GROUND_TRUTH", num_random_points=3000,
sampling="EQUALIZED_STRATIFIED_RANDOM")
            .save(Create_random_training_points_and_add_classvalue)


        # Process: Join on classValue Field and add className (Join Field) (management)
        with arcpy.EnvManager(scratchWorkspace=r"C:\Users\[redacted]\model.gdb",
workspace=r"C:\Users\[redacted]\model.gdb"):
            Output_training_points_final = arcpy.management.JoinField(in_data=Output_training_points, in_field="GrndTruth",
join_table=_80_of_ground_truth_polygons, join_field="classvalue", fields=["classname", "classvalue"])[0]

        # Process: Train Random Trees Classifier (Train Random Trees Classifier) (ia)
        Output_classifier_file_RF = "C:\\[redacted]\\classifierRF.ecd"
        with arcpy.EnvManager(scratchWorkspace=r"C:\Users\[redacted]\model.gdb",
workspace=r"C:\Users\[redacted]\model.gdb"):
            arcpy.ia.TrainRandomTreesClassifier(in_raster=Raster_stack, in_training_features=Output_training_points_final,
out_classifier_definition=Output_classifier_file_RF, in_additional_raster="", max_num_trees=500, max_tree_depth=60,
max_samples_per_class=None, used_attributes=["COLOR", "MEAN"], dimension_value_field="classvalue")
            .save(Train_Random_Trees_Classifier)


        # Process: Classify raster with RF (Classify Raster) (ia)
        Output_RF_classification = "C:\\[redacted]\\RF_classification.tif"
        Classify_raster_with_RF = Output_RF_classification
        with arcpy.EnvManager(scratchWorkspace=r"C:\Users\[redacted]\model.gdb",
workspace=r"C:\Users\[redacted]\model.gdb"):
            Output_RF_classification = arcpy.ia.ClassifyRaster(in_raster=Raster_stack,
in_classifier_definition=Output_classifier_file_RF, in_additional_raster="")
            Output_RF_classification.save(Classify_raster_with_RF)


        # Process: Create random accuracy points and add classvalue (Create Accuracy Assessment Points) (ia)
        Output_accuracy_points = "C:\\[redacted]\\accuracypRT.shp"
        arcpy.ia.CreateAccuracyAssessmentPoints(in_class_data=_20_of_ground_truth_polygons,
out_points=Output_accuracy_points, target_field="GROUND_TRUTH", num_random_points=750,
sampling="EQUALIZED_STRATIFIED_RANDOM")
        .save(Create_random_accuracy_points_and_add_classvalue)
```

```
        # Process: Add the classvalue of the RF classification to the points (Update Accuracy Assessment Points) (ia)
        Output_accuracy_points_RF_final = "C:\\[redacted]\\output_accuracypRT.shp"
        arcpy.ia.UpdateAccuracyAssessmentPoints(in_class_data=Output_RF_classification, in_points=Output_accuracy_points,
out_points=Output_accuracy_points_RF_final, target_field="CLASSIFIED")
        .save(Add_the_classvalue_of_the_RF_classification_to_the_points)


        # Process: Compute Confusion Matrix RF (Compute Confusion Matrix) (ia)
        Output_error_matrix_RF = "C:\\[redacted]\\errorMatrixRT.dbf"
        arcpy.ia.ComputeConfusionMatrix(in_accuracy_assessment_points=Output_accuracy_points_RF_final,
out_confusion_matrix=Output_error_matrix_RF)
        .save(Compute_Confusion_Matrix_RF)


        # Process: Train Maximum Likelihood Classifier (Train Maximum Likelihood Classifier) (ia)
        Output_classifier_file_ML = "C:\\[redacted]\\classifierML.ecd"
        with arcpy.EnvManager(scratchWorkspace=r"C:\[redacted]\model.gdb",
workspace=r"C:\Users\[redacted]\model.gdb"):
            arcpy.ia.TrainMaximumLikelihoodClassifier(in_raster=Raster_stack,
in_training_features=Output_training_points_final, out_classifier_definition=Output_classifier_file_ML,
in_additional_raster="", used_attributes=["COLOR", "MEAN"], dimension_value_field="classvalue")
            .save(Train_Maximum_Likelihood_Classifier)


        # Process: Classify Raster with ML (Classify Raster) (ia)
        Output_ML_classification = "C:\\[redacted]\\ML_classification.tif"
        Classify_Raster_with_ML = Output_ML_classification
        with arcpy.EnvManager(scratchWorkspace=r"C:\Users\[redacted]\model.gdb",
workspace=r"C:\Users\[redacted]\model.gdb"):
            Output_ML_classification = arcpy.ia.ClassifyRaster(in_raster=Raster_stack,
in_classifier_definition=Output_classifier_file_ML, in_additional_raster="")
            Output_ML_classification.save(Classify_Raster_with_ML)


        # Process: Add the classvalue of the ML classification to the points (Update Accuracy Assessment Points) (ia)
        Output_accuracy_points_ML_final = "C:\\[redacted]\\output_accuracypRT.shp"
        arcpy.ia.UpdateAccuracyAssessmentPoints(in_class_data=Output_ML_classification, in_points=Output_accuracy_points,
out_points=Output_accuracy_points_ML_final, target_field="CLASSIFIED")
        .save(Add_the_classvalue_of_the_ML_classification_to_the_points)


        # Process: Compute Confusion Matrix ML (Compute Confusion Matrix) (ia)
        Output_error_matrix_ML = "C:\\[redacted]\\errorMatrixRT.dbf"
        arcpy.ia.ComputeConfusionMatrix(in_accuracy_assessment_points=Output_accuracy_points_ML_final,
out_confusion_matrix=Output_error_matrix_ML)
        .save(Compute_Confusion_Matrix_ML)


if __name__ == '__main__':
    Model()
```

K4. Random forest model in Erdas Imagine

Training model

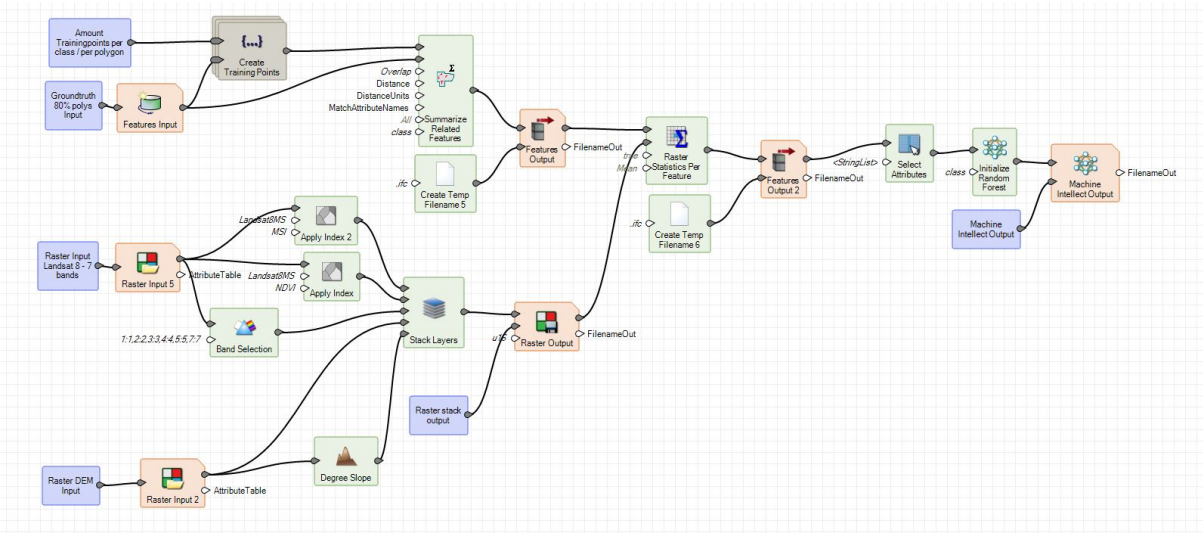

'Create training points':

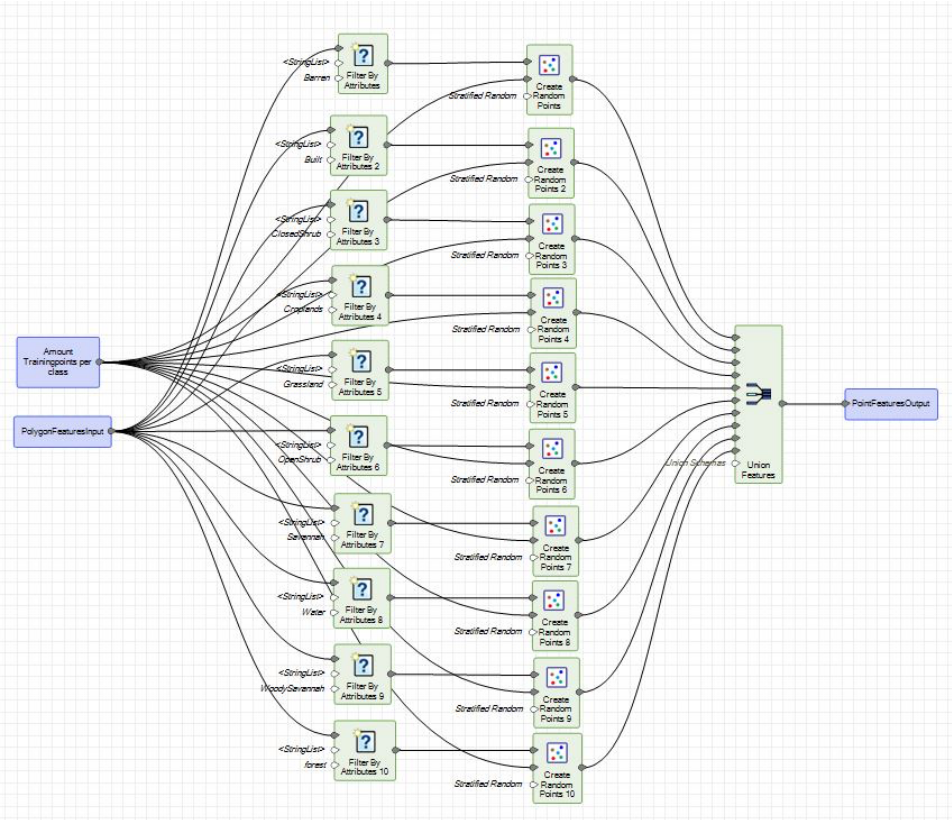

Classification model